

Fossil

Record

26 (2) 2023

Fossil Record

An International Journal of Palaeontology

Editor-in-Chief

Florian Witzmann

Museum für Naturkunde Berlin
Invalidenstraße 43
10115 Berlin
E-Mail: florian.witzmann@mfn-berlin.de
Tel: +49 30 889140 - 8820
Fax: +49 30 889140 - 8565

Editorial Secretary

Boryana Ovcharova

Pensoft Publishers,
Prof. Georgi Zlatarski Street 12
1700 Sofia, Bulgaria
Tel: +359-2-8704281
Fax: +359-2-8704282
E-Mail: journals@pensoft.net

Editorial Board

Anne-Claire Fabre, Bern, Switzerland
Carolin Haug, Munich, Germany
Christian Klug, Zürich, Switzerland
Johannes Müller, Berlin, Germany
Torsten Scheyer, Zurich, Switzerland
Alexander Schmidt, Göttingen, Germany
Florian Witzmann, Berlin, Germany
Hui-ting Wu, Beijing, China

Fossil Record

2023. Volume 26. Issue 2

ISSN: 2193-0066 (print), 2193-0074 (online)

In Focus

The cover picture shows a dorsal view of the carapace of *Denazinemys nodosa* (DMNH EPV.64550).

See paper of **Spicher GE, Sertich JJW, Girard LC, Joyce WG, Lyson TR, Rollot Y** A description of a *Denazinemys nodosa* specimen (Testudinata, Baenidae) from the Late Cretaceous Kaiparowits Formation of southern Utah.

Cover design



Fossil Record

An International Journal of Palaeontology

Content of volume **26 (2)** 2023

- Spicher GE, Sertich JJW, Girard LC, Joyce WG, Lyson TR, Rollot Y**
A description of a *Denazinemys nodosa* specimen (Testudinata, Baenidae) from the Late Cretaceous Kaiparowits Formation of southern Utah 151
- Augustin FJ, Ósi A, Csiki-Sava Z**
The Rhabdodontidae (Dinosauria, Ornithischia), an enigmatic dinosaur group endemic to the Late Cretaceous European Archipelago 171
- Zippel A, Haug C, Elverdi Z, Müller P, Haug JT**
Possible fungus-eating cucujiformian beetle larvae with setiferous processes from Cretaceous and Miocene ambers 191

Abstract & Indexing Information

Biological Abstracts® (Thompson ISI)
BIOSIS Previews® (Thompson ISI)
Cambridge Scientific Abstracts (CSA/CIG)
Web of Science® (Thompson ISI)
Zoological Record™ (Thompson ISI)

A description of a *Denazinemys nodosa* specimen (Testudinata, Baenidae) from the Late Cretaceous Kaiparowits Formation of southern Utah

Gaël E. Spicher^{1,2}, Joseph J. W. Sertich^{3,4}, Léa C. Girard¹, Walter G. Joyce¹, Tyler R. Lyson⁵, Yann Rollot¹

¹ Department of Geosciences, University of Fribourg, 1700 Fribourg, Switzerland

² Institute of Geosciences, Section Paleontology, Rheinische Friedrich-Wilhelms-Universität Bonn, Nußallee 8, 53115 Bonn, Germany

³ Department of Geosciences, Warner College of Natural Resources, Colorado State University, Fort Collins, Colorado, USA

⁴ Smithsonian Tropical Research Institute, Panama City, Panama

⁵ Department of Earth Sciences, Denver Museum of Nature & Science, Denver, Colorado, USA

<https://zoobank.org/A97F2AE5-019E-46D2-9B7B-584CB48CAFE0>

Corresponding author: Gaël E. Spicher (spicher.gael@gmail.com)

Academic editor: Florian Witzmann ♦ Received 22 February 2023 ♦ Accepted 14 June 2023 ♦ Published 31 July 2023

Abstract

Denazinemys nodosa is a Late Cretaceous representative of the North American turtle clade Baenidae diagnosed, among others, by a shell surface texture consisting of raised welts. We provide a detailed description of a partial skeleton from the late Campanian Kaiparowits Formation of Utah, USA, including bone-by-bone analysis of its cranium based on images obtained using micro-computed tomography. A revised phylogenetic analysis confirms placement of *Denazinemys nodosa* close to *Eubaena cephalica* and *Boremys* spp. within the clade Eubaeninae. Comparison with a second skull from the Kaiparowits Formation previously assigned to *Denazinemys nodosa* questions its referral to this taxon. An assortment of specimens from the Early to Late Campanian of Mexico and the USA had previously been referred to *Denazinemys nodosa* based on shell surface texture alone, even though this characteristic is known to occur in other baenids. Our review of all available material concludes that *Denazinemys nodosa* is currently only known from the Late Campanian of New Mexico and Utah.

Key Words

Baenidae, Baenodda, Campanian, Kaiparowits Formation, Late Cretaceous, Paracryptodira, Testudinata, Utah

Introduction

Baenidae is a clade of typically riverine paracryptodiran turtles that lived in North America from the Early Cretaceous to Eocene (Joyce and Lyson 2015). A conspicuous representative of the clade, easily diagnosed even in the field by the nodular surface texture of its shell, is *Denazinemys nodosa* (Gilmore, 1916). To date, well diagnosed material has been recovered from the Late Campanian of the Fruitland and Kirtland formations of New Mexico (Gilmore 1916, 1919; Wiman 1933; Lucas and Sullivan 2006; Sullivan et al. 2013; Dalman and

Lucas 2016; Lichtig and Lucas 2017) and the Kaiparowits Formation of Utah, USA (Hutchison et al. 2013; Lively 2016). Although this taxon was historically only known from shells, two skulls were recently reported and briefly described from the Kaiparowits Formation of Utah (Lively 2016).

Over the course of the last several decades, X-ray micro-computed tomography (μ CT) has proven itself essential in yielding novel insights into the cranial anatomy of turtles (e.g., Brinkman et al. 2006, 2009; Sterli et al. 2010), including baenids (Lipka et al. 2006; Rollot et al. 2018, 2022a, b; Evers et al. 2021), as this method provides a

non-destructive means to visualize structures hidden from external view and evaluate cryptic interelement sutures. As the above-mentioned skulls of *Denazinemys nodosa* are expected to provide additional insights into the taxonomy, phylogenetic relationships, and ecology of this turtle, we here provide a detailed description of one of them (DMNH EPV.64550) based on μ CT scans. We also provide a more detailed description of its shell based on 3D surface scans. These novel insights are then utilized to update the diagnosis of this turtle, to provide a novel phylogenetic hypothesis of baenid relationships, and to highlight possible paleoecological and paleogeographic implications. A difficult issue with which we were confronted during this study is the apparent differences between DMNH EPV.64550 and the second available skull of *Denazinemys nodosa* (BYU 19123), which cannot be explained satisfactorily for the moment.

Institutional abbreviations: BYU, Brigham Young University, Provo, Utah, USA; DMNH, Denver Museum of Nature & Science, Denver, Colorado, USA.

Materials and methods

Geologic setting

Specimen DMNH EPV.64550 was recovered from the middle unit of the Kaiparowits Formation (DMNH Loc. 4418), within the central Kaiparowits Plateau of Grand Staircase-Escalante National Monument, southern Utah (Fig. 1). The locality is approximately 200–300 meters above the lower contact with the Wahweap Formation, located stratigraphically higher than Ash Bed KP-07 of Roberts et al. (2013), U-Pb dated to 76.394 ± 0.040 Ma, and below Ash Bed KBC-109, dated to 75.609 ± 0.015 Ma (Ramezani et al. 2022), thus placing the locality at approximately 76 Ma. The youngest certain occurrence of *Denazinemys nodosa*, the type locality in the De-Na-Zin Member of the Kirtland Formation, is capped by Ash J (Fassett and Steiner 1997), dated to 73.496 ± 0.039 Ma (Ramezani et al. 2022). This established stratigraphic range for the taxon, between ~ 76 Ma and ~ 73.5 Ma is potentially extended by fragmentary remains recovered from older units in the southern portion of the Western Interior, including the Lower Shale Member of the Aguja Formation (~ 80 – 77 Ma; Lehman et al. 2019), the Allison Member of the Menefee Formation (~ 83 – 80 Ma; Lichtig and Lucas 2015), and the Coyote Point Member of the Wahweap Formation (~ 81 – 80 Ma; Holroyd and Hutchison 2016; Beveridge et al. 2022). However, none of this material is necessarily diagnostic of *Denazinemys nodosa* per se, as other turtles from the Campanian are known to have a nodular surface texture, such as *Boremys* spp. and *Scabremys ornata* (Gilmore 1935; Sullivan et al. 2013, see Discussion below).

In addition to the associated shell and skull of *Denazinemys nodosa* (DMNH EPV.64550), fossil specimens recovered from DMNH Loc. 4418 include a small partial dentary of the alligatoroid c.f. *Brachychampsia*

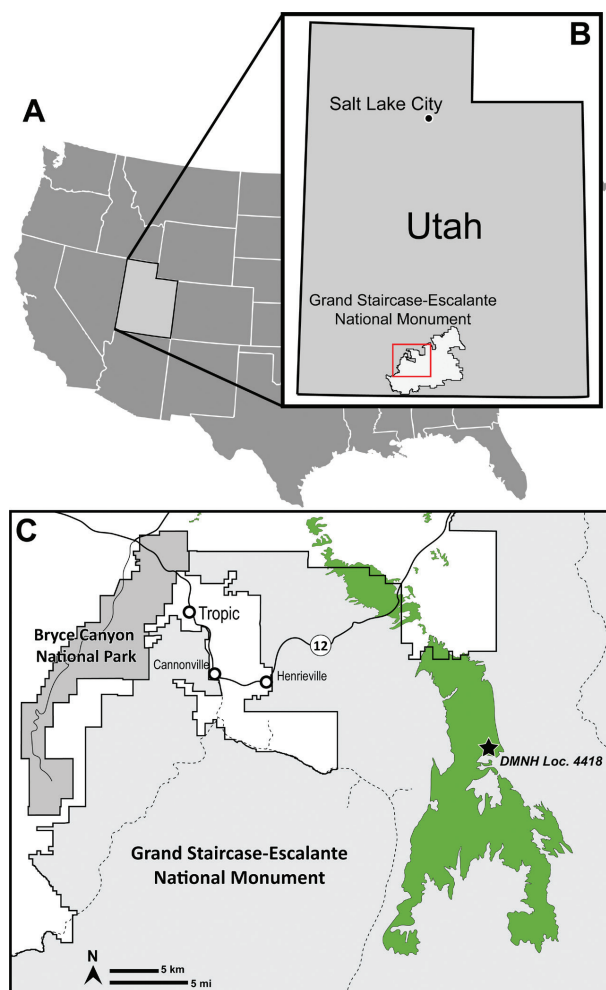


Figure 1. Map showing the location of DMNH Loc. 4418 on the Kaiparowits Plateau of Grand Staircase-Escalante National Monument, southern Utah, U.S.A. (A), with inset of Utah (B), and the location of the main exposures of the Kaiparowits Formation in and around Grand Staircase-Escalante National Monument (C). Green areas represent aerial exposure of the Kaiparowits Formation.

sp. and rounded fragments of other turtle taxa typical of aquatic assemblages in the Kaiparowits Formation. The sediment at the locality consists of a fine-grained, sandy mudstone associated with overbank floodplain deposition in a ponded setting (Facies Association 8 of Roberts [2007]). Shell elements were disarticulated and chaotically oriented in an area of less than $\frac{1}{4}$ square meter, with many elements cleanly broken prior to, or during, deposition. Breaks of shell elements ranged from mild offsets to widely scattered pieces, with some portions of individual elements recovered from different sides of the association and later repaired in the laboratory. This suggests the pre-depositional disarticulation of an individual, possibly at the bottom of a shallow pond, followed by a higher energy depositional event (e.g., flood, avulsion) that rearranged and disturbed elements but did not carry them far before final deposition. The skull was found within the cluster of chaotically arranged shell elements, surrounded by portions of shell within the sediment. All shell elements

referred to *D. nodosa* from the site are consistent in size and preservation. This, combined with the absence of duplicated elements, strongly suggests that the locality preserved only one individual of *D. nodosa* and that the closely associated skull can be confidently assigned to the same individual. Smaller elements, including appendicular elements, vertebrae, and mandibles, may have been lost to winnowing during deposition or scavenged, though the remaining elements do not show evidence of scavenging by a large-bodied vertebrate such as a crocodyliform or non-avian theropods.

Visualization

μCT-scan: We used high-resolution X-ray micro-computed tomography to obtain the internal cranial morphology of DMNH EPV.64550. The scan was undertaken at the University of Texas High-Resolution X-ray Computed Tomography Facility in Austin, Texas, USA with a NSI scanner with 3600 projections, a voltage of 180 kV, a current of 160 μA, and an aluminum filter. The projections were converted into 1930 coronal slices with a voxel size of 33.1 μm. To generate and visualize the bones and canals of DMNH EPV.64550 in three dimensions, we used the software program Amira (version 6.1.1; <https://www.thermofisher.com/>). We utilized the brush and lasso tools of Amira to manually highlight the boundaries of all bones and canals preserved in the specimen in every third slice in the x-axis. The reconstructions were then obtained through interpolation using the appropriate tool. Isosurface models were exported as .ply files. The visualization of the 3D models was made in the software Blender (version 2.79b; <https://www.blender.org>). The image stack and the 3D models are available at Morphosource (<https://www.morphosource.org/projects/000483670>).

Surface scanning: The carapace and plastron of DMNH EPV.64550 were scanned using a portable surface scanner Artec Space Spider at DMNS. The scans were acquired and treated with the software Artec Studio 16 Professional: scans from different angles were performed to acquire the full 3D morphology of each shell part, each scan was cleaned, landmarks were manually applied to align and fuse scans, and holes automatically filled to produce a single, watertight 3D model. Models were exported as .obj files with an associated texture as .png file. The models were later loaded into MeshLab to merge mesh and texture on a single .ply model for each piece of the shell. The 3D models are available at Morphosource (<https://www.morphosource.org/projects/000483670>).

Phylogenetic analysis

To explore the phylogenetic relationships of *Denazinemys nodosa* with other baenids, we modified the character/taxon matrix of Rollot et al. (2022b). We utilized the herein new observations to score the cranial anatomy of

Denazinemys nodosa, thereby partially replicating the efforts of Lively (2016) in capturing the cranial anatomy of this taxon. The previously existing postcranial scorings for this taxon were updated by reference to the shell of DMNH EPV.64550, in particular characters 35 (preneural; 0/1 [variously present], not ?), 48 (placement of anal scutes; 1 [z-shaped], not 0), 49 (xiphiplastron/hypoplastron suture; 1 [z-shaped], not ?), 88 (proportions of neural V; 1 [longer than wide], not ?), and 89 (neural VI contacts; 1 [contacts costals V, VI, and VII], not ?). We furthermore updated the scoring of *Goleremys mckennai* by reference to Hutchison (2004), as this taxon was deemed to be problematic by some previous analyses (e.g., Lyson and Joyce 2010; Lyson et al. 2019), in particular characters 63 (parietal width versus length; 1 [combined width greater than length], not ?), 73 (size of external narial opening; 0 [much smaller than orbit], not ?), 96 (basipterygoid processes; 2 [absent], not ?), and 101 (bones contributing to occipital condyle; 1 [basiooccipital only], not ?). The final matrix consists of 105 characters scored for 48 taxa and can be found in Suppl. material 1.

The matrix was subjected to a parsimony analysis using TNT (Goloboff et al. 2008). Unless stated otherwise, we used the default settings. Characters 5, 9, 13, 15, 17, 25, 26, 29, 32, 37, 38, 39, 44, 46, 58, 61, 78, 86, 93, 95, 96, 99 (here and elsewhere, we are not using the numeration of TNT) form morphoclines and were ordered. 1,000 replicates of random addition sequences were followed by a second round of tree bisection-reconnection. As we are doubtful about the common presence of 12 peripherals in baenodds (see Discussion), we deactivated character 36, which captured its purported distribution across the ingroup. We furthermore deactivated character 57 (presence of horizontal tubercles of the basiooccipital), as we are unable to replicate its current meaning or coding.

Systematic paleontology

Testudinata Klein, 1760 (Joyce et al., 2020a)
Paracryptodira Gaffney, 1975 (Joyce et al., 2021)
Baenidae Cope, 1873 (Joyce et al., 2021)
***Denazinemys* Lucas & Sullivan, 2006**

***Denazinemys nodosa* (Gilmore, 1916)**

Holotype. USNM 8345, an almost complete shell (Gilmore 1916, figs 34, 35, pl. 76; Sullivan et al. 2013, fig. 20.2a, b).

Type locality and horizon. Locality 60, Willow Wash, 2 miles northwest of Ojo Alamo store, San Juan County, New Mexico (Gilmore 1916), USA; De-na-zin Member, Kirtland Formation, upper Campanian, Upper Cretaceous (Sullivan et al. 2013).

Referred material and range. Upper Cretaceous (Campanian) Fruitland and Kirtland formations of New Mexico (Gilmore 1916, 1919; Wiman 1933; Lucas and Sullivan 2006; Sullivan et al. 2013; Dalman and

Lucas 2016; Lichtig and Lucas 2017) and Kaiparowits Formation of Utah (Hutchison et al. 2013; Lively 2016) (see Discussion for justification).

Revised diagnosis. *Denazinemys nodosa* can be identified as a representative of Baenodda by the contribution of vertebral V to the posterior margin of the shell, an omega-shaped femoral-anal sulcus, and a midline contact between both extragulars posterior to the gulars and a representative of Eubaeninae by the presence of a subdivided cervical, the presence of prepleurals, and a vertebral III that is longer than wide. Among eubaenines *Denazinemys nodosa* can be differentiated by the following combination of characters: presence of welt-like ornamentation on the carapace (also present in *Boremys* spp. and *Scabremys ornata*), absence of a posterodorsal extension of the quadratojugal that crests the cavum tympani (also absent in *Baena arenosa* and *Chisternon undatum*), the presence of epipterygoids, large mandibular condyles, and a nasal/frontal suture that is anteriorly convex (Joyce and Lyson 2015).

Description. General. The cranium is generally well preserved, despite minor crushing mainly affecting the right side of the specimen (Figs 2, 3). The right quadratojugal and right squamosal are missing. Portions of the right quadrate and paroccipital process of the right opisthotic dislocated from the remainder of the cranium but are preserved as an articulated fragment that was μ CT scanned together with the skull, though not in the position it was originally found. The sutures of the cranium can be distinguished with relative ease in the μ CT scan. The skull is about 65 mm long from the anterior tip of the nasals to the posterior end of the supraoccipital crest, and 48 mm wide between the outside edge of the mandibular condyles. The skull is wedge-shaped in dorsal view and possesses a distinct, pinched snout (Fig. 2A). The less deformed left side suggests that the orbits were oriented dorsolaterally. The upper temporal emargination protrudes anteriorly beyond the level of the anterior margin of the cavum tympani (Fig. 2B). The last three observations are in broad agreement with other baenodds (Joyce and Lyson 2015). The dorsal skull roof is decorated with fine crenulations, but distinct scute sulci appear to be absent.

Nasal. The nasals are flat and narrow elements that roof the nasal cavity (Fig. 2). In dorsal view, the nasal is longer than broad and contacts its counterpart medially and the frontals posteriorly and posteromedially. The nasal is prevented from contacting its counterpart for nearly half of its length posteriorly by an anterior extension of the frontal (Fig. 2A). This anterior process of the frontal also covers the posteromedial aspect of the nasal. Within the nasal cavity, the nasal contacts the prefrontal posterolaterally, but such a contact is prevented externally by an extended contact between the frontal and maxilla (Fig. 2C, E). On the uncrushed, left side of the skull, the apertura narium externa forms a posteriorly oriented slit starting from its dorsolateral margin. The slit extends posteriorly and reaches the frontal, thus preventing the nasal from contacting the maxilla (Fig. 2A). As

preserved, the right nasal contacts the right maxilla along a straight contact, but deformation in combination with a lack of apparent articulation sites suggest that this is due to compression. The nasal of *Denazinemys nodosa*, therefore, differs from the more elongated nasal that contacts the maxilla of *Eubaena cephalica* (Gaffney 1972; Rollot et al. 2018), *Goleremys mckennai* (Hutchison 2004), and *Saxochelys gilberti* (Lyson et al. 2019).

Prefrontal. The prefrontals are well preserved despite some shearing on both sides. The dorsal plate is greatly reduced in size as in the majority of baenodds (Joyce and Lyson 2015). The dorsal plate of the prefrontal is developed as a small, rectangular lappet that forms the anterodorsal margin of the orbit (Fig. 2A, C, E). The dorsal process of the prefrontal contacts the maxilla anteriorly and the frontal dorsally and posteriorly. The dorsal process furthermore contacts the nasal within the roof of the nasal cavity, as in *Eubaena cephalica* (Rollot et al. 2018). The descending process of the prefrontal frames the orbit anteriorly and forms the anterior margin of the foramen interorbitale and the anterior half of the foramen orbito-nasale, which is posteriorly framed by the palatine. Anteriorly, the descending process of the prefrontal broadly contacts the maxilla ventrolaterally along a straight suture, the vomer posteroventrolaterally, and the palatine on both sides of the foramen orbito-nasale. A blunt, sheet-like ridge along the medial aspect of the descending process of the prefrontal might be apparent on the right side, but a constriction of the fissura ethmoidalis as that observed in some early branching baenids is not apparent in *Denazinemys nodosa* (Rollot et al. 2022a).

Frontal. The frontal is a flat and elongate element, trapezoidal in dorsal view, mediolaterally wider posteriorly than anteriorly (Fig. 2A, C–E). The frontal contacts the nasal anteriorly along a deeply concave suture, the maxilla anterolaterally, the dorsal process of the prefrontal lateroventrally, the postorbital posterolaterally, the parietal posteriorly, and its counterpart medially for its entire length. The frontoparietal suture is located posterior to the orbit. The left frontal likely has a minute contribution to the posterior margin of the slit-like opening located between the nasal and maxilla, which had previously not been noted (Lively 2016). The frontal bears a pointed anterior process that deeply protrudes between the nasals, preventing the latter to contact one another along their posterior half. At about two thirds of its length, the frontal is slightly expanded laterally to form the dorsal margin of the orbit (Fig. 2C, E). Ventrally, the frontal is thickened to form a low crista cranii that separates the orbit from the low but broad sulcus olfactorius. The crista cranii is not continuous with the parietal posteriorly.

Parietal. The parietals are complete but slightly damaged, mostly along the ventral aspect of their descending process (Fig. 2A). The parietal forms the anteromedial wall of the temporal fossa, the posterior margin of the foramen interorbitale, and the anterior and medial margin of the upper temporal emargination. The dorsal part of the parietal forms a thin plate of bone

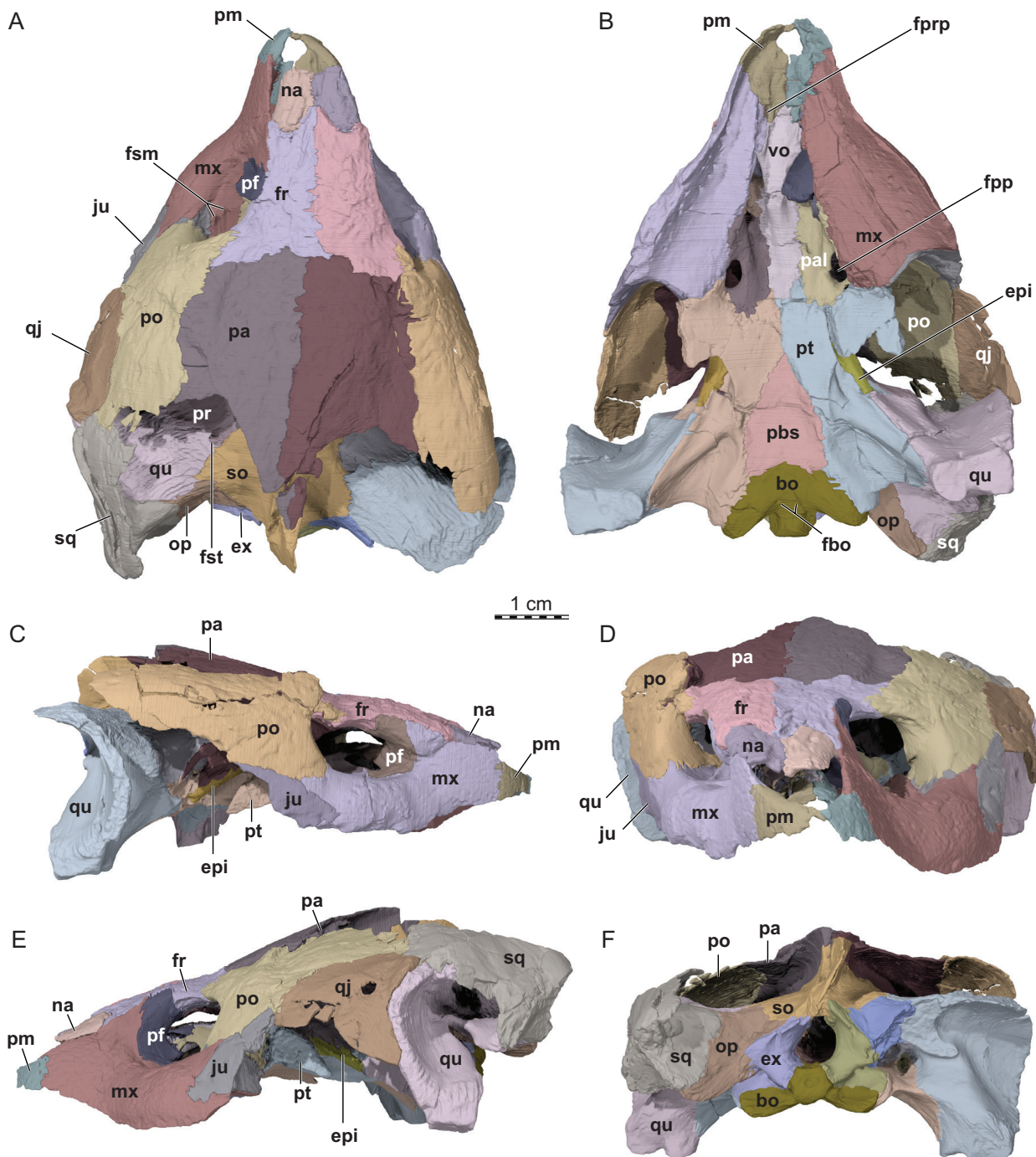


Figure 2. Skull of *Denazinemys nodosa* (DMNH EPV.64550), Late Cretaceous (Campanian) of southern Utah, U.S.A. Three-dimensional renderings of the skull in: **A.** Dorsal; **B.** Ventral; **C.** Right lateral; **D.** Anterior; **E.** Left lateral, and **F.** Posterior views. Abbreviations: bo, basioccipital; epi, epipterygoid; ex, exoccipital; fbo, foramen basioccipitale; fpp, foramen palatinum posterius; fprp, foramen praepalatinal; fr, frontal; fsm, foramen supramaxillare; fst, foramen stapedio-temporale; ju, jugal; mx, maxilla; na, nasal; op, opisthotic; pbs, parabasisphenoid; pa, parietal; pal, palatine; pf, prefrontal; pm, premaxilla; po, postorbital; pr, prootic; pt, pterygoid; qj, quadratojugal; qu, quadrate; so, supraoccipital; sq, squamosal; vo, vomer.

that is slightly broader anteriorly than posteriorly, but the combined width of the parietals is about as great as their length. The dorsal plate contacts the frontal anteriorly, the postorbital laterally, the supraoccipital posteriorly, and its counterpart medially. Within the upper temporal fossa, the vertical process of the parietal, or processus inferior parietalis, contacts the prootic laterally and the supraoccipital

posteriorly. A distinct ridge extends posteroventrally along the lateral surface of the processus inferior parietalis, starting from the contact with the postorbital to nearly reach the ventral contact with the epipterygoid. Within the lower temporal fossa, the processus inferior parietalis contacts the pterygoid anteroventrally, the epipterygoid ventrally, again the pterygoid posteroventrally along the

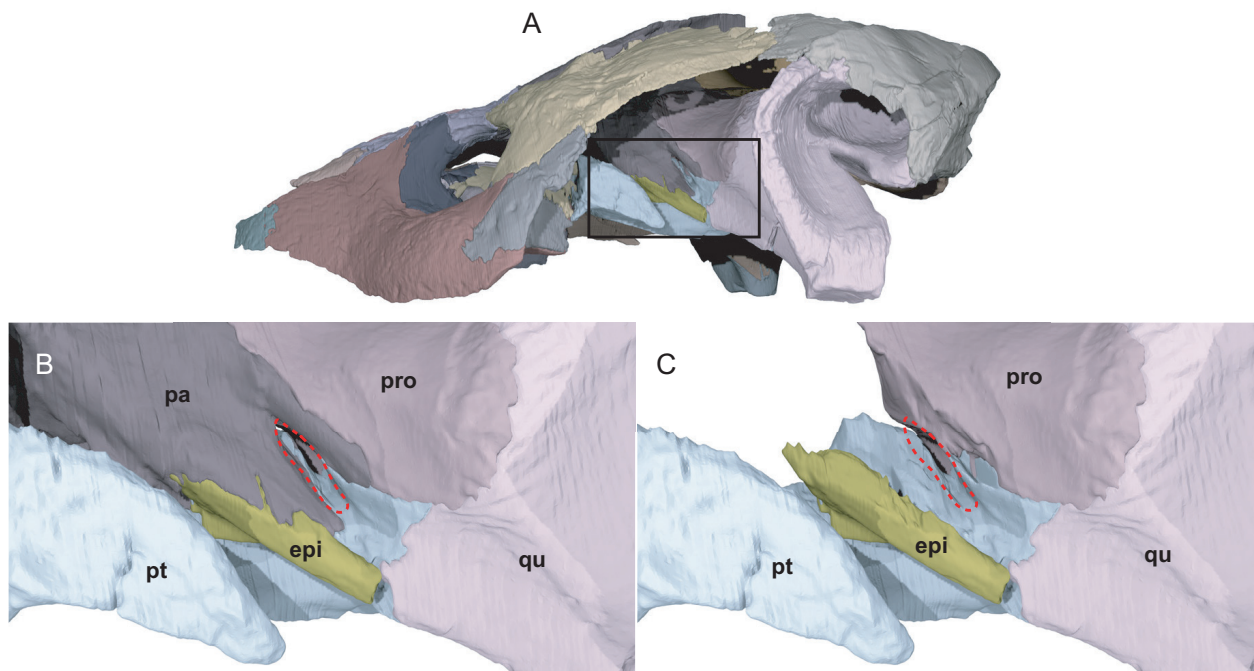


Figure 3. Three-dimensional renderings of the left trigeminal foramen of DMNH EPV.64550. **A.** Left lateral view of DMNH EPV.64550 showing the area of interest; **B.** Close-up on the left trigeminal foramen area highlighting its external margin; **C.** Close-up on the left trigeminal foramen area showing its internal margin. The margins of the trigeminal foramen are highlighted by the dashed red circles. Abbreviations: epi, epipterygoid; pa, parietal; pro, prootic; pt, pterygoid; qu, quadrate.

posterior margin of the foramen nervi trigemini, and the prootic posteriorly (Fig. 3). Within the braincase, the processus inferior parietalis additionally contacts the parabasisphenoid posteroventrally. Two finger-like processes of the parietal frame the anteroventral and posterodorsal margins of the trigeminal foramen and, independently from one another, contact the pterygoid ventrally. Although these contacts prevent the prootic from contributing to the external margin of the foramen nervi trigemini, as is the case in *Boremys pulchra* (Brinkman and Nicholls 1991), the prootic roofs the latter foramen from the inside, similar to the condition observed in *Lakotemys australodakotensis* (Rollot et al. 2022a). The parietal and epipterygoid jointly form a thickened ridge that runs diagonally from the dorsal skull roof to the articular surface of the quadrate just anteroventrally to the trigeminal foramen (Fig. 2B, C and E).

Postorbital. Despite some fractures, both postorbitals are overall well preserved. The anterior part of the postorbital is ventrally expanded as a mediolaterally thickened septum orbitotemporale (sensu Evers et al. 2020) that forms the posterior aspect of the fossa orbitalis and broadly rests on the jugal dorsally (Fig. 2A–E). The resulting, posteriorly constricted opening between the orbit and temporal fossa resembles the condition observed in other paracryptodires, but also pleurodires (Evers et al. 2020). Within the orbit, the postorbital mainly contacts the jugal ventrally, but additional contacts can be identified along the most posterior aspect of the orbital floor with the

maxilla anterolaterally and the pterygoid posterolaterally (Fig. 2B, C, and E). Along the posteroventral corner of the right orbit, the postorbital contacts the maxilla anteroventrally, which prevents the jugal from contributing to the orbital margin. On the left side, small portions of the jugal are inserted between the postorbital and maxilla in some areas (Fig. 2D). These repeated slight exposures of the jugal are somewhat unusual in comparison to other paracryptodires that either lack a jugal contribution to the orbital margin, or exhibit a clear jugal contribution to that margin. The condition exhibited on the left side likely corresponds to a preservational artefact, and we interpret the bony arrangement on the right side as being correct (Fig. 2A and D). A contact between the maxilla and postorbital along the posteroventral margin of the orbit was also reported in *Boremys pulchra* (Brinkman and Nicholls 1991), *Eubaena cephalica* (Gaffney 1972; Rollot et al. 2018), and *Saxochelys gilberti* (Lyson et al. 2019).

The posterior part of the postorbital is developed as a flat and elongate piece of bone (Fig. 2). Although the posterior margin of both postorbitals is damaged, the intact margins of the surrounding elements strongly suggest that the postorbital broadly contributed to the upper temporal emargination. On the skull roof, the postorbital contacts the frontal anteromedially, the parietal medially, the jugal anterolaterally, the quadratojugal laterally, and the squamosal posterolaterally.

Jugal. The jugals are both damaged and their posterior portion is not preserved (Fig. 2C and E). The jugal

is a small element that forms the anterodorsal margin of the cheek emargination. The right jugal preserves a small portion of that margin, indicating that the cheek emargination likely reached the level of the ventral margin of the orbit at the most. In lateral view, the jugal contacts the maxilla anteriorly and anteroventrally and the postorbital dorsally. A contact with the quadratojugal posteriorly is preserved on the left side only (Fig. 2E). The jugal forms a thick process medially that lies beneath the postorbital and is partially exposed within the orbit, where it contacts the maxilla anteriorly and medially along a V-shaped suture. The jugal contacts the postorbital dorsally. A small exposure of the jugal is apparent on the left side (Fig. 2A, D), but this is likely due to some damage or shearing, and the bony arrangement along the posteroventral corner of the right orbit appears to be the usual condition for DMNH EPV.64550 (see Postorbital above). Within the lower temporal fossa, the medial process of the jugal contacts the pterygoid posteromedially, anterior to the external process of the latter (Fig. 2B).

Quadratojugal. Only the left quadratojugal is preserved in DMNH EPV.64550 (Fig. 2A, C, and E). The quadratojugal is a flat, subtriangular element that forms the posterodorsal margin of the lower temporal emargination. The quadratojugal contacts the jugal anteriorly, the postorbital dorsally, the squamosal posterodorsally, and the quadrate posteriorly (Fig. 2E). A contribution of the quadratojugal to the margin of the cavum tympani is not apparent.

Squamosal. The right squamosal is missing in DMNH EPV.64550, but its left counterpart is entirely preserved, albeit crossed by various fractures (Fig. 2A, B and E, F). The squamosal forms the posterodorsal aspect of the skull and contributes to the posterodorsal rim of the cavum tympani, the posterolateral margin of the upper temporal emargination, and the posterior and lateral margins of a deep antrum postoticum (Fig. 2E). On the skull roof, the squamosal contacts the quadratojugal anterolaterally and the postorbital anteromedially, and broadly contacts the quadrate ventrally. Within the upper temporal fossa, the squamosal contacts the quadrate anteromedially and the paroccipital process of the opisthotic medially (Fig. 2A, F). The squamosal broadly covers the posterodorsolateral aspects of the quadrate to form a deep antrum postoticum. The ridge that runs from the posterior tip of the squamosal towards the paroccipital process is damaged on the left side of the skull. As a result, the pit behind the antrum postoticum, best seen in lateral view (Fig. 2E), for attachment of the *M. depressor mandibulae* is incomplete.

Premaxilla. The premaxilla forms the floor of the fossa nasalis and the ventral margin of the apertura narium externa (Fig. 2A–E). The premaxillae are visible in dorsal view, as in other eubaenines. The premaxilla contacts the vomer posteriorly, the maxilla posterolaterally, and its counterpart medially. The premaxillae form a relatively large, rounded opening along their median suture that resembles the intermaxillary foramen of trionychians (Fig. 2A, B). This foramen, perhaps the result of taphonomic damage, is not homologous with the foramen praepalatinum, as the latter

is preserved along the most posterior aspect of the premaxilla. The foramen praepalatinum is mostly formed by the premaxilla, with contributions of the maxilla posterolaterally, as in *Eubaena cephalica* (Gaffney 1972; Rollot et al. 2018) but not other eubaenines for which this area is known (Gaffney 1972; Hutchison 2004). The premaxilla forms the anterior aspects of the labial margin, contributes only little to the triturating surfaces, and defines a distinct median tongue groove, much as in *Stygiochelys estesi* (Gaffney and Hiatt 1971), *Chisternon undatum* (Gaffney 1972), *Eubaena cephalica* (Gaffney 1972; Rollot et al. 2018), and *Saxochelys gilberti* (Lyson et al. 2019), but likely not *Goleremys mckennai* (Hutchison 2004). A lingual ridge is not present.

Maxilla. The maxilla forms the anterior and ventral margins of the orbit, the lateral margin of the apertura narium externa, the lateral wall of the fossa nasalis, minor aspects of the lateral margin of the foramen palatinum posterius, and floors the fossa orbitalis (Fig. 2A–E). The ascending process of the maxilla forms a thin sheet of bone bordered by the apertura narium externa anteriorly and the orbit posteriorly. The ascending process contacts the frontal dorsally and the prefrontal posteriorly. On the right side of the skull, the maxilla contacts the nasal, but this contact is likely due to shearing, as such a contact appears to be absent on the left. The maxilla contacts the premaxilla anteriorly. Within the fossa orbitalis, the maxilla contacts the descending process of the prefrontal anteromedially, the palatine medially, the pterygoid posteromedially, and the postorbital posterolaterally, and broadly underlies the jugal, which results in a V-shaped suture located just lateral for the foramen supramaxillare. The foramen is developed singularly on the right side, but is doubled on the left. In either case, the foramina are connected to a canal, that runs below the surface of the orbit and connects to a network of sub-canal that feed numerous nutritive foramina that are dispersed across the ventral side of the maxilla (Fig. 2B). The maxilla forms triturating surfaces that broaden posteriorly, as in *Stygiochelys estesi* (Gaffney and Hiatt 1971), *Eubaena cephalica* (Gaffney 1972; Rollot et al. 2018), *Boremys pulchra* (Brinkman and Nicholls 1991), *Goleremys mckennai* (Hutchison 2004), *Saxochelys gilberti* (Lyson et al. 2019), and *Palatobaena* spp. (Archibald and Hutchison 1979; Lyson et al. 2009; Lyson et al. 2021). Anteriorly, the triturating surface bears a distinct lingual ridge that delineates a broad tongue groove. The medial margin of the triturating surface is slightly thickened, but does not form a distinct ridge, much as in *Eubaena cephalica* (Gaffney 1972; Rollot et al. 2018). In ventral view, the maxilla contacts the premaxilla anteriorly, the vomer anteromedially, the palatine medially and posteromedially, and the pterygoid posteriorly.

Palatine. The palatine is a laminar bone that forms most of the foramen palatinum posterius and the posterior half of the foramen orbito-nasale (Fig. 2B). The palatine contacts the prefrontal anterodorsally, the vomer medially along a straight suture for most of its length, the maxilla ventrolaterally, and the pterygoid posteriorly.

The palatine only contributes minorly to the triturating surface. A contact with the jugal is absent, which differs from the condition observed in *Eubaena cephalica* (Rollot et al. 2018). The right palatine has a short contact with the descending process of the right parietal within the interorbital fossa, but such a contact is not present on the left side of the skull.

Vomer. The vomer is a single, elongated, and narrow bone (Fig. 2). The vomer floors the posterior part of the nasal cavity and forms the medial wall of the internal nares. The vomer contacts the premaxilla anteriorly, the maxilla anterolaterally, the prefrontal dorsolaterally, and the pterygoid posteriorly. The vomer also contacts the palatine laterally for most of its length, which prevents the latter from contacting its counterpart. The dorso-lateral processes of the vomer for articulation with the descending process of the prefrontals are very low, nearly nonexistent. Dorsally, a narrow sulcus vomeri is apparent along the posterior half of the bone.

Pterygoid. The pterygoids are well preserved with the exception of minor cracks. The anterior half of the pterygoid contacts the vomer anteromedially, the palatine anteriorly, the maxilla anterolaterally, and the jugal anterodorsolaterally (Fig. 2B, C, E). The pterygoid forms a reduced anterior process that barely protrudes between the vomer and palatine and extends only to the level of the posterior margin of the foramen palatinum posterius (Fig. 2B). Such a reduced anterior process contrasts with the elongate process of pleurosternids (Evers et al. 2020; Rollot et al. 2021) and early branching baenids (Evers et al. 2021; Rollot et al. 2022a; Rollot et al. 2022b), but resembles the condition of more derived baenids (Gaffney and Hiatt 1971; Gaffney 1972; Archibald and Hutchison

1979; Brinkman 2003; Hutchison 2004; Lyson and Joyce 2009a; Lyson and Joyce 2009b; Lyson and Joyce 2010; Lively 2015; Lyson et al. 2019; Lyson et al. 2021). The pterygoid forms a minor portion of the foramen palatinum posterius, which is apparent within its posterolateral corner. The pterygoid forms a well-defined external pterygoid process (Fig. 2C, E). The well-developed vertical flange has a broad contact with the overlying postorbital. The posterior half of the pterygoid has an elongate contact with the parabasisphenoid medially and the quadrate laterally (Figs 2B, 4). The pterygoid also contacts the basioccipital posteromedially for most of the length of the latter bone as in other baenids (Gaffney and Hiatt 1971; Gaffney 1972; Archibald and Hutchison 1979; Brinkman and Nicholls 1993; Brinkman 2003; Hutchison 2004; Lipka et al. 2006; Lyson and Joyce 2009a; Lyson and Joyce 2009b; Lively 2015; Lyson et al. 2019; Lyson et al. 2021; Rollot et al. 2022a; Rollot et al. 2022b) but which contrasts with the condition observed in pleurosternids (Evans and Kemp 1976; Gaffney 1979; Rollot et al. 2021). Posteriorly, the pterygoid forms a deep pterygoid fossa and the anterolateral half of the basioccipital tubercle. Within the lower temporal fossa, the pterygoid contacts the descending process of the parietal anterodorsally, the epipterygoid dorsally, and the prootic posterodorsally behind the foramen nervi trigemini, of which it forms the posterior margin (Fig. 3). The preserved portion of the pterygoid shows that the crista pterygoidea was likely low, but this area is difficult to assess given the shearing that is apparent in this area. Within the cavum acustico-jugulare, the pterygoid contacts the prootic anteriorly and anteromedially, the quadrate laterally, the exoccipital and basioccipital posteromedially. A contact with the processus

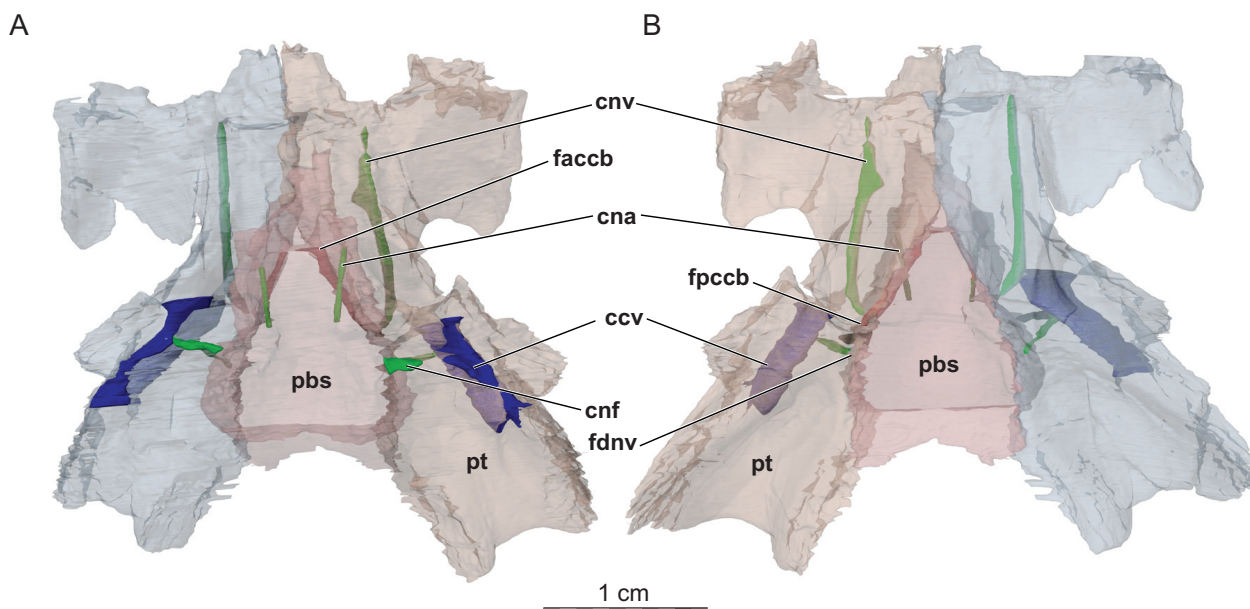


Figure 4. Three-dimensional renderings of the parabasisphenoid and the left and right pterygoids of the skull of *Denazinemys nodosa* (DMNH EPV.64550). **A.** Dorsal view and **B.** Ventral view of the bones rendered transparent showing the internal carotid artery and facial nerve systems. Abbreviations: ccv, canalis cavernosus; cna, canalis nervus abducentis; cnf, canalis nervus facialis; cnv, canalis nervus vidianus; faccb, foramen anterius canalis carotici basisphenoidalis; fdnv, foramen distalis nervi vidiani; fpccb, foramen posterius canalis carotici basisphenoidalis; pbs, parabasisphenoid; pt, pterygoid.

interfenestralis of the opisthotic was likely present dorso-medially as well, but can only partially be observed on the right side because of the shearing that affects the skull. The canalis cavernosus is mostly formed by the pterygoid and the prootic only forms the dorsal margin of the canal (Fig. 4). The foramen cavernosum is formed by the pterygoid and prootic and leads into the sulcus cavernosus anteriorly, which is formed by the pterygoid laterally and ventrally and minor contributions of the parabasisphenoid medially.

A short, anteroposteriorly oriented groove is located at about mid-length along the suture between the pterygoid and parabasisphenoid (Fig. 2B). This groove is inferred to have housed the internal carotid artery and two foramina can be identified along its posterolateral and anterior margins (Fig. 4). The posterolateral foramen is the foramen distalis nervi vidiani, which serves as a passage for the vidian nerve from the canalis pro ramo nervi vidiani to the carotid groove (Fig. 4). The foramen distalis nervi vidiani is formed by the pterygoid only, albeit located just lateral to the pterygoid-parabasisphenoid suture. The anterior foramen is the foramen posterius canalis carotici interni, which leads into the canalis caroticus internus. Just anterolateral to the foramen posterius canalis carotici interni, the canalis nervus vidianus bifurcates from the canalis caroticus internus and extends anteriorly through the pterygoid. The canalis nervus vidianus can be traced anteriorly close to the level of the suture between the pterygoid and palatine, just posterior to the foramen palatinum posterius, but crushing of the skull prevents us to determine the exact location and bony contributions to the foramen anterius canalis nervi vidiani. The canalis caroticus internus becomes the canalis caroticus basisphenoidalis just anterior to the split between the former canal and the canalis nervus vidianus, and extends anteromedially through the parabasisphenoid. The canalis caroticus basisphenoidalis joins the sella turcica by means of the foramen anterius canalis carotici basisphenoidalis, which is formed by the parabasisphenoid. The canalis caroticus lateralis, when present, typically extends anteriorly along the pterygoid-parabasisphenoid suture and joins the sulcus cavernosus. In DMNH EPV.64550, we are not able to identify any canal in this position, and the canalis caroticus lateralis is, therefore, considered absent in *Denazinemys nodosa*. The circulatory pattern of *Denazinemys nodosa* is overall very similar to that of *Eubaena cephalica* (Rollot et al. 2018), with the exception that the foramen distalis nervi vidiani is not ventrally exposed in *Eubaena cephalica*.

Epipterygoid. The epipterygoid is a small, rod-like bone, which is located anteroventral to the trigeminal foramen, but does not contribute to its formation (Figs 2B, C, E, 3). A notable ascending process is lacking. The epipterygoid contacts the pterygoid medially and ventrally and the parietal dorsally and anteriorly. A minor concavity at its posterior end marks remnants of the palatoquadrate cartilage (see Discussion for the known distribution of epipterygoids among baenodds).

Quadrate. The quadrate is a large bone that forms most of the middle ear, in particular the evenly rounded

cavum tympani, the medial aspects of the antrum postoticum, the posteriorly open incisura columella auris, the lateral wall of the cavum acustico-jugulare, and the mandibular condyle (Fig. 2). Within the upper temporal fossa, the quadrate contacts the prootic anteromedially, the supraoccipital medially, the opisthotic posteromedially, and the squamosal posteriorly (Fig. 2A). The contact between the quadrate and supraoccipital is extensive and prevents the opisthotic from contributing to the margin of the foramen stapedio-temporale, as in *Eubaena cephalica* (Rollot et al. 2018) and *Saxochelys gilberti* (Lyson et al. 2019), but not *Chisternon undatum* (Gaffney 1972) and *Stygiochelys estesi* (Gaffney 1972), in which the contact is either extremely reduced or completely absent, respectively. On the lateral skull surface, the quadrate forms a broad, C-shaped suture with the quadratojugal anteriorly and contacts the squamosal dorsally (Fig. 2E). In ventral view, the quadrate has an elongate contact with the posterior process of the pterygoid medially (Fig. 2B). An anterior contact with the epipterygoid is hindered by a rounded cavity that likely held the remnants of the palatoquadrate cartilage. The mandibular condyles are small, ventrally oriented, and consist of two concave facets, the lateral of which is larger than the medial one. The foramen stapedio-temporale is formed by the quadrate laterally, the prootic anteriorly, and the supraoccipital laterally and posterolaterally (Fig. 2A). The opisthotic has a minor contribution to the right canalis stapedio-temporalis internally, much as in *Eubaena cephalica* (Rollot et al. 2018). The quadrate and prootic also jointly form the processus trochlearis oticum, which is developed as a relatively broad ridge-like protrusion. Within the cavum acustico-jugulare, the quadrate contacts the prootic anterodorsomedially, the opisthotic posterodorsomedially, and the pterygoid ventromedially, and forms the lateral margin of the aditus canalis stapedio-temporalis.

Prootic. The prootic forms the medial half of the processus trochlearis oticum and the medial wall of the canalis stapedio-temporalis (Fig. 2A). The prootic is excluded from the lateral margin of the foramen nervi trigemini by a contact of the parietal with the pterygoid (Fig. 3B), but contributes to the foramen internally within the skull (Fig. 3C), as has previously been observed for *Lakotemys australodakotensis* (Rollot et al. 2022a). The prootic contacts the parietal anteriorly, the supraoccipital posteromedially, the quadrate posteriorly and posterolaterally, the pterygoid ventrolaterally, and the parabasisphenoid ventromedially. The prootic forms the anterior half of the cavum labyrinthicum, canalis semicircularis anterior, and canalis semicircularis horizontalis, and the anterior margin of the hiatus acusticus and fenestra ovalis. We are not able to determine if the fenestra ovalis is fully surrounded by bone because of damage to the processus interfenestralis of the opisthotic on both sides. The prootic also forms the dorsal margin of the canalis cavernosus and foramen cavernosum. The canalis nervus facialis extends laterally through the prootic from the fossa acustico-facialis and joins the medial margin of the

canalis cavernosus (Fig. 4). The geniculate ganglion, i.e. where the facial nerve splits into the vidian and hyoman-dibular nerves, is inferred to have been located within the canalis cavernosus. The canalis pro ramo nervi vidiani, which held the vidian nerve, extends ventromedially from the canalis cavernosus through the pterygoid and joins the carotid groove by means of the foramen distalis nervi vidiani. The vidian nerve is then inferred to have extended anteriorly alongside the internal carotid artery within the carotid groove into the canalis caroticus internus, and split from the latter to enter the canalis nervus vidianus just anterior to the foramen posterius canalis carotici interni. The canalis nervus vidianus is formed by the pterygoid.

Opisthotic. The opisthotics are damaged – the left lacks the processus interfenestralis and the right lacks most of the paroccipital process (Fig. 2A, B, F). The opisthotic forms the posterior margin of the hiatus acusticus and the posterior half of the cavum labyrinthicum, canalis semicircularis horizontalis, and canalis semicircularis posterior. Anteriorly, within the upper temporal fossa, the opisthotic contacts the supraoccipital medially and the quadrate laterally. A broad anterior contact with the prootic is hidden from dorsal view by a sheet of bone formed by the supraoccipital that laterally contacts the quadrate (Fig. 2A, F). The paroccipital process of the opisthotic forms the dorsal rim of the fenestra postotica, which is fully confluent with the foramen jugulare posterius, and contacts the exoccipital medially and squamosal laterally. The right opisthotic also slightly contributes to the posterior wall of the canalis stapedio-temporalis. Although the processus interfenestralis is absent on the left side and badly damaged on the right, we are able to assess most of its bony contributions. A contact with the pterygoid might have occurred ventrally, but the apparent contact on the right side seems to be the result of crushing. The foramen internum nervi glossopharyngei and foramen externum nervi glossopharyngei of the glossopharyngeal nerve (IX) are both preserved along the dorsal base of the processus interfenestralis. The processus interfenestralis forms the posterior margin of the fenestra ovalis but, as mentioned above (see Prootic), damage prevents us from determining if the fenestra ovalis was fully surrounded by bone. The processus interfenestralis also forms the dorsal margin of the foramen jugulare anterius, which is otherwise formed by the exoccipital and a small anterior contribution from the pterygoid. As preserved, the fenestra perilymphatica has a slit-like appearance, but this may be a result of compression.

Supraoccipital. The supraoccipital is complete, although some damage affects the crista supraoccipitalis, which is fragmented into two bony pieces (Fig. 2A, C, E, F). The supraoccipital forms the posteromedial tip of the skull roof, where it is only slightly exposed. The supraoccipital also forms the medial margin of the foramen stapedio-temporale, the dorsal margin of the hiatus acusticus, and the dorsal margin of the foramen magnum, and roofs the cavum cranii. The crista supraoccipitalis is moderately tall and thin and, despite some damage and slight displacement, appears to be complete, and the crista

barely protrudes beyond the level of the foramen magnum. The supraoccipital contacts the parietal anterodorsally, the prootic anterolaterally, the quadrate laterally, the opisthotic posterolaterally, and the exoccipital posteriorly. The supraoccipital roofs the cavum labyrinthicum and forms the posterior half of the canalis semicircularis anterior and the anterior half of the canalis semicircularis posterior. The foramen aqueducti vestibuli is not preserved.

Basioccipital. The basioccipital is an unpaired element that floors the posterior portion of the cavum cranii and forms the ventral margin of the foramen magnum and a low crista dorsalis basioccipitalis (Fig. 2B, F). In ventral view, the basioccipital is trapezoidal in shape and contacts the parabasisphenoid anteriorly and the posterior process of the pterygoid laterally for all its length. The parabasisphenoid, however, underlaps the anterior fifth of the basioccipital by means of a thin sheet of bone. Together with the pterygoid, the basioccipital forms two well-defined tubercula basioccipitale, which are buttressed from above by the exoccipital. The right exoccipital minutely contributes to the articular surface of the condylus occipitalis. The left exoccipital is damaged in this region, but a minor contribution seems plausible on this side as well. Two foramina basioccipitale are present on the ventral surface of the basioccipital, as in *Eubaena cephalica* (Rollot et al. 2018).

Exoccipital. The exoccipital forms the lateral wall of the cavum cranii, the lateral margin of the foramen magnum, the medial margin of the foramen jugulare anterius, and the medial wall of the recessus scalae tympani (Fig. 2A, F). The exoccipital closely approaches the condylus occipitalis and a minor contribution of the right exoccipital to the articular surface of the latter is visible. The same region is damaged for the left exoccipital and no contribution to the articular surface of the condylus occipitalis is visible. However, it seems plausible that a minor contribution was present on this side as well. The exoccipital contacts the supraoccipital dorsally, the opisthotic laterally, the pterygoid ventrolaterally and the basioccipital ventrally, and buttresses the tuberculum basioccipitale from above (Fig. 2F). Along the braincase wall, we are able to identify 4 small foramina on the medial surface of the exoccipital, but only one larger foramen on its external surface. Cranial nerves X, XI, and XII typically branch off the brain as multiple small branches that merge shortly after having left the brain (Soliman 1964; Kardong 2012). The arrangement observed in DMNH EPV.64550 perfectly illustrates this condition, in which 4 small hypoglossal nerve branches (XII) depart from the brain to enter the exoccipital through separate foramina, and merge within the latter bone to exit the skull by means of a single, enlarged foramen nervi hypoglossi. Unlike in *Eubaena cephalica* (Rollot et al. 2018), the exoccipitals and the basioccipital are clearly distinguishable in the CT scan, which suggests that this specimen likely belongs to a skeletally immature specimen.

Parabasisphenoid. The parabasisphenoid is a thick triangular bone that forms the ventral margin of the hiatus acusticus, the medial wall of the sulcus cavernosus,

and most of the floor of the cavum cranii (Figs 2B, 4). Ventrally, the parabasisphenoid broadly contacts the pterygoids laterally along straight sutures. The posterior contact with the basioccipital is transverse, but a surficial lamina of bone, likely homologous to the parasphenoid (Sterli et al. 2010), underlaps the basioccipital to yield a concavely curved suture. The parabasisphenoid otherwise contacts the prootic dorsolaterally. The rostrum basisphenoidale is flat and short, only representing about one third of the total length of the parabasisphenoid, and contacts the pterygoids ventrally (Fig. 2B). At the posterior limit of the rostrum basisphenoidale is the sella turcica, in which the two foramina arteria carotica interna are located (Fig. 4). The sella turcica is overhung by a tall dorsum sellae. Distinct retractor bulbi pits are not apparent. The short, wing-like clinoid processes, as seen in the 3D models, partially roof the sulcus cavernosus. The foramen posterius canalis nervi abducentis is located on the dorsal surface of the parabasisphenoid at about mid-length between the dorsum sellae and the posterior end of the bone. The canalis nervus abducentis is mostly formed by the parabasisphenoid, but the pterygoid forms the lateral margin of the right foramen arteria carotica interna, as in the pleurosternid *Pleurosternon bullockii* (Evers et al. 2020) and the early branching baenid *Arundelemys dardeni* (Evers et al. 2021). Ventrally, the parabasisphenoid forms the medial portion of most of the carotid groove, but the foramen posterius canalis carotici interni is only formed by the pterygoid, albeit extremely close to the pterygoid-parabasisphenoid suture. Shortly anterior to the foramen posterius canalis carotici interni, the canalis caroticus internus becomes the canalis caroticus basisphenoidalis, which is formed by the parabasisphenoid. The basiptyergoid process is absent.

Shell. The shell associated with the skull was reassembled, as it was disarticulated during burial. Although some bones are missing, those that remain are preserved in three dimensions (Figs 5, 6). The surface of the carapace is covered by numerous welts (Fig. 5A). Elongate welts are oriented anteroposteriorly, roughly parallel to the sagittal plane, and most densely arranged over the medial half of the costals. Most sulci can be traced with ease, with the exception of those in the nuchal area, which are difficult to discern. The shell is highly vaulted. The posterior margin of the carapace is scalloped and exhibits a broad pygal notch. The anterior margin is lightly scalloped as well. The skin-scutum sulcus runs along the margins of the visceral side of both carapace and plastron (Fig. 6).

The carapace likely consists of a nuchal, preneural, nine neural elements of which eight are interpreted as regular and one as supernumerary, a suprapygal, a pygal, eight pairs of costals, and twelve pairs of peripherals (Fig. 5A). The preneural and neural I have four sides and only contact costal I laterally. Neurals II–V are elongate, hexagonal, and have short anterolateral sides that contact the anterior costal. Neurals VI and VII are missing, but can be inferred to have been short, hexagonal elements. The surrounding elements suggest the presence of a short,

irregular neural that was squeezed between neurals VII and neural VIII, which we do not count as a full element of the neural series. Neural VIII is an elongate hexagon with short anterolateral sides. The suprapygal is crescent-shaped, has four contacts, and is about the size of the preneural. The pygal is much broader than long, forms much of the posterior margin of the shell, and exhibits a deep anterior concavity for articulation with the suprapygal. As in most baenids, costals I–IV are large elements, while costals V–VIII are reduced in size. Costal I is in contact with four peripherals and its rib inserts laterally into the fourth peripheral element. As the first costal rib seems to insert into the third peripheral universally among turtles (Joyce and Rollet 2020), this suggests that the small peripherals at the very front of the series are supernumerary elements relative to other turtles. To avoid propagating incorrect homology, we highlight the first pair of elements as supernumerary peripherals and start counting the regular peripheral series with the second element. As other *Denazinemys nodosa* shells only display three peripherals associated with costal I (Wiman 1933; Lichtig and Lucas 2015), this could be used as evidence for a distinct species. However, as the shell of baenids often exhibits irregular bone or scute arrangements (e.g., Wiman 1933; Gaffney 1972; Joyce and Lyson 2015), we interpret this as an anomaly until it can be consistently demonstrated among additional individuals. A peripheral count of 12 is reported for numerous baenids in the literature (e.g., Gaffney 1972) and is used as character evidence in baenid trees going back to Gaffney and Meylan (1988), but we find it doubtful that this characteristic exists in the first place (see Discussion below). The nuchal is a narrow, trapezoidal element that laterally contacts peripheral I on the right side only. The supernumerary peripheral is a small, triangular element that posteriorly contacts costal I on the left side only. As the axillary buttress reaches the very front of the shell, the posterior margin of peripheral I is V-shaped in cross section. The inguinal buttress is only partially preserved, but the posterior peripherals, at least peripherals VIII–XI, are flat in cross section.

The carapace was likely covered by five vertebrals, one pair of prepleurals, four pairs of pleurals, and twelve pairs of regular marginals, and one pair of supernumerary marginals (Fig. 5A). We are not able to determine the number of cervicals beyond one. Vertebral I is constricted anteriorly by the adjacent prepleurals. Vertebrals II–IV have six contacts, but are mostly square to rectangular in shape. Vertebral V is constricted posteriorly by marginals XII and contributes to the margin of the shell. The intervertebral sulci are located above neural I, III, V, and VIII, while the interpleural one are located above costals II, IV, VI, and VIII.

The plastron consists of an entoplastron and paired epi-, hyo-, meso-, hypo-, and xiphiplastra (Figs 5B, 6B). The anterior plastral lobe is short and triangular, the bridge region broad, and the posterior lobe short, but squared. The entoplastron is diamond-shaped in external view, but notably T-shaped in visceral view due to the development of a broad posterior entoplastral process. The mesoplastra

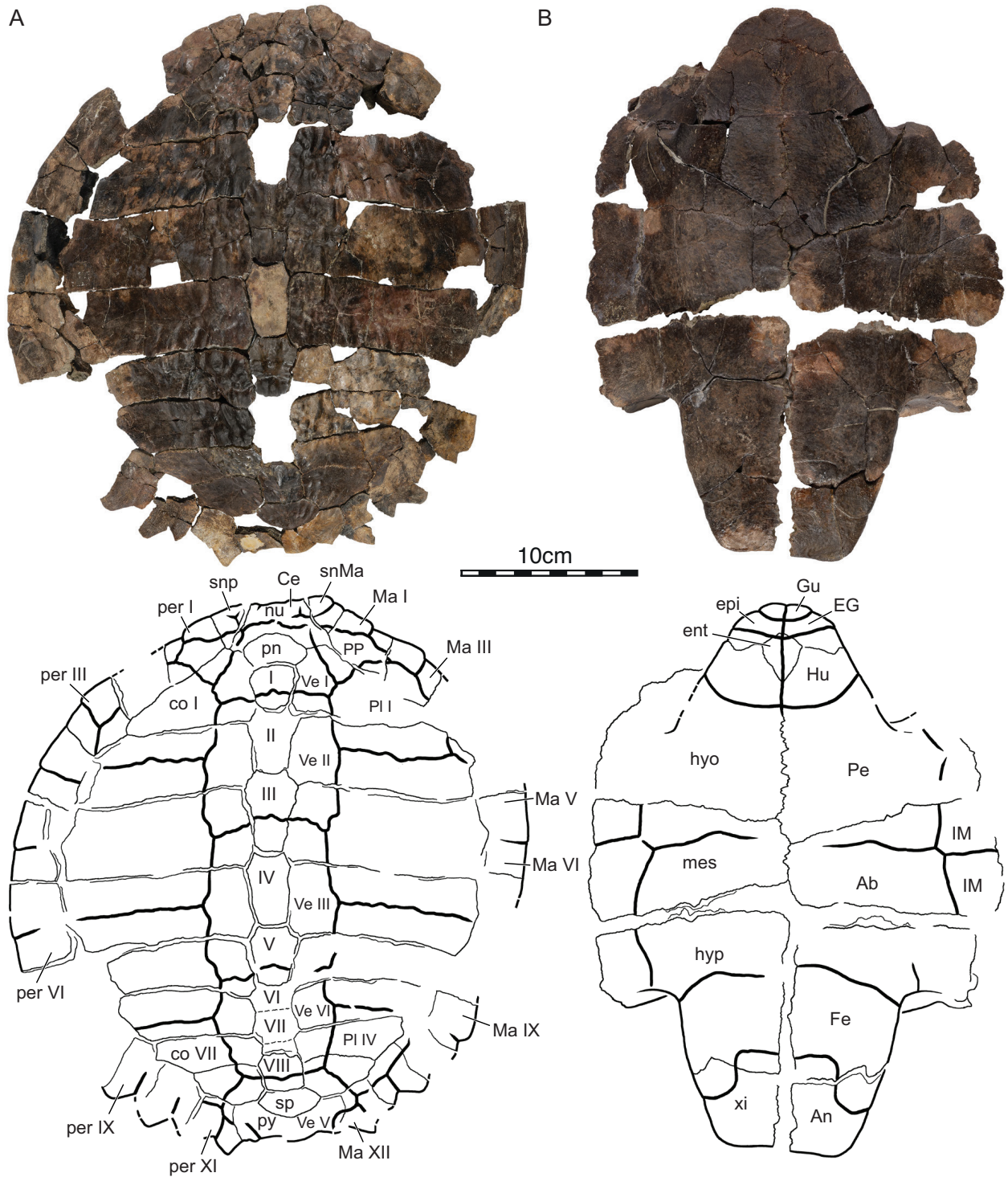


Figure 5. Photographs and interpretive line drawings of the exterior of the shell of DMNH EPV.64550. **A.** Dorsal view of the carapace, and **B.** Ventral view of the plastron. Abbreviations: Ab, abdominal scute; An, anal scute; Ce, cervical scute; co, costal; EG, extragular scute; ent, entoplastron; epi, epiplastron; Fe, femoral scute; Gu, gular scute; Hu, humeral scute; hyo, hyoplastron; hyp, hypoplastron; IM, inframarginal scute; Ma, marginal scute; mes, mesoplastron; nu, nuchal; Pe, pectoral scute; per, peripheral; PI, pleural scute; pn, preneural; PP, prepleural; py, pygal; snMa, supernumerary marginal; snp, supernumerary peripheral; sp, suprapygale; Ve, vertebral scute; xi, xiphiplastron. Neurals are given in Roman numerals.

show a broad, slightly asymmetric midline contact as in *Compsemys* (Gaffney, 1972). The hyoplastra form large, winglike axillary buttresses that reach anteriorly to contact the posterior corner of peripheral I and then articulate with nearly the full width of costal I from below.

The hypoplastra similarly form large, wing-like inguinal buttresses that articulate with a broad ridge formed at the contact of costals V and VI.

The plastron was likely once covered by paired gulars, extragulars, humerals, pectorals, abdominals, femorals,

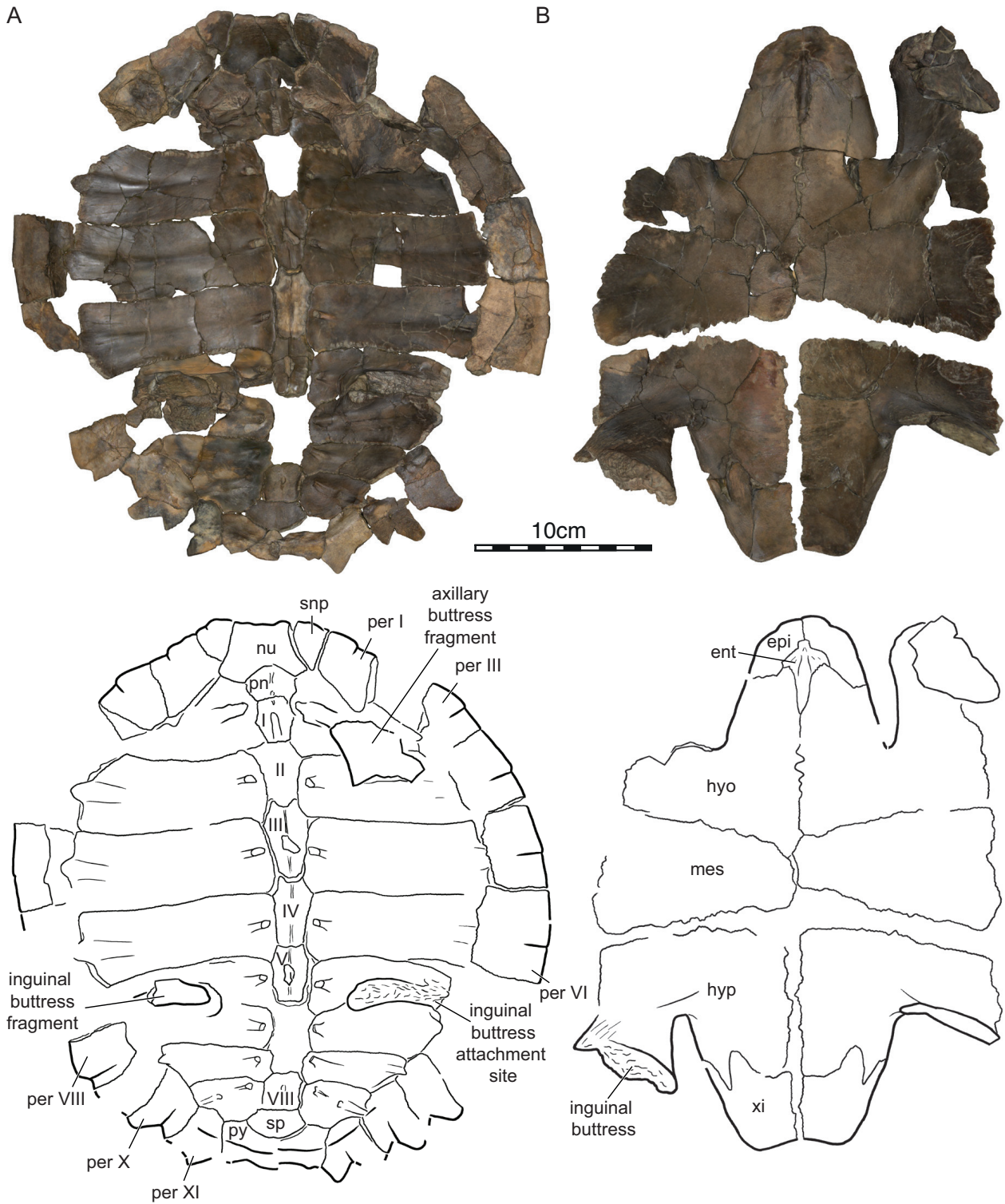


Figure 6. Three-dimensional renderings and interpretative drawings of the shell of DMNH EPV.64550 showing the inner part of the shell in **A**. Ventral view of the carapace, and **B**. Dorsal view of the plastron. Abbreviations: ent, entoplastron; epi, epiplastron; hyo, hyoplastron; hyp, hypoplastron; mes, mesoplastron; nu, nuchal; per, peripheral; pn, preneural; py, pygal; snp, supernumerary peripheral; sp, suprapygal; xi, xiplastron. Neurals are given in Roman numerals.

and anals (Fig. 5B). The gulars and extragulars are relatively small elements that are oriented transversely and have midline contacts with their counterparts. The extragular only barely covers the most anterior tip of the entoplastron. The humeral-pectoral sulcus is rounded and

located far behind the entoplastron. The femoral-anal sulcus is omega-shaped and crosses onto the hypoplastron. The exact number of inframarginals is not clear, but a complete series was certainly present that separated the carapacial scutes from contacting the plastral ones.

Discussion

Supernumerary peripherals in baenids

In the vast majority of turtles, 11 pairs of peripherals are developed, of which elements III through X are normally associated with costal ribs I through VIII. Notable exceptions are basal turtles from the Triassic, which often exhibit additional peripheral elements, although the exact count remains unclear, and kinosternids and carettochelyids, which universally exhibit only 10 pairs (Joyce 2007). The historic literature sometimes implies that baenids may have had 12 pairs of peripherals (e.g., Hay 1908; Gaffney 1972). Gaffney and Meylan (1988), therefore, more recently suggested that the presence of 12 peripherals may be a synapomorphy for the clade Baenodda (their Baenodd). This character was retained in more recent phylogenetic analyses (e.g., Lyson and Joyce 2009a; Lively 2015; Joyce et al. 2020b; Rollot et al. 2022b). The unambiguous presence of 12 peripheral elements in DMNH EPV.64550 through the inclusion of additional elements to the front of the shell led us to review the distribution of this character. The best previously documented occurrence of supernumerary peripherals is available for the Campanian *Plesiobaena antiqua*. Brinkman (2003) documented for this taxon four well preserved shells, of which three exhibit 11 pairs of peripherals, of which the two most anterior elements are fused. The fourth individual, by contrast, exhibits on the left side of the shell what looks to be a subdivided eleventh peripheral. The marginal count remains at twelve. Hay (1908) otherwise documented 12 pairs of peripherals for the holotypes of “*Baena hatcheri*” (currently *Eubaena hatcheri*), “*Baena clara*” (currently *Baena arenosa*), and “*Baena emiliae*” (currently *Baena arenosa*). In all cases, however, the associated figures indicate that sutures are not actually preserved in the posterior parts of the shell, although a count of 13 marginals appears plausible. Hay (1908) also depicts “*Baena riparia*” (currently *Baena affinis*) as having 12 pairs of peripherals, but the relevant part of the shell is not actually preserved. We are therefore unaware of any baenid specimen that unambiguously documents the presence of twelve pairs of peripherals. At first sight, this conclusion appears somewhat surprising as baenids are extremely common in the fossil record, but this statement is put into perspective by the fact that baenids were riverine turtles with deterministic growth: smaller individuals with unfused shells typically disarticulate, which obscures their peripheral count, while adult specimens with better preservation potential exhibit fused shells. Our summary of the literature is insufficient to conclude that no baenid has twelve peripherals, but does highlight the fact that previous studies may have been guided by the presumption that twelve pairs may be present. We therefore deactivated the relevant character from our matrix and suggest that future research focus on this character.

Epipterygoid

The presence versus absence of a separately ossified epipterygoid is currently used as a character to resolve baenid relationships, but it remains unclear if the apparent variation is taxonomic, ontogenetic (as suggested by Brinkman (2003) based on variation seen in *Plesiobaena antiqua*), or the result of observational error. If variation is taxonomic, we would expect all, or at least most individuals of a species to display the same character state. If variation is ontogenetic (i.e., the result of fusion to a neighboring element), we would expect large specimens to consistently lack epipterygoids relative to younger individuals of the same species. Of course, it may also be possible that the epipterygoid only ossifies late in ontogeny. Finally, varying degrees of preservation could be the result of observational error, for instance, in that epipterygoids are incorrectly reported to be absent in crushed specimens, or that epipterygoids are apparent in CT scans, but look to be absent in external view of the same specimen. At present, we conclude that not enough data are available to resolve this question with confidence, but we suspect a mixture of all three factors.

Differences with BYU 19123

Lively (2016) provided figures and brief descriptions for two baenid skulls from the Kaiparowits Formation that he referred to *Denazinemys nodosa*. Although Lively (2016) was not able to observe many sutures in external view, we are able to confirm most of his observations for DMNH EPV.64550 using the μ CT scans available to us. However, we note some puzzling differences with BYU 19123, the second skull described by Lively (2016). First, while BYU 19123 has deep upper and lower temporal emarginations, those of DMNH EPV.64550 are relatively shallow. Second, while the orbits of DMNH EPV.64550 are oriented dorso-laterally, those of BYU 19123 are oriented more laterally. Third, while the parietal-frontal contact is oriented transversely in DMNH EPV.64550, it is oriented obliquely in BYU 19123. As a result, the parietals of DMNH EPV.64550 end bluntly and the frontals contact one another along their full length, but the parietals of BYU 19123 form enlarged anterior processes that protrude into the interorbital space and broadly hinder the frontals from contacting one another. Fourth, while DMNH EPV.64550 has jugals located just posteroventrally to the orbit, those of BYU 19123 are located posteriorly only. Fifth, while DMNH EPV.64550 has tall maxillae, those of BYU 19123 are notable slim. The depressor fossa behind the cavum tympani of DMNH EPV.64550 furthermore seems to be smaller than that of BYU 19123, but that appears to be the result of damage. The skull of DMNH EPV.64550 was found in close association among disarticulated shell elements referable to *Denazinemys nodosa* (see Geological Setting above). Notes on BYU localities from the Kaiparowits Formation are extremely limited to nonexistent, by contrast, preventing

confident association of the skull of BYU 19123 with the recovered shell material.

The morphological differences listed above suggest that the two skulls belong to two distinct species, thus questioning the attribution of one to *Denazinemys nodosa*. Although we are not able to further resolve this issue for the moment, we see two primary possibilities. On the one hand, as studies based on CT scans can retrieve sutures with confidence quite different from those apparent in external view (e.g., Rollet et al. 2022b), it is possible that the listed differences are errors in the interpretation of BYU 19123, perhaps amplified by differential damage to both specimens. If this is the case, attribution of either skull to *Denazinemys nodosa* is unproblematic. On the other hand, it is also possible that further study of BYU 19123 confirms the differences listed above, which either implies that the shell of *Denazinemys nodosa* is associated with two skull morphotypes, or that one of the two skulls simply does not belong to *Denazinemys nodosa*, even if it was found in close proximity to a diagnostic shell. The resulting parataxonomic conundrum (i.e., taxonomic instability caused by uncertain attributions of separate body parts to the same taxon) is typical for turtles, including baenids (e.g., Lyson and Joyce 2009a, b; Lyson et al. 2011). In contrast to BYU 19123, which was collected at least four decades ago without detailed field notes, we can personally vouch for the fact that the skull of DMNH EPV.64550 was found among the elements of a single shell, which resembles the holotype of *Denazinemys nodosa*, at a locality that otherwise did not yield abundant remains of other turtles. In addition, an unpublished skull found associated with another *Denazinemys nodosa* shell (RAM 31605 A.A. Farke, pers comm.) broadly confirms the morphology of DMNH EPV.64550. We, therefore, conclude this association to be the correct one until proven otherwise, with ambiguous association of skull and shell in BYU 19123.

Stratigraphic range of *Denazinemys nodosa*

Denazinemys nodosa was originally described based on a near complete shell from what is now classified as the Late Campanian De-na-zin Member at the top of the Kirtland Formation of New Mexico (Gilmore 1916; Sullivan and Lucas 2003, 2006). Soon after, a large sample of additional specimens was described by Wiman (1933), of which many likely originate from the underlying Late Campanian Hunter Wash Member of the Kirtland Formation (Sullivan et al. 2013). Sullivan et al. (2013) reported on the presence of *Denazinemys nodosa* in the Late Campanian Fruitland Formation of New Mexico, which regionally underlies the Kirtland Formation, but specimens were not figured. The reported presence of complete shells, however, provides us with confidence that the referred specimens are diagnostic of *Denazinemys nodosa*. Numerous additional specimens have since been described from New Mexico, but all fit within this stratigraphic range (Lucas and Sullivan 2006; Sullivan et al.

2013; Dalman and Lucas 2016; Lichtig and Lucas 2017). Hutchison et al. (2013) and Lively (2016) more recently described complete, diagnostic shells from the Late Campanian Kaiparowits Formation of Utah, which extend to temporal range of *D. nodosa* approximately 1 million years older (see Geological Settings above). The currently known range for this taxon based on diagnostic material is therefore restricted to the Late Campanian within a time interval of approximately 2.5 Ma (~76–73.5 Ma).

A number of additional remains have otherwise been referred to *Denazinemys nodosa* as well, including specimens from the Middle to Late Campanian Aguja Formation of Coahuila and Texas (Tomlinson 1997; Lehman et al. 2019; López-Conde et al. 2020), the Middle Campanian Wahweap Formation of Utah (Holroyd and Hutchison 2016), and the Lower Campanian Menefee Formation of New Mexico (Lichtig and Lucas 2015). In all cases, the material is highly fragmentary and diagnosed as *Denazinemys nodosa* by the presence of welts on carapace elements. Welts indeed are a highly conspicuous characteristic of *Denazinemys nodosa*, but they also occur in other baenids, including *Boremys pulchra* (Lambe 1902) from the Late Campanian of Alberta and Montana (e.g., Brinkman and Nicholls 1991), *Boremys grandis* Gilmore, 1935 from the Late Campanian of New Mexico (e.g., Sullivan et al. 2013), and *Scabremys ornata* (Gilmore 1935) from the Late Campanian of New Mexico. As these turtles appear to be closely related (see Phylogeny below), we note that this characteristic appears to be a synapomorphy of a clade, not an autapomorphy of *Denazinemys nodosa*. Sullivan et al. (2013) highlighted differences in shell surface texture between the above-listed taxa based on the complete shells that were available to them but similarly concluded that fragmentary remains cannot be identified to the species level. We, therefore, question the attribution of all Lower to Middle Campanian turtle fragments with welted carapace ornamentation to this taxon and await descriptions of more complete specimens from these older units.

Phylogeny

Our phylogenetic analysis resulted in 35 equally parsimonious solutions with 361 steps (see Suppl. material 2 for list of common synapomorphies). The strict consensus tree finds *Denazinemys nodosa* as the immediate sister to *Eubaena cephalica* (Fig. 7). This late Maastrichtian taxon was already previously found in the vicinity (Lyson et al. 2011, 2016, 2021) or as the immediate sister to *Denazinemys nodosa* (Lively 2015). This contrasts the results of Sullivan et al. (2013), who retrieved *D. nodosa* nested within a clade of Eocene baenids. Our analysis recovers two synapomorphies uniting the latter two taxa: orbits that are smaller than the height of the maxilla (character 4, state 1) and the presence of swollen maxillae (character 10, state 1). We are somewhat surprised by this result, as we had informally noticed many shape similarities between these two taxa during this project. However, this also may be an artifact

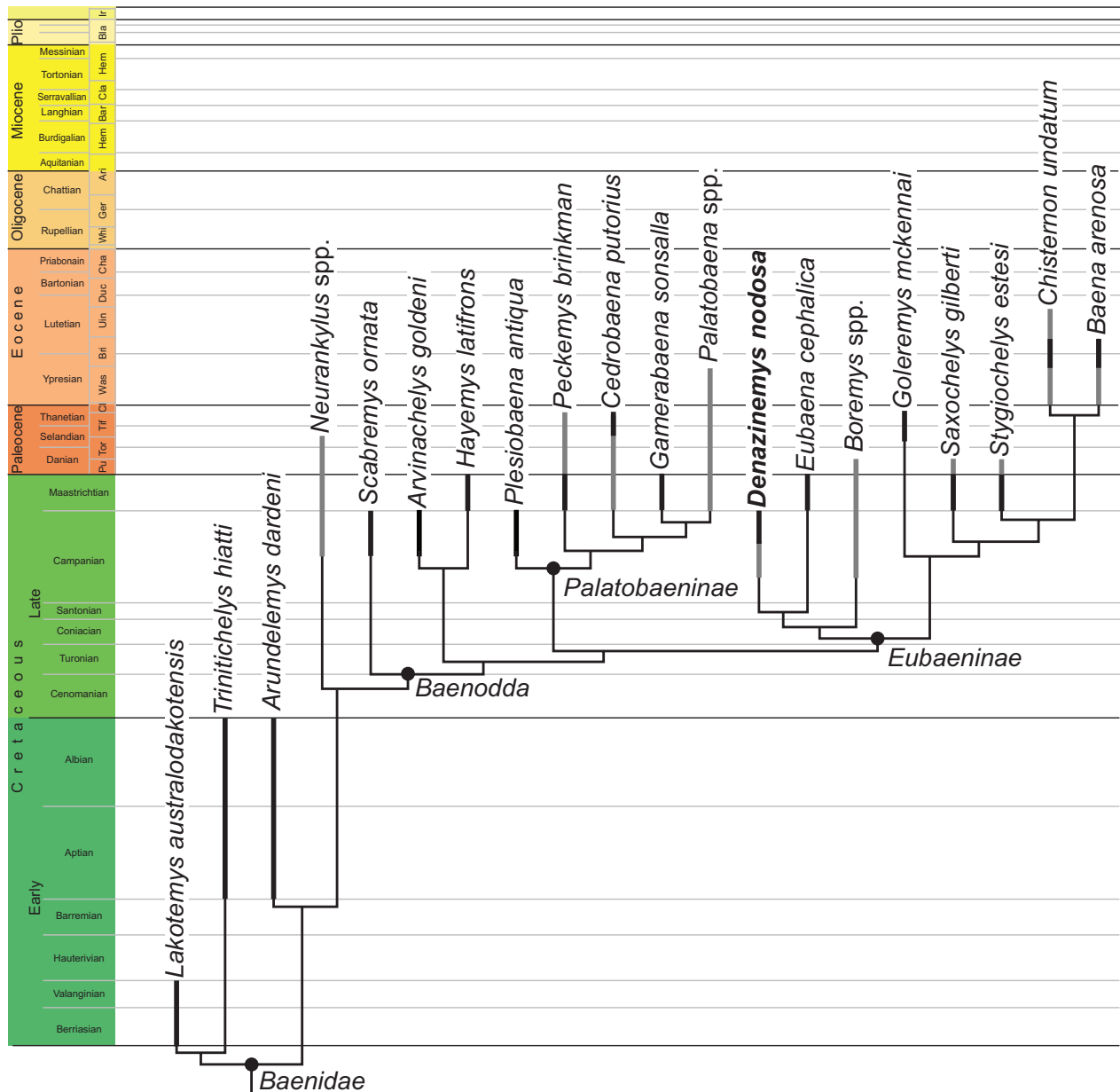


Figure 7. Strict consensus tree obtained in the phylogenetic analysis and mapped against the stratigraphic ranges for each taxon. Black lines indicate temporal distribution based on type material. Gray lines indicate temporal distribution based on referred material. For simplicity, taxa are referred to full time bins (i.e., the entire Maastrichtian or the entire late Campanian).

of sampling, as CT scans are also available for *Eubaena cephalica* (Rollot et al. 2018). Our hypothesis predicts that the shell of *Eubaena cephalica* should broadly resemble that of *Denazinemys nodosa*, but no shell material is known from the Maastrichtian that replicates the unique surface texture.

The sister group relationship of *Denazinemys nodosa* relative to *Eubaena cephalica* raises the question if the former may be ancestral to the latter. Although *Denazinemys nodosa* is thought to be restricted to the south-central portion of Laramidia and *Eubaena cephalica* to the north-central portion, we do not believe biogeography provides particularly strong evidence for or against this idea. However, our analysis indicates that *Denazinemys nodosa* has four autapomorphies, which would need to be secondarily lost if the latter is ancestral

to *Eubaena cephalica*, in particular the absence of a posterodorsal extension of the quadratojugal that crests the cavum tympani (character 19, state 1), presence of an epipterygoid (character 27, state 0), large mandibular condyles (character 60, state 1), and an anteriorly convex nasal/frontal suture (character 67, state 1). *Denazinemys nodosa*, therefore, does not fulfill the criteria of an ancestral metataxon for the moment (sensu Archibald 1994).

Our analysis retrieves *Boremys* spp. as the sister group to the clade formed by *Denazinemys nodosa* and *Eubaena cephalica*, broadly, once again, replicating previous results (Lyson et al. 2011, 2016, 2021; Lively 2015; see Sullivan et al. 2013 for different results). Three synapomorphies, which are common to all most parsimonious trees, are apparent: distinct scalloping of posterior shell margin (character 32,

state 2), gulars that are as large as the extragulars (character 46, state 1), and an anteriorly scalloped shell (character 51, state 1). An additional feature that unites these taxa is the distinct shell sculpturing consisting of raised welts, but it was not retrieved as a synapomorphy in the analysis.

An interesting insight gained by our analysis is the placement of *Goleremys mckennai*. This late Paleocene taxon had variously been found in previous analyses as a eubaenine (Lyson and Joyce 2009a, b; Lively 2015), a palatobaenine (Lyson et al. 2016), or a wildcard taxon (Lyson and Joyce 2010; Lyson et al. 2019; Rollot et al. 2022b). We, too, had initially found *Goleremys mckennai* to be a wildcard/rogue taxon, but then noticed that this may perhaps be the result of inconsistent scoring. After adjustment of the scorings of four characters (see Materials and Methods), we would expect this taxon to have a more stable placement within eubaenines. We now retrieve *Goleremys mckennai* as the sister taxon to the clade formed by *Baena arenosa*, *Chisternon undatum*, *Saxochelys gilberti*, and *Stygiochelys estesi*. Our result replicates the results of Lyson and Joyce (2009a, b), but not Lively (2015). The common synapomorphies for this arrangement formed by *G. mckennai* include the absence of a prefrontal exposure on the skull roof (character 13, state 2), a maximum combined width of parietals greater than their length (character 63, state 1) and the occipital condyle only formed by the basioccipital (character 101, state 1).

Our analysis retrieves the following 9 common synapomorphies uniting eubaenines: the absence of a palatine contribution to the triturating surface (character 8, state 0; 0/1 for *Denazinemys nodosa*), a reduced splenial (character 29, state 1; unknown for *Denazinemys nodosa*), the presence of preneurals (character 35, state 1; 0/1 for *Denazinemys nodosa*), the presence of two or more cervical scutes (character 38, state 2), the vertebral length greater than its width (character 39, state 2), the presence of a nuchal scute (character 40, state 1), the presence of prepleural scutes (character 41, state 1), a small suprapygal size (character 87, state 1), and an internal carotid artery canal that is anteriorly ossified and a foramen distalis nervi vidiani that is ventrally exposed (character 99, state 1).

Data availability

The specimen described herein is available to the public at the Denver Museum of Nature & Science (DMNS), Denver, Colorado, an approved repository for specimens from Bureau of Land Management (BLM) lands. The CT data and the 3D mesh models generated from it are available at MorphoSource (<https://www.morphosource.org/projects/000483670>).

Author contributions

WGJ, TRL, and JJWS designed the study. GES segmented cranial CT data and exported 3D mesh

models. LCG produced and exported the 3D mesh models of the shell. WGJ illustrated the shell and assembled figures. GES and WGJ assembled character matrix and conducted phylogenetic analyses. GES, TRL, YR, JJWS, LCG and WGJ prepared the manuscript and contributed to editing.

Competing interests

The authors declare that they have no conflict of interest.

Financial support

This research was supported by a grant from the Swiss National Science Foundation to WGJ (SNF 200021_178780/1), as well as the National Science Foundation (NSF-DEB-1947025) to TRL.

Acknowledgements

Specimen DMNH EPV.64550 was discovered by Geoff Lee and collected by JJWS under Bureau of Land Management (USA) permit UT11-011GS. Thanks to Alan Titus and Scott Foss for assistance with permits and additional thanks to Alan Titus for logistical support within GSENM. The specimen was expertly prepared in the DMNH labs by Jim Englehorn under the supervision of Bryan Small and Heather Finlayson. Additional mechanical preparation and repair of the shell was undertaken by Salvador Bastien for this study. Rick Wicker (DMNH) is thanked for professional specimen photography. The Kaiparowits Plateau, where the specimen was collected, is now protected as part of Grand Staircase-Escalante National Monument and managed by the BLM, is part of the ancestral lands of the Nuwuvi (Southern Paiute), Núu-ágha-tuvu-pú (Ute), Diné (Navajo), and Puebloan peoples. We are also grateful to Spencer Lucas and Juliana Sterli, who provided helpful comments that improved the quality of the manuscript.

References

- Archibald JD (1994) Metataxon concepts and assessing possible ancestry using phylogenetic systematics. *Systematic Biology* 43(1): 27–40. <https://doi.org/10.1093/sysbio/43.1.27>
- Archibald JD, Hutchison JH (1979) Revision of the genus *Palatobaena* (Testudines, Baenidae) with the description of a new species. *Postilla* 177: 1–19.
- Beveridge TL, Roberts EM, Ramezani J, Titus AL, Eaton JG, Irmis RB, Sertich JJW (2022) Refined geochronology and revised stratigraphic nomenclature of the Upper Cretaceous Wahweap Formation, Utah, U.S.A. and the age of early Campanian vertebrates from southern Laramidia. *Palaeogeography, Palaeoclimatology, Palaeoecology* 591: 1–22. <https://doi.org/10.1016/j.palaeo.2022.110876>

- Brinkman DB (2003) Anatomy and systematics of *Plesiobaena antiqua* (Testudines: Baenidae) from the mid-Campanian Judith River Group of Alberta, Canada. *Journal of Vertebrate Paleontology* 23(1): 146–155. [https://doi.org/10.1671/0272-4634\(2003\)23\[146:AASOPA\]2.0.CO;2](https://doi.org/10.1671/0272-4634(2003)23[146:AASOPA]2.0.CO;2)
- Brinkman DB, Hart M, Janniczky H, Colbert M (2006) *Nichollsemys baieri* gen. et sp. nov., a primitive chelonoid turtle from the late Campanian of North America. *Paludicola* 5: 111–124.
- Brinkman DB, Nicholls EL (1991) Anatomy and relationships of the turtle *Boremys pulchra* (Testudines: Baenidae). *Journal of Vertebrate Paleontology* 11(3): 302–315. <https://doi.org/10.1080/02724634.1991.10011400>
- Brinkman DB, Nicholls EL (1993) The skull of *Neurankylus eximius* (Testudines: Baenidae) and a reinterpretation of the relationships of this taxon. *Journal of Vertebrate Paleontology* 13(3): 273–281. <https://doi.org/10.1080/02724634.1993.10011509>
- Brinkman DB, Aquillon-Martinez MC, De Leon Dávila CA, Janniczky H, Eberth DA, Colbert M (2009) *Euclastes coahuilaensis* sp. nov., a basal cheloniid turtle from the late Campanian Cerro del Pueblo Formation of Coahuila State, Mexico. *PaleoBios* 28: 76–88.
- Cope ED (1873) On the extinct Vertebrata of the Eocene of Wyoming, observed by the expedition of 1872, with notes on the geology. *United States Geological Survey of the Territories* 6: 545–649.
- Dalman SG, Lucas SG (2016) Frederic Brewster Loomis and the 1924 Amherst College paleontological expedition to the San Juan Basin, New Mexico. In: Sullivan RM, Lucas SG (Eds) *Fossil Record 5*, New Mexico Museum of Natural History and Science Bulletin 74, Albuquerque, NM, USA, 61–66. <https://doi.org/10.56577/SM-2016.397>
- Evans J, Kemp TS (1976) A new turtle skull from the Purbeckian of England and a note on the early dichotomies of cryptodire turtles. *Palaeontology* 19: 317–324.
- Evers SW, Rollot Y, Joyce WG (2020) Cranial osteology of the Early Cretaceous turtle *Pleurosternon bullockii* (Paracryptodira: Pleurosternidae). *PeerJ* 8: e9454. <https://doi.org/10.7717/peerj.9454>
- Evers SW, Rollot Y, Joyce WG (2021) New interpretation of the cranial osteology of the Early Cretaceous turtle *Arundelemys dardeni* (Paracryptodira). *PeerJ* 9: e11495. <https://doi.org/10.7717/peerj.11495>
- Fassett JE, Steiner MB (1997) Precise age of C33N-C32R magnetic-polarity reversal, San Juan Basin, New Mexico and Colorado. In: *Mesozoic geology and paleontology of the Four Corners Region: New Mexico Geological Society, Forty-eighth Annual Field Conference, October 1–4, 1997*, 48, 239–247. <https://doi.org/10.56577/FFC-48.239>
- Gaffney ES (1972) The systematics of the North American family Baenidae (Reptilia, Cryptodira). *Bulletin of the American Museum of Natural History* 147: 241–320.
- Gaffney ES (1975) A phylogeny and classification of the higher categories of turtles. *Bulletin of the American Museum of Natural History* 155: 387–436.
- Gaffney ES (1979) The Jurassic turtles of North America. *Bulletin of the American Museum of Natural History* 162: 91–135.
- Gaffney ES, Hiatt R (1971) A new baenid turtle from the Upper Cretaceous of Montana. *American Museum Novitates* 2443: 1–9.
- Gaffney ES, Meylan PA (1988) A phylogeny of turtles. In: Benton MJ (Ed.) *The Phylogeny and Classification of the Tetrapods, Volume 1*. Oxford: Clarendon Press, 157–219.
- Gilmore CW (1916) Description of two new species of fossil turtles, from the Lance Formation of Wyoming. *Proceedings of the United States National Museum* 50(2137): 641–646. <https://doi.org/10.5479/si.00963801.50-2137.641>
- Gilmore CW (1919) Reptilian faunas of the Torrejon, Puerco, and underlying Upper Cretaceous formations of San Juan County, New Mexico. *United States Geological Survey Professional Paper*, 119, 1–68. <https://doi.org/10.3133/pp119>
- Gilmore CW (1935) On the Reptilia of the Kirtland Formation of New Mexico, with descriptions of new species of fossil turtles. *Proceedings of the United States National Museum* 83(2978): 159–188. <https://doi.org/10.5479/si.00963801.83-2978.159>
- Goloboff PA, Farris JS, Nixon KC (2008) TNT: A free program for phylogenetic analysis. *Cladistics* 24(5): 774–786. <https://doi.org/10.1111/j.1096-0031.2008.00217.x>
- Hay OP (1908) *The Fossil Turtles of North America*. Washington, DC: Carnegie Institution of Washington. (Publications 75.) 568.
- Holroyd PA, Hutchison JH (2016) Fauna and setting of the *Adelolophus hutchisoni* type locality of the Upper Cretaceous (Campanian) Wahweap Formation of Utah. *PaleoBios* 33: 1–9. <https://doi.org/10.5070/P9331031196>
- Hutchison JH (2004) A new eubaenine, *Goleremys mckennai*, gen. et sp. N., (Baenidae: Testudines) from the Paleocene of California. *Bulletin of the Carnegie Museum of Natural History* 36: 91–96. [https://doi.org/10.2992/0145-9058\(2004\)36\[91:ANEGMG\]2.0.CO;2](https://doi.org/10.2992/0145-9058(2004)36[91:ANEGMG]2.0.CO;2)
- Hutchison JH, Knell MJ, Brinkman DB (2013) Turtles from the Kaiparowits Formation, Utah. In: Titus AL, Loewen MA (Eds) *At the top of the Grand Staircase: the Late Cretaceous of southern Utah*, Indiana University Press, Bloomington, 295–318.
- Joyce WG (2007) Phylogenetic relationships of Mesozoic turtles. *Bulletin - Peabody Museum of Natural History* 48(1): 3–102. [https://doi.org/10.3374/0079-032X\(2007\)48\[3:PROMT\]2.0.CO;2](https://doi.org/10.3374/0079-032X(2007)48[3:PROMT]2.0.CO;2)
- Joyce WG, Lyson TR (2015) A review of the fossil record of turtles of the clade Baenidae. *Bulletin - Peabody Museum of Natural History* 56(2): 147–183. <https://doi.org/10.3374/014.056.0203>
- Joyce WG, Parham JF, Anquetin J, Claude J, Danilov IG, Iverson JB, Kear B, Lyson TR, Rabi M, Sterli J (2020a) *Testudinata*. In: de Queiroz K, Cantino PD, Gauthier JA (Eds) *Phylogeny – A Companion to the PhyloCode*, Boca Raton, CRC Press, 1045–1048.
- Joyce WG, Rollot Y (2020) An alternative interpretation of *Peltochelys duchastelii* as a paracryptodire. *Fossil Record* 23: 83–93. <https://doi.org/10.5194/fr-23-83-2020>
- Joyce WG, Rollot Y, Cifelli RL (2020b) A new species of baenid turtle from the Early Cretaceous Lakota Formation of South Dakota. *Fossil Record (Weinheim)* 23(1): 1–13. <https://doi.org/10.5194/fr-23-1-2020>
- Joyce WG, Anquetin J, Cadena EA, Claude J, Danilov IG, Evers SW, Ferreira GS, Gentry AD, Georgalis GL, Lyson TR, Perez-Garcia A, Rabi M, Sterli J, Vitek NS, Parham JF (2021) A nomenclature for fossil and living turtles using phylogenetically defined clade names. *Swiss Journal of Palaeontology* 140(5): 1–45. <https://doi.org/10.1186/s13358-020-00211-x>
- Kardong KV (2012) *Vertebrates: Comparative anatomy, function, evolution*, 6th edn. McGraw-Hill, New York, 794 pp.
- Klein IT (1760) *Klassifikation und kurze Geschichte der vierfüßigen Thiere*. Lübeck, Jonas Schmidt.
- Lambe LM (1902) New genera and species from the Belly River Series (mid-Cretaceous). *Contributions to Canadian Paleontology* 3: 25–81.
- Lehman TM, Wick SL, Brink AA, Shiller TA II (2019) Stratigraphy and vertebrate fauna of the lower shale member of the Aguja Formation (lower Campanian) in West Texas. *Cretaceous Research* 99: 291–314. <https://doi.org/10.1016/j.cretres.2019.02.028>

- Lichtig AJ, Lucas SG (2015) Turtles of the Lower Eocene San Jose Formation, San Juan Basin, New Mexico. *New Mexico Museum of Natural History and Science Bulletin* 67: 161–177. <https://doi.org/10.56577/SM-2014.226>
- Lichtig AJ, Lucas SG (2017) Sutures of the shell of the Late Cretaceous-Paleocene baenid turtle *Denazinemys*. *Neues Jahrbuch für Geologie und Paläontologie. Abhandlungen* 283(1): 1–8. <https://doi.org/10.1127/njgpa/2017/0622>
- Lipka TR, Therrien F, Weishampel DB, Jamniczky HA, Joyce WG, Colbert MW, Brinkman DB (2006) A new turtle from the Arundel Clay facies (Potomac Formation, Early Cretaceous) of Maryland, U.S.A. *Journal of Vertebrate Paleontology* 26(2): 300–307. [https://doi.org/10.1671/0272-4634\(2006\)26\[300:ANTFTA\]2.0.CO;2](https://doi.org/10.1671/0272-4634(2006)26[300:ANTFTA]2.0.CO;2)
- Lively JR (2015) A new species of baenid turtle from the Kaiparowits Formation (Upper Cretaceous, Campanian) of southern Utah. *Journal of Vertebrate Paleontology* 35(6): e1009084. <https://doi.org/10.1080/02724634.2015.1009084>
- Lively JR (2016) Baenid turtles of the Kaiparowits Formation (Upper Cretaceous: Campanian) of southern Utah, USA. *Journal of Systematic Palaeontology* 14(11): 891–918. <https://doi.org/10.1080/14772019.2015.1120788>
- López-Conde OA, Chavarría-Arellano ML, Montellano-Ballesteros M (2020) Nonmarine turtles from the Aguja Formation (Late Cretaceous, Campanian) of Chihuahua, Mexico. *Journal of South American Earth Sciences* 102: 102668. <https://doi.org/10.1016/j.jsames.2020.102668>
- Lucas SG, Sullivan RM (2006) *Denazinemys*, a new name for some Late Cretaceous turtles from the Upper Cretaceous of the San Juan Basin, New Mexico. *New Mexico Museum of Natural History and Science Bulletin* 35: 223–227.
- Lyson TR, Joyce WG (2009a) A new species of *Palatobaena* (Testudines: Baenidae) and a maximum parsimony and Bayesian phylogenetic analysis of Baenidae. *Journal of Paleontology* 83(3): 457–470. <https://doi.org/10.1666/08-172.1>
- Lyson TR, Joyce WG (2009b) A revision of *Plesiobaena* (Testudines: Baenidae) and an assessment of baenid ecology across the K/T boundary. *Journal of Paleontology* 83(6): 833–853. <https://doi.org/10.1666/09-035.1>
- Lyson TR, Joyce WG (2010) A new baenid turtle from the Upper Cretaceous (Maastrichtian) Hell Creek Formation of North Dakota and a preliminary taxonomic review of Cretaceous Baenidae. *Journal of Vertebrate Paleontology* 30(2): 394–402. <https://doi.org/10.1080/02724631003618389>
- Lyson TR, Joyce WG, Knauss GE, Pearson DA (2011) *Boremys* (Testudines, Baenidae) from the latest Cretaceous and early Paleocene of North Dakota: An 11-million-year range extension and an additional K/T survivor. *Journal of Vertebrate Paleontology* 31(4): 729–737. <https://doi.org/10.1080/02724634.2011.576731>
- Lyson TR, Joyce WG, Lucas SG, Sullivan RN (2016) A new baenid turtle from the early Paleocene (Torrejonian) of New Mexico and a species-level phylogenetic analysis of Baenidae. *Journal of Paleontology* 90(2): 305–316. <https://doi.org/10.1017/jpa.2016.47>
- Lyson TR, Saylor JL, Joyce WG (2019) A new baenid turtle, *Saxochelys gilberti*, gen. et sp. nov., from the uppermost Cretaceous (Maastrichtian) Hell Creek Formation: Sexual dimorphism and spatial niche partitioning within the most speciose group of Late Cretaceous turtles. *Journal of Vertebrate Paleontology* 39(4): e1662428. <https://doi.org/10.1080/02724634.2019.1662428>
- Lyson TR, Petermann H, Toth N, Bastien S, Miller IM (2021) A new baenid turtle, *Palatobaena knellerorum* sp. nov. from the lower Paleocene (Danian) Denver Formation of South-Central Colorado, U.S.A. *Journal of Vertebrate Paleontology* 41(2): e1925558. <https://doi.org/10.1080/02724634.2021.1925558>
- Ramezani J, Beveridge TL, Rogers RR, Eberth DA, Roberts EM (2022) Calibrating the zenith of dinosaur diversity in the Campanian of the Western Interior Basin by CA-ID-TIMS U-Pb geochronology. *Scientific Reports* 12(1): 1–20. <https://doi.org/10.1038/s41598-022-19896-w>
- Roberts EM (2007) Facies architecture and depositional environments of the Upper Cretaceous Kaiparowits Formation, southern Utah. *Sedimentary Geology* 197(3–4): 207–233. <https://doi.org/10.1016/j.sedgeo.2006.10.001>
- Roberts EM, Sampson SD, Deino AL, Bowring SA, Buchwaldt R (2013) The Kaiparowits Formation: a remarkable record of late Cretaceous terrestrial environments, ecosystems, and evolution in western North America. In: Titus AL, Loewen MA (Eds) *At the Top of the Grand Staircase: the late Cretaceous of Southern Utah*, Indiana University Press, Bloomington, IN, USA, 85–106.
- Rollot Y, Lyson TR, Joyce WG (2018) A description of the skull of *Eubaena cephalica* (Hay, 1904) and new insights into the cranial circulation and innervation of baenid turtles. *Journal of Vertebrate Paleontology* 38(3): e1474886. <https://doi.org/10.1080/02724634.2018.1474886>
- Rollot Y, Evers SW, Joyce WG (2021) A redescription of the Late Jurassic (Tithonian) turtle *Uluops uluops* and a new phylogenetic hypothesis of Paracryptodira. *Swiss Journal of Palaeontology* 140(1): 1–30. <https://doi.org/10.1186/s13358-021-00234-y>
- Rollot Y, Evers SW, Cifelli RL, Joyce WG (2022a) New insights into the cranial osteology of the Early Cretaceous paracryptodiran turtle *Lakotemys australodakotensis*. *PeerJ* 10: e13230. <https://doi.org/10.7717/peerj.13230>
- Rollot Y, Evers SW, Pierce SE, Joyce WG (2022b) Cranial osteology, taxonomic reassessment, and phylogenetic relationships of the Early Cretaceous (Aptian-Albian) turtle *Trinitichelys hiatti* (Paracryptodira). *PeerJ* 10: e14138. <https://doi.org/10.7717/peerj.14138>
- Soliman MA (1964) Die Kopfnerven der Schildkröten. *Zeitschrift für Wissenschaftliche Zoologie* 169: 216–312.
- Sterli J, Müller J, Anquetin J, Hilger A (2010) The parabasisphenoid complex in Mesozoic turtles and the evolution of the testudinate basicranium. *Canadian Journal of Earth Sciences* 47(10): 1337–1346. <https://doi.org/10.1139/E10-061>
- Sullivan RM, Lucas SG (2003) The Kirtlandian, a new land-vertebrate “age” for the Late Cretaceous of Western North America: New Mexico Geological Society, 54th Field Conference, Guidebook, 369–377. <https://doi.org/10.56577/FFC-54.369>
- Sullivan RM, Lucas SG (2006) The Kirtlandian land-vertebrate “age”-faunal composition, temporal position and biostratigraphic correlation in the nonmarine Upper Cretaceous of western North America. *New Mexico Museum of Natural History and Science Bulletin* 35: 7–29.
- Sullivan RM, Jasinski SE, Lucas SG (2013) Re-Assessment of late Campanian (Kirtlandian) turtles from the Upper Cretaceous Fruitland and Kirtland Formations, San Juan Basin, New Mexico, USA. In: Brinkman DB, Holroyd PA, Gardner JD (Eds) *Morphology and Evolution of Turtles*, Dordrecht, Netherlands, Springer, 337–387. https://doi.org/10.1007/978-94-007-4309-0_20
- Tomlinson SL (1997) Late Cretaceous and Early Tertiary turtles from the Big Bend region, Brewster County, Texas [dissertation]. Lubbock, TX, Texas Tech University, 194 pp.
- Wiman C (1933) Über Schildkröten aus der oberen Kreide in New Mexico. *Nova Acta Regiae Societatis Scientiarum Upsaliensis* 9(5): 1–34.

Supplementary material 1

Mesquite file of the character matrix used for the phylogenetical analysis

Authors: Gaël E. Spicher, Joseph J. W. Sertich, Léa C. Girard, Walter G. Joyce, Tyler R. Lyson, Yann Rollot

Data type: Character matrix

Copyright notice: This dataset is made available under the Open Database License (<http://opendatacommons.org/licenses/odbl/1.0>). The Open Database License (ODbL) is a license agreement intended to allow users to freely share, modify, and use this Dataset while maintaining this same freedom for others, provided that the original source and author(s) are credited.

Link: <https://doi.org/10.3897/fr.26.102520.suppl1>

Supplementary material 2

Common synapomorphies mapped onto the strict consensus tree

Authors: Gaël E. Spicher, Joseph J. W. Sertich, Léa C. Girard, Walter G. Joyce, Tyler R. Lyson, Yann Rollot

Data type: Phylogenetic

Copyright notice: This dataset is made available under the Open Database License (<http://opendatacommons.org/licenses/odbl/1.0>). The Open Database License (ODbL) is a license agreement intended to allow users to freely share, modify, and use this Dataset while maintaining this same freedom for others, provided that the original source and author(s) are credited.

Link: <https://doi.org/10.3897/fr.26.102520.suppl2>

The Rhabdodontidae (Dinosauria, Ornithischia), an enigmatic dinosaur group endemic to the Late Cretaceous European Archipelago

Felix J. Augustin¹, Attila Ósi^{2,3}, Zoltán Csiki-Sava⁴

¹ Department of Geosciences, University of Tübingen, Hölderlinstraße 12, 72074 Tübingen, Germany

² Department of Palaeontology, Institute of Geography and Earth Sciences, ELTE Eötvös Loránd University, Pázmány Péter Sétány 1/C, Budapest 1117, Hungary

³ Hungarian Natural History Museum, Baross u. 13, Budapest 1088, Hungary

⁴ Faculty of Geology and Geophysics, University of Bucharest, 1 Nicolae Bălcescu Avenue, 010041 Bucharest, Romania

<https://zoobank.org/3168FE10-A551-4F73-8D99-0FE627D642C0>

Corresponding author: Felix J. Augustin (felix.augustin@uni-tuebingen.de)

Academic editor: Florian Witzmann ♦ Received 3 July 2023 ♦ Accepted 11 August 2023 ♦ Published 28 August 2023

Abstract

The Rhabdodontidae was one of the most important dinosaur groups inhabiting the Late Cretaceous European Archipelago. Currently, the clade comprises nine species within six genera, which have been found in southern France, northern Spain, eastern Austria, western Hungary and western Romania, ranging from the Santonian to the late Maastrichtian. Phylogenetic analyses consistently place the Rhabdodontidae at the very base of the iguanodontian radiation, whereas the in-group relationships of rhabdodontids are relatively poorly understood; nevertheless, the clade seems to have had a rather complicated biogeographical history. Generally, rhabdodontids were small- to medium-sized, probably habitually bipedal herbivores, characterised by a rather stocky build and a comparatively large, triangular skull. Several lines of evidence suggest that they were presumably gregarious animals, as well as selective browsers that fed on fibrous plants and occupied different ecological niches than sympatric herbivorous dinosaur clades. Moreover, the sympatry of at least two rhabdodontid taxa was rather common and can be explained, at least in some instances, by niche partitioning. While rhabdodontids disappeared prior to the K/Pg extinction event in Western Europe, they survived close to the end of the Cretaceous in Eastern Europe, where they were amongst the last non-avian dinosaurs still present before the end of the Cretaceous. In this paper, we provide an overview of the rhabdodontid taxonomic history, diversity, phylogenetic relationships and palaeobiogeographic history, as well as palaeoecology and extinction. In addition, we also highlight still open questions on each of these topics and suggest potential future research directions.

Key Words

Iguanodontia, Late Cretaceous European Archipelago, palaeobiogeography, palaeoecology, Rhabdodontidae, taxonomy

Introduction

Amongst the various dinosaur groups that inhabited the Late Cretaceous European Archipelago, the Rhabdodontidae is one of the most important, as these animals seem to have been exceptionally abundant and also relatively diverse, representing the most common medium-sized herbivores of Europe during the largest part of the later Late Cretaceous (Weishampel et al. 2004; Csiki-Sava et al. 2015). Currently, the Rhabdodontidae

comprises nine species within six genera, which have been found in southern France, northern Spain, eastern Austria, western Hungary and western Romania (Fig. 1) and which range in age from the Santonian to the late Maastrichtian (Matheron 1869; Bunzel 1871; Seeley 1881; Nopcsa 1902; Buffetaut and Le Loeuff 1991; Weishampel et al. 2003; Ósi et al. 2012; Godefroit et al. 2017; Párraga and Prieto-Márquez 2019; Augustin et al. 2022). The group looks back on a rather complicated taxonomic history that spans more than 150 years (see

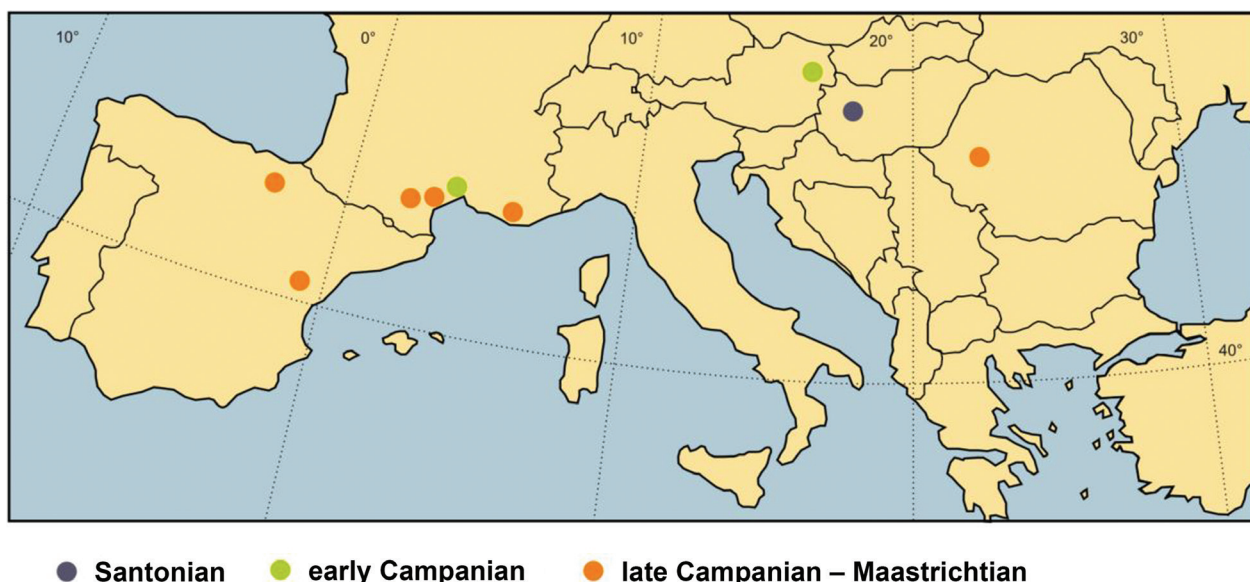


Figure 1. Distribution of the localities yielding remains of the Rhabdodontidae in Europe.

below), starting with the description of the eponymous *Rhabdodon* from southern France (Matheron 1869). In general, rhabdodontids were small- to medium-sized, probably habitually bipedal herbivores, characterised by a rather stocky build, with strong hind limbs, short forelimbs, a long tail and a comparatively large, triangular skull that tapers anteriorly and ends in a pointy snout (Weishampel et al. 1991, 2003; Garcia et al. 1999; Pincemaille-Quillevere 2002; Chanthasit 2010; Ósi et al. 2012).

Interestingly, unquestionable remains of rhabdodontids are currently only known from Upper Cretaceous (i.e. Santonian and younger) strata of Europe and, accordingly, the clade appears to have been endemic to the Late Cretaceous European Archipelago (Weishampel et al. 2003; Ósi et al. 2012; Godefroit et al. 2017; Párraga and Prieto-Márquez 2019; Augustin et al. 2022). A potential Early Cretaceous rhabdodontid from northern Spain, the unnamed ‘Vegagete ornithopod’, has been described recently and referred to the clade (Dieudonné et al. 2016, 2020; Yang et al. 2020), but according to a subsequent assessment, it might be a close relative of the Rhabdodontidae instead (Dieudonné et al. 2021). Within Ornithopoda, the Rhabdodontidae has consistently been found to be a basal clade of iguanodontians (see below), which, combined with their fossil record being limited to the Late Cretaceous, indicates a particularly long ghost lineage. Mapping their distribution and phylogenetic relationships offers intriguing insights into the complicated biogeographical history of these animals, but also that of the Late Cretaceous European Archipelago palaeofaunas overall (see below). Furthermore, several studies have focused on certain aspects of the palaeoecology of rhabdodontids, including their peculiar masticatory apparatus, potential niche partitioning, as well as their posture and locomotion (e.g. Weishampel et al. 2003; Bojar et al. 2010; Godefroit et al. 2017; Augustin et al. 2022; Ósi et al. 2022; Dieudonné et al. 2023).

In the past decades, a wealth of new rhabdodontid material has been discovered throughout Europe (e.g. Chanthasit 2010; Ósi et al. 2012; Godefroit et al. 2017) Párraga and Prieto-Márquez 2019; Augustin et al. 2022), which, combined with the renewed interest in this peculiar dinosaur group, has led to a dramatic increase of our knowledge on the Rhabdodontidae in recent years. This is well exemplified by the fact that three of the six genera currently recognised were named in the last decade (see below). Nevertheless, numerous new and, so far, undescribed specimens remain to be studied and several rhabdodontids still await taxonomic revision, likely leading to an even better understanding of rhabdodontids in the near future. The aims of this paper are to summarise the current state of the knowledge concerning their taxonomic history and diversity, phylogenetic relationships and palaeobiogeographic history, as well as their palaeoecology and extinction. Moreover, we highlight open questions on each of these topics and suggest potential future directions. Therefore, this overview is intended as a baseline for future research on rhabdodontids.

Institutional abbreviations

LPB (FGGUB), Laboratory of Paleontology, Faculty of Geology and Geophysics, University of Bucharest, Bucharest, Romania; **MTM**, Hungarian Natural History Museum, Budapest, Hungary; **MCD**, Museu de la Conca Dellà, Isona, Spain; **MDE**, Musée des Dinosauriens, Espéraza, France; **MHN**, Muséum d’Histoire Naturelle d’Aix-en-Provence, Aix-en-Provence, France; **MMS/VBN**, Musée du Moulin seigneurial, Velaux-La Bastide Neuve, France; **MPLM**, Palais Longchamp Museum, Marseille, France; **NHMUK**, Natural History Museum, London, UK; **PIUW**: Paläontologisches Institut der Universität Wien, Vienna, Austria; **UBB**, Babeş-Bolyai University, Cluj-Napoca, Romania.

The taxonomic history and diversity of the Rhabdodontidae

For the taxonomic history of the Rhabdodontidae presented here, only unquestionable members of the family were considered; other putative rhabdodontids that were, however, subsequently mostly placed outside of the Rhabdodontidae (within the more inclusive clade Rhabdodontomorpha), are discussed in the following section (see also there the formal definitions of the two clades, Rhabdodontidae and Rhabdodontomorpha).

The first rhabdodontid that was scientifically described and which later served as the basis for the name of the family is *Rhabdodon priscum* (later amended to *R. priscus* by Brinkmann (1986), see below) from the uppermost Cretaceous (Campanian–middle Maastrichtian) of southern France (Matheron 1869). The material upon which Matheron (1869) erected *Rhabdodon priscum* included a fragmentary left dentary (Fig. 2A) and some postcranial elements. The fragmentary left dentary (MPLM 30) was later selected as the lectotype of *Rhabdodon priscus* (Brinkmann 1988), but has since deteriorated (Pincemaille-Quillevere 2002). The material was originally discovered in the 1840s at the construction site of a railway tunnel at la Nerthe in Bouches-du-Rhône, southern France (Taquet 2001). A few years after the discovery, Philippe Matheron, a geologist tasked with supervising the drilling work of the tunnelling project, preliminarily described the first vertebrate remains from La Nerthe, including a tooth that was reminiscent of *Iguanodon* (Matheron 1846; Taquet 2001). More than two decades later, he based a new genus and species of dinosaur, *Rhabdodon priscum*, on the material from la Nerthe (Matheron 1869).

Additional material of *Rhabdodon priscum* was described by Matheron (1892) and, much later, by Lapparent (1947). As a consequence of the intensified research on the Late Cretaceous vertebrates from southern France since the later part of the 20th century, numerous specimens have been uncovered and referred to *Rhabdodon* (e.g. Garcia et al. 1999; Pincemaille-Quillevere 2002; Allain and Suberbiola 2003; Pincemaille-Quillevere et al. 2006; Chanthasit 2010). The most important of the more recently collected specimens from southern France is a partial associated skeleton missing the cranium, forelimbs and several caudal vertebrae (MHN AIX PV 199) from the lower Maastrichtian of Vitrolles (Bouches-du-Rhône, southern France), which is one of the most complete rhabdodontid individuals known thus far (Garcia et al. 1999; Pincemaille-Quillevere 2002). In addition to the occurrences from southern France, *Rhabdodon* has also been reported from the Upper Cretaceous of north-eastern Spain (e.g. Pereda-Suberbiola and Sanz 1999; Ortega et al. 2006, 2015; Pereda-Suberbiola et al. 2015).

However, the referral of all of this material to just one species or even genus is currently debated and usually at least a second species, *R. septimanicus* from southern

France, is recognised (Buffetaut and Le Loeuff 1991; Chanthasit 2010). This second species was erected based on an isolated and incomplete right dentary of a juvenile individual (MDE D-30; Fig. 2B) from the upper Campanian–lower Maastrichtian “Grès à Reptiles Formation” of Montouliers (Hérault), southern France (Buffetaut and Le Loeuff 1991). Although they noted a high degree of variability in the *Rhabdodon* material from southern France, Allain and Pereda-Suberbiola (2003) regarded all this material as pertaining to just one species, characterised by a high degree of intraspecific variation and/or sexual dimorphism and, thus, considered *R. septimanicus* as a junior synonym of *R. priscus*. Later, Chanthasit (2010) described additional cranial and postcranial material from the upper Campanian–lower Maastrichtian of Hérault (southern France) referred to *R. septimanicus*, concluding that it, indeed, represents a valid species. In this context, it is worth noting that Ősi et al. (2012), in their analysis of histological thin sections of *Rhabdodon* long bones from southern France, have documented extreme differences in body size occurring within a single ontogenetic stage (i.e. adult individuals) indicating the presence of at least two, but possibly even more, different taxa.

The geologically oldest material ascribed to the genus *Rhabdodon* comes from the lower Campanian of the Villeveyrac Basin (Hérault, southern France) and comprises four teeth, dorsal and caudal vertebrae, a humerus and a partial femur (Buffetaut et al. 1996). The authors assigned the teeth to the genus *Rhabdodon*, while the vertebrae were referred to as cf. *Rhabdodon priscus* (Buffetaut et al. 1996). Conversely, the youngest occurrence of the genus comes from the upper Maastrichtian of Vitrolles-la-Plaine (Bouches-du-Rhône, southern France) and includes several isolated teeth (Valentin et al. 2012). Remarkably, the material from Vitrolles-la-Plaine also represents the youngest rhabdodontid occurrence from south-western Europe in general (see below); nevertheless, it should be noted that the vertebrate remains from this site might have been reworked (as indicated by weathering and abrasion of the fossils) and, thus, could ultimately turn out be older than currently thought (Valentin et al. 2012; Vila et al. 2016).

Soon after the description of *Rhabdodon* by Matheron (1869), a closely related taxon from the Upper Cretaceous (lower Campanian) of eastern Austria (Muthmannsdorf) was reported by Bunzel (1871), as *Iguanodon suessi*, for which Seeley (1881) later coined the new genus name *Mochlodon* (as *M. suessi*). The specimens referred to *Mochlodon suessi* were found in the ‘coal-bearing series’ of Muthmannsdorf, which was mined until the end of the 19th century and which is assignable to the lower Campanian Grünbach Formation of the Gosau Group (Bunzel 1871; Seeley 1881; Summesberger et al. 2007; Csiki-Sava et al. 2015). The first vertebrate fossil collected from Muthmannsdorf was an isolated tooth found by Ferdinand Stoliczka in 1859 during an excursion led by Professor Eduard Suess, which resembled

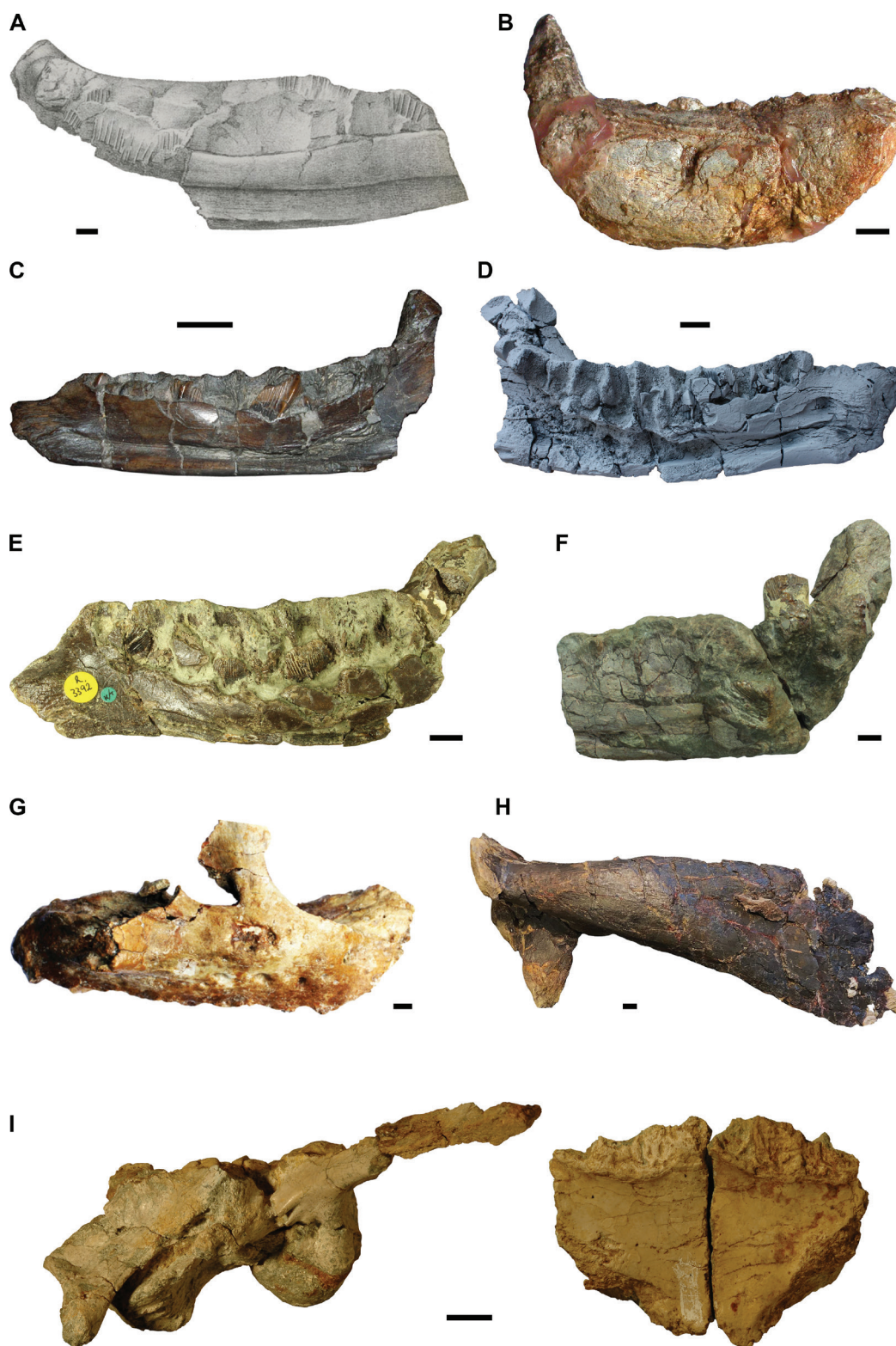


Figure 2. Type specimens of the nine rhabdodontid species described so far. **A.** The original drawing of the lectotype of *Rhabdodon priscus*, MPLM 30, a partial left dentary. The specimen has since deteriorated (Pincemaille-Quillevere 2002). Modified after Matheron (1869). **B.** Holotype of *Rhabdodon septimanicus*, MDE D-30, an incomplete right dentary. Photo kindly provided by Eric Buffetaut. **C.** Lectotype of *Mochlodon suessi*, PIUW 2349/2, a right dentary. **D.** Holotype of *Mochlodon vorosi*, MTM V 2010.105.1, a left dentary. **E.** Holotype of *Zalmoxes robustus*, NHMUK R.3392, a right dentary. Photo kindly provided by János Magyar. **F.** Holotype right dentary of *Zalmoxes shqiperorum*, NHMUK R.4900. Note that the holotype of *Z. shqiperorum* also comprises several postcranial elements that presumably belong to the same individual as the dentary. Photo kindly provided by János Magyar. **G.** Holotype of *Matheronodon provincialis*, MMS/VBN-02-102, a right maxilla. Modified after Godefroit et al. (2017). **H.** Holotype of *Pareisactus evrostos*, MCD 5371, a left scapula. Modified after Párraga and Prieto-Márquez (2019). **I.** Holotype of *Transylvanosaurus platycephalus*, LPB (FGGUB) R.2070, a partial skull comprising the articulated basicranium and both frontals. Scale bars: 1 cm.

the teeth of *Iguanodon* (Bunzel 1871). Following this discovery, more vertebrate material was collected by the mining manager Pawlowitsch and eventually described by the physician and amateur palaeontologist Emanuel Bunzel (1871), who erected the new species *Iguanodon suessi*. After further material had been collected, Harry Govier Seeley was invited to Vienna in 1879 to study the additional specimens, which resulted in a revision of the vertebrate material from Muthmannsdorf and the erecting of the new genus *Mochlodon* (Seeley 1881). Originally, Seeley (1881) also erected the taxa *Ornithomerus gracilis*, *Rhadinosaurus alcemus* and *Oligosaurus adelus* based on various fragmentary appendicular elements; subsequently, however, all three taxa have been considered to be synonymous with *M. suessi* (Norman 2004; Sachs and Hornung 2006). As the mining activity has stopped at Muthmannsdorf in the late 19th century, no further fossil vertebrate material has been collected at this site (Csiki-Sava et al. 2015).

The material assigned to *Mochlodon suessi* comprises a right dentary (Fig. 2C), a partial parietal, two teeth and fragmentary postcranial elements (Bunzel 1871; Seeley 1881), of which the dentary (PIUW 2349/2) was selected as the lectotype of the taxon by Sachs and Hornung (2006). Subsequently, *Mochlodon* was synonymised with *Rhabdodon* by Nopcsa (1915), a view that was upheld for decades (e.g. Abel 1919; Romer 1933, 1956; Huene 1956; Müller 1968; Steel 1969; Brinkmann 1988; Norman and Weishampel 1990). Much later, Sachs and Hornung (2006) considered *Mochlodon* to be a nomen dubium and referred the Austrian material to the genus *Zalmoxes* that was named shortly before (see below). However, more recent work showed that *Mochlodon*, indeed, likely represents a valid genus that is distinct from *Rhabdodon* and *Zalmoxes* (Ösi et al. 2012). Moreover, a second species of *Mochlodon*, *M. vorosi*, was also recently described by Ösi et al. (2012) from the Upper Cretaceous (Santonian) of Hungary based on a left dentary (holotype, MTM V 2010.105.1; Fig. 2D), as well as a referred left postorbital, two right quadrates, additional dentaries, isolated teeth and postcranial elements. The presence of rhabdodontids in the Upper Cretaceous of Hungary was originally reported a few years earlier based on three isolated teeth referred to an indeterminate rhabdodontid (Ösi 2004).

It is noteworthy that the name *Rhabdodon* was abandoned in favour of *Mochlodon* for several years during the 1980s (Bartholomai and Molnar 1981; Weishampel and Weishampel 1983; Milner and Norman 1984; Norman 1984, 1985; Weishampel 1984; Sereno 1986), when it was recognised that the genus name *Rhabdodon* was pre-occupied by a colubrid snake (Fleischmann 1831). As a consequence, a case was submitted to the ICZN in 1985 (No. 2536) by Brinkmann (1986) to conserve the name for the dinosaur. In the same submission, Brinkmann (1986) also suggested to change the species name from *R. priscum* to *R. priscus*. A decision by the ICZN on this case was reached in 1987 (opinion 1483), when it was decided unanimously to conserve the genus name for the dinosaur and change the species name to *R. priscus*,

as proposed by Brinkmann (1986) two years before (International Commission on Zoological Nomenclature 1988). Therefore, *Rhabdodon* is the valid genus name of the taxon described and named by Matheron (1869).

The first mentions of basal ornithopods from Transylvania (western Romania) were made by Nopcsa (1897, 1899a, b) in three short notes on the geology of the region around Sânpetru ('Szentpéterfalva') in the Hațeg Basin, referring the material to 'mochlodons', as well as to 'camptosaurus' (the latter being known mainly from the Upper Jurassic of the United States). Subsequently, Nopcsa (1900), in his monograph on the hadrosauroid dinosaur *Telmatosaurus* (originally named '*Limnosaurus*'), commented on three lower jaws that were found together with the type material of *Telmatosaurus* at his most prolific site, his 'Nest 1' (Quarry 1) from the Sibișel Valley near Sânpetru and which he referred to basal ornithopods. Two of these jaws were assigned to two new species, *Camptosaurus inkeyi* and *Mochlodon robustum* (Fig. 2E), whereas the third was referred to *Mochlodon suessi*. Despite erecting two new species and reporting the presence of a third one, Nopcsa (1900) did not figure the dentaries in this monograph and only very briefly described the element he assigned to *Camptosaurus inkeyi* in a footnote. The first thorough study of rhabdodontid material from the Hațeg Basin was published by Nopcsa (1902). In this monograph, he described a few cranial elements (three dentaries, an articular, two quadrates, three squamosals and several isolated teeth belonging to four individuals) referred to *Mochlodon* and synonymised *Mochlodon robustum* with *Mochlodon suessi*.

Two years later, Nopcsa published a second monograph on the cranial anatomy of *Mochlodon* reporting new elements (frontal, premaxilla, maxilla, nasal, prementary and tentatively referred braincases) from Sânpetru (Nopcsa 1904). In this publication, Nopcsa also re-identified the type dentary of *Camptosaurus inkeyi* as a maxilla and considered this taxon to be a junior synonym of *Mochlodon* (Nopcsa 1904: p. 245–246). The initial draft for this publication also included a new genus and species, *Onychosaurus hungaricus*, which was based on a right premaxillary (NHMUK R.3411) and a prementary (NHMUK R.3410), but the manuscript was subsequently retracted by Nopcsa himself (Nopcsa 1903) and *Onychosaurus* was referred to *Mochlodon* as Individual G (Nopcsa 1904: p. 231). Subsequently, Nopcsa (1905) regarded *Mochlodon robustum* again a valid species and listed both *M. robustum* and *M. suessi* as occurring at Sânpetru (Nopcsa 1905: p. 170). After first-hand examination of the *Rhabdodon* material from southern France described by Matheron (1869), Nopcsa (1915) synonymised *M. robustum* and *M. suessi* with *Rhabdodon priscum* and regarded the two former *Mochlodon* species from Transylvania as sexual variants of a single species (Nopcsa 1915: p. 4–7). Several years later, Nopcsa published his third monograph on the rhabdodontids from the Hațeg Basin, this time describing the vertebral column (Nopcsa 1925) and

mentioning, for the first time, the inventory numbers of his Transylvanian specimens housed in the London collection (NHMUK), to which Nopcsa previously sold his collection. In this third monograph, Nopcsa noted once again the presence of two morphotypes within his ‘*Rhabdodon*’ sample that he interpreted as most likely representing male and female individuals of the same species (Nopcsa 1925), a view later reiterated in an article on sexual dimorphism in ornithomimid dinosaurs (Nopcsa 1929), his last work dealing with the ornithomimid dinosaurs from the Hațeg Basin.

Following the work of Nopcsa, the rhabdodontids and, in fact, the entire latest Cretaceous vertebrate fauna from the Hațeg Basin slid into oblivion for several decades. Renewed interest began to form again in the 1970s and 1980s, with systematic excavations taking place at several of Nopcsa’s classical sites, as well as at new localities (for an overview of this restart, see Grigorescu 2010). As a consequence, an extensive review of the geology, taphonomy and palaeontology of the Hațeg Basin was given by Grigorescu (1983), incorporating both old and newly acquired data. Additionally, Weishampel et al. (1991) provided an updated overview of the dinosaur fauna from the Hațeg Basin with a discussion treatment of *Rhabdodon priscus* mainly based on the original Nopcsa specimens, but also reporting newly discovered material. A few years later, Jianu (1994) described a new dentary specimen from Sânpetru and assigned it to *Rhabdodon priscus*. Eventually, an extensive revision of the rhabdodontid material from the Hațeg Basin, both old and new, was published by Weishampel et al. (2003), in which the authors noted several important differences between *Rhabdodon* from southern France and the material from Romania. Consequently, the new genus *Zalmoxes* was erected for the rhabdodontid material from Romania, containing two species, the type species *Z. robustus* and *Z. shqiperorum*. The former represents a resurrection of Nopcsa’s *Mochlodon robustum* (amended to *robustus*), whereas the latter is a new species based primarily on a partial skeleton excavated by Nopcsa (NHMUK R.4900; Fig. 2F). These authors also designated the holotype of *Z. robustus*, represented by the right dentary (NHMUK R.3392; Fig. 2E), upon which Nopcsa (1900) originally based *M. robustum* and which he figured and described a few years later (Nopcsa 1902). In the same publication, Weishampel et al. (2003) also formally established the family Rhabdodontidae, at that time including the genera *Rhabdodon*, *Mochlodon* and *Zalmoxes*.

It is important to note, nonetheless, that the holotype of *Zalmoxes shqiperorum* does not come from the south-western Transylvanian Basin as stated by Weishampel et al. (2003), but from the Hațeg Basin. The locality of the type specimen of *Z. shqiperorum*, individual NHMUK R.4900, was originally given as “Unnamed formation (‘Bozeș strata’; upper Maastrichtian-Paleocene); Vurpăr, near Vințu de Jos, Alba County, Romania” (Weishampel et al. 2003: p. 95) and this information was later repeated by several other authors (e.g. Brusatte et al. 2013).

However, when first mentioning this individual, Nopcsa (1925: p. 286) clearly wrote that NHMUK R.4900 (his individual I) comes from Sânpetru (‘Szentpéterfalva’) in the south-central part of the Hațeg Basin. Accordingly, we amend here some of the basic information concerning *Zalmoxes shqiperorum* as stated by Weishampel et al. (2003: p. 95), respectively the position and identity of the type locality and horizon for this taxon; instead of Vurpăr, in the Transylvanian Basin, the corrected type locality is represented by the ‘Sibișel Valley, south of Sânpetru, Hațeg Basin, Hunedoara County, Romania’, whereas the type horizon can now be specified as the ‘Sânpetru Formation (Maastrichtian)’. Incidentally, since the only currently diagnostic rhabdodontid individual found at Vurpăr according to Nopcsa (1905) and identified later as Individual H (Nopcsa 1925; but indicated as originating from Vințu de Jos in this monograph), respectively specimen NHMUK R.3813, was referred to *Z. robustus* by Weishampel et al. (2003), the presence of a second species of *Zalmoxes* at this locality remains unsupported by currently available information. Although the occurrence of relatively abundant rhabdodontid remains had been reported subsequently from Vurpăr (e.g. Codrea et al. 2010; Vremir 2010; Vremir et al. 2015), these were not described in detail and were only generically referred to *Zalmoxes* (Codrea et al. 2010; Vremir et al. 2015). As such, the presence of *Zalmoxes shqiperorum* at Vurpăr, as well as the sympatry of *Z. robustus* and *Z. shqiperorum* in this locality (as proposed by, for example, Godefroit et al. 2009; Vremir et al. 2015) remains questionable for the time being.

In the years following the revision of the Transylvanian rhabdodontids by Weishampel et al. (2003), additional material referred to *Zalmoxes* was described from various parts of the Hațeg Basin, the Transylvanian Basin and the Ruscă Montană Basin, in Romania (Codrea and Godefroit 2008; Codrea et al. 2010, 2012; Brusatte et al. 2013, 2017; Dumbravă et al. 2013; Vremir et al. 2014, 2017; Botfalvai et al. 2017). Amongst these newly discovered specimens, a partial skull and skeleton referred to *Z. shqiperorum* from Nălaț-Vad (UBB NVZ1) is particularly noteworthy, as it represents one of the most complete *Zalmoxes* individuals known so far (Godefroit et al. 2009); recently, however, the referral of the entirety of this material to just one individual (or even taxon) was questioned (Brusatte et al. 2017; Augustin et al. 2023). Although the large majority of the material assigned to *Zalmoxes* comes from Maastrichtian strata (Csiki-Sava et al. 2016), one site from the south-western Transylvanian Basin (Petrești-Arini) yielded remains referred to *Zalmoxes* sp. from the uppermost Campanian (Vremir et al. 2014, 2015), representing the oldest rhabdodontid material from western Romania reported so far.

Besides *Rhabdodon*, *Mochlodon* and *Zalmoxes*, three more rhabdodontid genera were recently named and described, all of which are monospecific. The first of these is *Matheronodon provincialis*, which was based on a single, well preserved right maxilla (MMS/

VBN-02-102; Fig. 2G) from the Upper Cretaceous (Upper Campanian) of the Aix-en-Provence Basin in southern France (Godefroit et al. 2017). The second, *Pareisactus evrostos*, is represented by a nearly complete left scapula (MCD 5371; Fig. 2H) that was discovered in the Upper Cretaceous (lower Maastrichtian) Conques Member of the Tremp Formation in north-eastern Spain (Párraga and Prieto-Márquez 2019). To date, no further material has been assigned to either *Matheronodon* or to *Pareisactus* and, thus, both taxa are only known from their respective holotypes. Finally, Augustin et al. (2022) described the new genus and species *Transylvanosaurus platycephalus* based on a partial skull from the Hațeg Basin. The holotype and only known specimen of this taxon, LPB (FGGUB) R.2070, comes from the ‘middle’ Maastrichtian of the ‘Pui Beds’ (Csiki-Sava et al. 2016) and comprises the articulated basicranium together with the associated left and right frontals (Fig. 2I). The description of this new Romanian rhabdodontid has important consequences. As pointed out by Brusatte et al. (2017) and Augustin et al. (2022), in the past, rhabdodontid remains from the uppermost Cretaceous of Transylvania have been indiscriminately referred to the genus *Zalmoxes*, often without positive supportive evidence, on the account that it was the sole taxon represented in the local faunas. However, with the recent description of *Transylvanosaurus*, this practice has to be re-considered as the taxonomic diversity of rhabdodontids seems to have been actually higher than previously thought (at least in the Hațeg Basin, but potentially also in the Transylvanian and Rusca Montană basins). For an overview of the different rhabdodontids, as well as their temporal and stratigraphical distribution, see Table 1.

The phylogenetic relationships of the Rhabdodontidae and palaeobiogeographic implications

From the very beginning onwards, a close relationship between rhabdodontids and iguanodontian ornithopods was recognised. In fact, already Matheron (1869), in his initial description of *Rhabdodon*, noted the similarity of this form to *Iguanodon*, as did Bunzel (1871) by assigning the rhabdodontid from Muthmannsdorf, Austria, to *Iguanodon*, as the new species *I. suessi* (later placed in its own genus *Mochlodon*, see above, previous section). Nopcsa (1901) was the first to assign the rhabdodontids known at that time to a higher taxon, placing *Rhabdodon* and *Mochlodon* (the latter also including the rhabdodontid material from the Hațeg Basin, later to be named *Zalmoxes*) within the Hypsilophodontidae. This group was, in turn, considered to be part of the family Kalodontidae, a newly erected, paraphyletic grouping of non-hadrosaurid ornithopods (Nopcsa 1901). Later, Nopcsa (1902) confirmed this assignment in his first monograph on the rhabdodontid dinosaurs from the Hațeg Basin, noting the close resemblance of this material to *Hypsilophodon* from the Lower Cretaceous of England. After examination of further cranial material (see above) in his second monograph on the rhabdodontids from the Hațeg Basin, Nopcsa (1904) still regarded *Mochlodon* as a close relative of *Hypsilophodon*, although he noted that it also appears to be similar to *Camptosaurus* (see also Nopcsa 1903). His view, however, changed again several years later, when he regarded *Rhabdodon* (now including specimens referred previously to *Mochlodon* from both Austria and Romania)

Table 1. Overview of the different rhabdodontid taxa, as well as their geographical and stratigraphical distribution (for details and references, see text).

Taxon	Locality	Age
<i>Rhabdodon</i> Matheron, 1869		
<i>R. priscus</i> Matheron, 1869	various lithostratigraphic units, southern France	Campanian–‘middle’ Maastrichtian
<i>R. septimanicus</i> Buffetaut & Le Loeuff, 1991	“Grès à Reptiles Formation”, Hérault, southern France	Late Campanian–early Maastrichtian
<i>Mochlodon</i> Seeley, 1881		
<i>M. suessi</i> Bunzel, 1871 (= <i>Iguanodon suessi</i> Bunzel, 1871; <i>Ornithomerus gracilis</i> Seeley, 1881; <i>Rhadinosaurus alcemus</i> Seeley, 1881; <i>Oligosaurus adelus</i> Seeley, 1881)	Grünbach Formation, Muthmannsdorf, eastern Austria	Early Campanian
<i>M. vorosi</i> Ősi et al., 2012	Csehbánya Formation, Iharkút, western Hungary	Santonian
<i>Zalmoxes</i> Weishampel et al., 2003		
<i>Z. robustus</i> Nopcsa, 1900 (= <i>Mochlodon robustum</i> Nopcsa, 1900; <i>Camptosaurus inkeyi</i> Nopcsa, 1900; <i>Onychosaurus hungaricus</i> Nopcsa, 1902)	Sânpetru Formation, Densuș-Ciula Formation, Hațeg Basin, western Romania	early–late Maastrichtian
<i>Z. shqiperorum</i> Weishampel et al., 2003	Sânpetru Formation, Densuș-Ciula Formation, ‘Râul Mare River section’, Hațeg Basin, Jibou Formation, northwestern Transylvanian Basin, western Romania	early–late Maastrichtian
<i>Matheronodon</i> Godefroit et al., 2017		
<i>M. provincialis</i> Godefroit et al., 2017	Unnamed formation, Aix-en-Provence Basin, southern France	Late Campanian
<i>Pareisactus</i> Párraga and Prieto-Márquez, 2019		
<i>P. evrostos</i> Párraga and Prieto-Márquez, 2019	Tremp Formation, Basturs Poble, north-eastern Spain	early Maastrichtian
<i>Transylvanosaurus</i> Augustin et al., 2022		
<i>T. platycephalus</i> Augustin et al., 2022	‘Pui Beds’, Hațeg Basin, western Romania	‘middle’ Maastrichtian

as a member of the more derived Camptosauridae (Nopcsa 1915), an opinion also expressed in his later works (Nopcsa 1923, 1934). During the next decades, most authors followed this classification and *Rhabdodon* was assigned to the Camptosauridae or, alternatively, to the Iguanodontidae, which, during that time, was often used as a somewhat more inclusive clade also containing taxa traditionally placed within Camptosauridae, such as *Camptosaurus* (Abel 1919; Romer 1933, 1945, 1956; Huene 1956; Müller 1968; Steel 1969).

In the early 1980s, however, this view was challenged by some workers who classified *Mochlodon* (at this time including *Rhabdodon* and the Romanian rhabdodontid material, see above) as a non-iguanodontid ornithopod (Bartholomai and Molnar 1981) or as a potential hypsilophodontid (Norman 1985) or, at least, questioned its iguanodontid affinities (Weishampel and Weishampel 1983). All of these taxonomic opinions convergently regarded *Rhabdodon* as a more basal ornithopod than previously thought. The advent of cladistics in ornithischian systematics during the mid-1980s (Norman 1984; Sereno 1984, 1986; Cooper 1985; Maryanska and Osmólska 1985) also had a profound impact on the classification of *Mochlodon* and *Rhabdodon* within the dinosaur family tree. In the framework of these first cladistic analyses, *Mochlodon* (including *Rhabdodon*) was regarded either as a dryosaurid (Milner and Norman 1984) or else as a basal member of the clade Iguanodontia (Sereno 1986). Meanwhile, based on its supposedly more basal phylogenetic position and its hypsilophodontid-like tooth morphology, Brinkmann (1988) classified *Rhabdodon* as a member of the Hypsilophodontidae. Norman (1990) rejected dryosaurid affinities of *Rhabdodon* and, instead, considered it to be a hypsilophodontian. In contrast, Norman and Weishampel (1990) followed Sereno (1986) and classified *Rhabdodon* as Iguanodontia incertae sedis. Similarly, Weishampel et al. (1998) and Pincemaille-Quillever (2002) regarded *Rhabdodon* as a basal iguanodontian.

In their extensive revision of the rhabdodontid material from the Hațeg Basin, Weishampel et al. (2003) finally erected the family Rhabdodontidae (at this time containing *Rhabdodon*, *Zalmoxes* and, provisionally, *Mochlodon*) and defined it as “a node-based taxon consisting of the most recent common ancestor of *Zalmoxes robustus* and *Rhabdodon priscus* and all the descendants of this common ancestor (Weishampel et al. 2003: p. 69). In their phylogenetic analysis, Weishampel et al. (2003) recovered it as the sister-clade to Iguanodontia. Since then, the Rhabdodontidae has been consistently placed at the base of the iguanodontian radiation (Butler et al. 2008; McDonald 2012; Ósi et al. 2012; Boyd 2015; Dieudonné et al. 2016, 2021; Verdú et al. 2018, 2020; Madzia et al. 2018; Bell et al. 2018, 2019; Yang et al. 2020; Poole 2022; Augustin et al. 2022). Such a basal phylogenetic position within Iguanodontia, combined with their fossil record being limited to the later Late Cretaceous (Santonian–Maastrichtian), indicates an exceptionally long ghost lineage for rhabdodontids. Soon after the Rhabdodontidae

was erected and first defined by Weishampel et al. (2003), Sereno (2005) proposed a new definition for this taxon as the most inclusive clade containing *Rhabdodon priscus*, but not *Parasaurolophus walkeri*.

Based on the results of their phylogenetic analysis (indicating a particularly close relationship of the Rhabdodontidae with *Muttaborrasaurus*), Dieudonné et al. (2016) later erected the more inclusive clade Rhabdodontomorpha and defined it as “a node-based taxon consisting of the most inclusive clade containing *Rhabdodon priscus* Matheron, 1869 and *Muttaborrasaurus langdoni* Bartholomai & Molnar, 1981” (Dieudonné et al. 2016: p. 5). Subsequently, Madzia et al. (2018) suggested another definition for Rhabdodontomorpha, i.e. as a branch-based taxon with *Rhabdodon priscus* and *Muttaborrasaurus langdoni* as internal specifiers and *Iguanodon bernissartensis* as an external specifier. This definition was in turn slightly amended by Madzia et al. (2020), who defined the clade as a branch-based taxon with *Rhabdodon priscus* as an internal specifier and *Iguanodon bernissartensis* as an external specifier. Recently, formal definitions of the two clades Rhabdodontidae and Rhabdodontomorpha in compliance with the International Code of Phylogenetic Nomenclature (ICPN or PhyloCode) have been provided by Madzia et al. (2021). According to these definitions, Rhabdodontidae is defined as the smallest (most exclusive) clade containing *Rhabdodon priscus* and *Zalmoxes robustus*, while Rhabdodontomorpha is defined as the largest (most inclusive) clade containing *Rhabdodon priscus*, but not *Hypsilophodon foxii* and *Iguanodon bernissartensis* (Madzia et al. 2021). Potential close relatives of the Rhabdodontidae, belonging to the more inclusive clade Rhabdodontomorpha, include the ‘Vegagete ornithopod’ from the Lower Cretaceous (Barremian–Aptian) of northern Spain (Dieudonné et al. 2016), *Tenontosaurus* from the Lower Cretaceous (Aptian–Albian) of the western United States (Poole 2022), *Muttaborrasaurus* from the Lower Cretaceous (Albian) of north-eastern Australia (Bartholomai and Molnar 1981), *Fostoria* from the lowermost Upper Cretaceous (lower Cenomanian) of eastern Australia (Bell et al. 2019) and *Iani* from the lowermost Upper Cretaceous (Cenomanian) of the western United States (Zanno et al. 2023), albeit it should be noted that alternative positions within Iguanodontia have also been suggested for four of these five taxa (i.e. the ‘Vegagete ornithopod’, *Tenontosaurus*, *Muttaborrasaurus* and *Fostoria*).

The ‘Vegagete ornithopod’ has been originally proposed to be the basal-most and earliest member of the Rhabdodontidae itself (Dieudonné et al. 2016), although under the definition of Weishampel et al. (2003; see also Madzia et al. 2021), it would fall outside Rhabdodontidae (as the sister-group to it). Subsequently, this taxon was recovered in a sister-group relationship with *Mochlodon suessi*, together forming the sister-group to *M. vorosi* (Yang et al. 2020); on its turn, this small clade was found to be in a polytomy with the other two well-established rhabdodontid genera known at that time (*Rhabdodon*, *Zalmoxes*), each of which was shown to be monophyletic.

In an attempt to achieve better resolution within their tree, these authors decided to remove taxa identified as wildcards from a second run of their phylogenetic analysis, including here both *Zalmoxes* and *Rhabdodon*. Thus, whereas their resulting fully resolved agreement subtree did still return the same ‘Vegagete ornithopod’-*Mochlodon* clade, ironically, whether this grouping belongs to Rhabdodontidae (or even to Rhabdodontomorpha) or not, cannot be ascertained any longer as the specifiers for these clades (regardless of the details of their definition) were not included in the analysis. Indeed, there is no way to delineate Rhabdodontidae or its parent clade Rhabdodontomorpha at all in the fully resolved agreement subtree of Yang et al. (2020). Finally, the Early Cretaceous Spanish taxon was also recovered as a member of the Rhabdodontidae, closely related to *Rhabdodon* (Herne et al. 2019); however, more recently, it was recovered as the closest outgroup of Rhabdodontidae within Rhabdodontomorpha (Dieudonné et al. 2021).

Although *Tenontosaurus* is usually recovered outside of Rhabdodontomorpha (e.g. Dieudonné et al. 2016, 2021; Madzia et al. 2018; Bell et al. 2018, 2019; Andrzejewski et al. 2019; Yang et al. 2020; Barta and Norell 2021; Augustin et al. 2022), it has recently also been placed within this clade (Poole 2022; Zanno et al. 2023). *Muttaburrasaurus* is often regarded as a basal rhabdodontomorph (Dieudonné et al. 2016, 2021; Madzia et al. 2018; Bell et al. 2018; Barta and Norell 2021; Augustin et al. 2022), but it has also been recovered in a polytomy with the rhabdodontids *Rhabdodon* and *Zalmoxes* (McDonald et al. 2010); alternatively, it has been identified either as a more basal (Bell et al. 2019) or a more derived (Boyd 2015; Herne et al. 2019) iguanodontian compared to rhabdodontids and their close kin. *Fostoria*, on the other hand, has been found to be either a basal rhabdodontomorph (Dieudonné et al. 2021; Augustin et al. 2022) or a more basal iguanodontian (Bell et al. 2019). Meanwhile, the very recently described *Iani* has been recovered as a rhabdodontomorph by the only phylogenetic analysis including this taxon (Zanno et al. 2023). Given that derived rhabdodontomorphs (i.e. rhabdodontids) are, so far, exclusively known from Europe, a European origin of the Rhabdodontidae seems likely.

In addition to the phylogenetic position of the Rhabdodontidae within Ornithopoda, the interrelationships of the different rhabdodontids have been thoroughly scrutinised as well (Fig. 3). In most previous phylogenetic analyses, *Rhabdodon* spp. from southern France and north-eastern Spain has been recovered as the sister-taxon to a clade comprising *Mochlodon* spp. from Austria and Hungary and *Zalmoxes* spp. from Romania (Ösi et al. 2012; Madzia et al. 2018; Verdú et al. 2018, 2020; Barta and Norell 2021; Dieudonné et al. 2021). Notably, only a single phylogenetic analysis has found a closer relationship between *Rhabdodon* and *Zalmoxes* instead (Dieudonné et al. 2016), whereas the three genera have also been recovered in a polytomy by some phylogenetic analyses (e.g. Bell et al. 2019). Based on the results of these phylogenetic analyses and the geographic

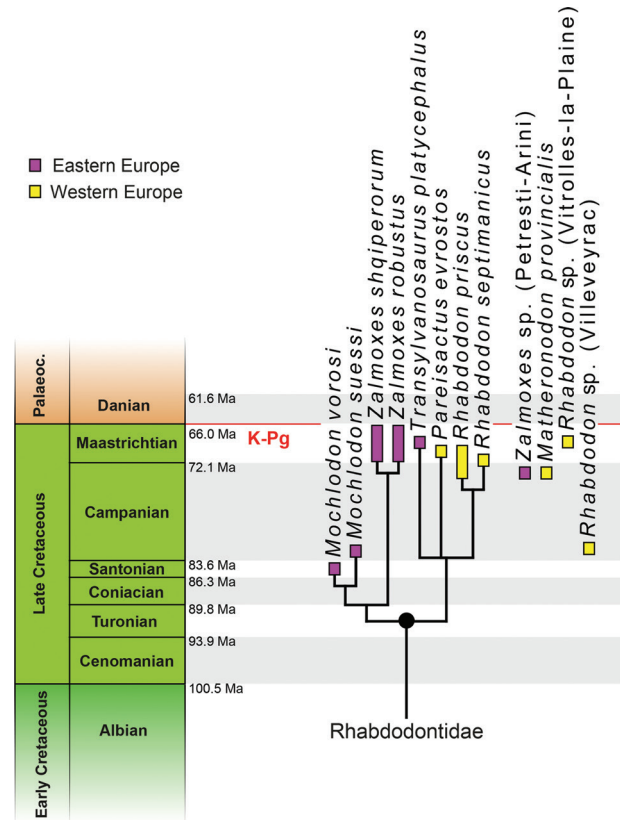


Figure 3. Phylogenetic relationships and temporal distribution of the Rhabdodontidae. The relationships within Rhabdodontidae primarily follow Dieudonné et al. (2021), as well as Párraga and Prieto-Márquez (2019) for the relationships of *Pareisactus*. The phylogenetic relationships of *Transylvanosaurus* follow Augustin et al. (2022), who suggested a particularly close relationship between this taxon and *Rhabdodon* spp. from southern France based on morphological comparisons. The relationships of *Matheronodon* have not yet been explored by a phylogenetic analysis nor by detailed comparisons and, thus, it is not included in the cladogram. Similarly, *Zalmoxes* sp. from Petrești-Arini, *Rhabdodon* sp. from Villevetryac and *Rhabdodon* sp. from Vitrolles-la-Plaine have not yet been incorporated into a phylogenetic analysis, but are included here, as these specimens represent the oldest respectively the youngest occurrences of rhabdodontids in Eastern and Western Europe (see text for explanations). The colour of the boxes denotes their distribution (purple for Eastern Europe, yellow for Western Europe).

distribution pattern of the then-known rhabdodontids, the presence of two rhabdodontid lineages has been suggested, one from Western Europe and the other from Eastern Europe (Ösi et al. 2012). The phylogenetic relationships of *Pareisactus evrostos* from north-eastern Spain were explored only by a single phylogenetic analysis that found it to be the sister-taxon to *Rhabdodon priscus*, thus making it a member of the same Western European rhabdodontid lineage (Párraga and Prieto-Márquez 2019). *Matheronodon* from southern France, on the other hand, has never been included in a phylogenetic analysis and, thus, its relationships with the other rhabdodontids remain currently unknown.

Intriguingly, a comparable ‘eastern vs. western’ dichotomous distribution pattern has been previously suggested for other latest Cretaceous European continental vertebrates as well, including turtles (Rabi et al. 2013; Csiki-Sava et al. 2015; Augustin et al. 2021), mammals (Csiki-Sava et al. 2015; Gheerbrant and Teodori 2021) and allodaposuchid crocodyliforms (Narváez et al. 2016; Blanco and Brochu 2017; Blanco 2021). Such a coherent pattern, as well as a high degree of regional faunal differences and endemism is usually linked to geographical isolation of the different islands of the Late Cretaceous European Archipelago (Fig. 4; for an overview, see Csiki-Sava et al. 2015). Meanwhile, the Santonian age of *Mochlodon vorosi* would indicate that the split between the western and the eastern rhabdodontid lineages must have occurred before the Santonian, after which the two clades evolved in isolation from each other through allopatric speciation (Ősi et al. 2012). Recently, however, this relatively simple and clear-cut biogeographical hypothesis has been challenged by Augustin et al. (2022), who postulated a particularly close relationship between the newly described *Transylvanosaurus* from western Romania and *Rhabdodon* spp. from southern France based on extensive morphological comparisons. Accordingly, these authors have, instead, suggested that at least one large-scale dispersal event must have happened within the ‘western’ European rhabdodontid lineage – either from western to eastern Europe or westward into the western European realm (Augustin et al. 2022).

At this point, it should be noted, however, that the in-group relationships of the Rhabdodontidae are still only

incompletely understood. One of the main reasons for this lies in the fact that several rhabdodontids are known from only relatively few and often non-overlapping elements (e.g. *Matheronodon*, *Pareisactus*, *Transylvanosaurus*), making it difficult to firmly establish phylogenetic hypotheses for these taxa. Moreover, the two best-known rhabdodontid taxa, *Rhabdodon* and *Zalmoxes*, both of which have regularly been included into phylogenetic analyses (e.g. McDonald 2012; Ősi et al. 2012; Dieudonné et al. 2016, 2021; Bell et al. 2018, 2019; Madzia et al. 2018; Verdú et al. 2018; Barta and Norell 2021; Augustin et al. 2022; Poole 2022), await taxonomic revision (see above). All of this currently hinders exploring the phylogenetic relationships of rhabdodontids in more detail, both within the group, but also with other ornithischian dinosaurs. Accordingly, the relationships of the different rhabdodontids, as well as the biogeographical scenarios based on these, should be viewed with caution pending the discovery of more complete specimens and the taxonomic revision of certain taxa.

The palaeoecology and extinction of the Rhabdodontidae

Assessments concerning rhabdodontid palaeoecology have been made early on and one of the first to hypothesise rather extensively on this topic was, again, Franz Nopcsa, considered one of the pioneers of dinosaur palaeobiology (Weishampel and Reif 1984). In his detailed description

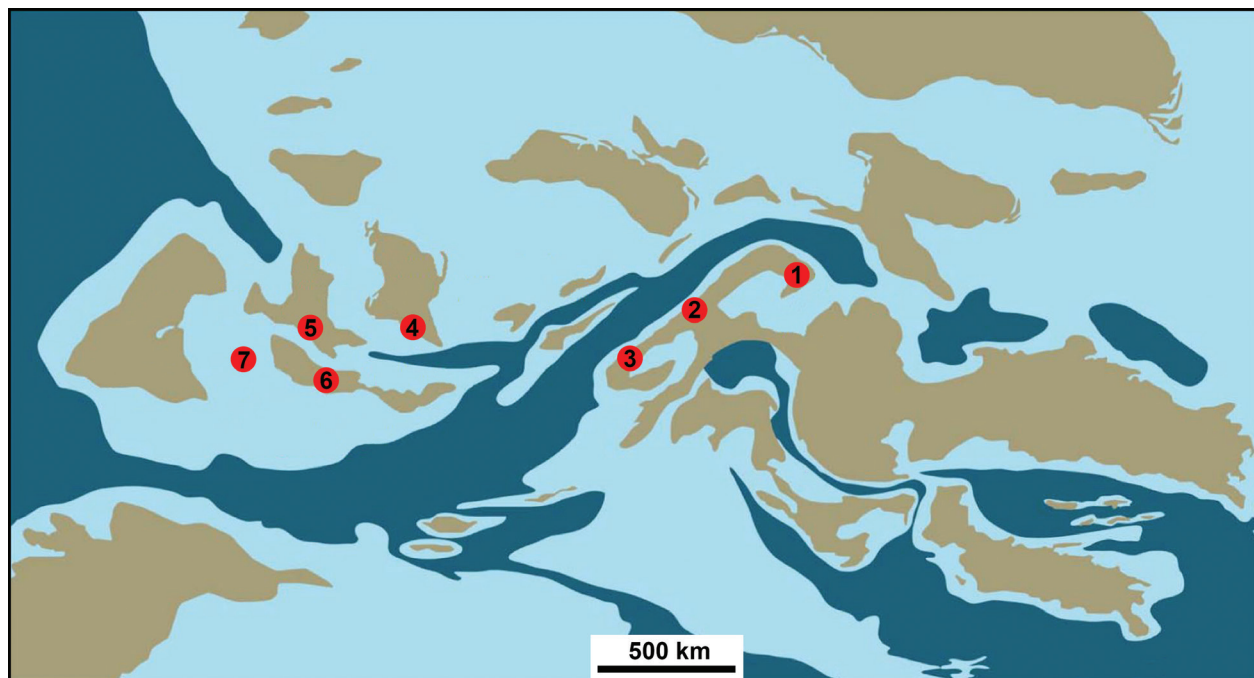


Figure 4. Palaeogeographic map of Europe during the latest Cretaceous (late Campanian), with the location of the most important rhabdodontid-bearing assemblages. **1** Transylvania (including the Hațeg, Transylvanian and Rusca Montană basins), western Romania. **2** Iharkút, western Hungary. **3** Muthmannsdorf, eastern Austria. **4** Eastern southern France. **5** Western southern France. **6** Northern Spain. **7** Central Spain. Note that the position and the extent of the different islands was slightly different before and after the late Campanian. In particular, during the Maastrichtian, the emergent landmasses were more extensive, meaning that the uppermost Cretaceous strata from central Spain (7) were deposited in a predominantly continental environment. Modified after Blanco (2021).

of the skull anatomy of the Transylvanian ‘*Mochlodon*’ (i.e. *Zalmoxes*), Nopcsa (1902) concluded that, based on tooth morphology, the movement of the jaws was exclusively vertical and that the abrasion pattern of the teeth indicates a scissor-like shearing action. He was, however, not the first to propose such a kind of masticatory mechanism since, two decades before, Seeley (1881) already suggested a scissor-like chewing action in *Mochlodon suessi* based on tooth wear. In addition, Nopcsa (1914) suggested that the presence of a sharp beak and the teeth adapted for chewing (Fig. 5A, G) indicate consumption of food items that were hard on the outside, but internally soft. He further reasoned that the rhabdodontids from ‘Szentpéterfalva’ (= Sânpetru) in the Hațeg Basin were living in the same area where their remains have been found, because they are so abundant at this locality and because juveniles have been found there (Nopcsa 1914). Since he interpreted the Sânpetru deposits as those of a shallow freshwater swamp, he regarded the rhabdodontids as swamp dwellers (Nopcsa 1914), a notion that he reiterated thereafter on several occasions (Nopcsa 1915, 1923). Contrary to Nopcsa’s interpretation, more recent sedimentological investigations demonstrated that the Sibișel Valley succession (i.e. the stratotype section of the Sânpetru Formation) were, in fact, deposited on a poorly channelised alluvial plain drained by braided river systems, which comprised active channels, wetlands, well-drained floodplains and higher-lying drier areas (e.g. Therrien 2006; Therrien et al. 2009).

Albeit this alternative sedimentological and palaeoenvironmental interpretation of the Sibișel Valley deposits was first proposed by Grigorescu (1983), he also noted that, based on taphonomical considerations, rhabdodontids (along with hadrosaurs and turtles) were likely residents of swampy areas within this diverse palaeoenvironmental mosaic – this conclusion appears to be largely a holdover of Nopcsa’s earlier habitat preference assessments. Subsequently, however, an extensive taphonomic survey of the latest Cretaceous vertebrates from the Hațeg Basin demonstrated that rhabdodontid remains are present in all of these different palaeoenvironmental settings and, despite earlier claims to the contrary, are commonly found in well-drained palaeoenvironments (Csiki et al. 2010). Therefore, these animals were almost certainly not limited to swamps or lacustrine environments as suggested before, but instead were inhabiting all palaeobiotopes represented by the deposits of the Hațeg Basin (Csiki et al. 2010). Interestingly, rhabdodontid remains with similar taphonomic features – and, thus, common taphonomic histories – pertaining to several different *Zalmoxes* individuals of different sizes have been found together in certain bonebeds in the Hațeg Basin, suggesting that these animals might have been gregarious (Csiki et al. 2010). A similar conclusion is suggested by the occurrence of at least six individuals of different sizes at the monotaxic Vegagete fossil locality that all belong to the ‘Vegagete ornithopod’, most probably a rhabdodontomorph (Dieudonné et al. 2020, 2021,

2023), indicating that the presence of a gregarious habit may have been the ancestral condition within this lineage.

During the past decades, especially the feeding behaviour and potential diet of rhabdodontids received a great deal of attention. In his monograph on ornithopod jaw mechanisms, Weishampel (1984) described the intracranial joints in more than 50 ornithopod taxa, including ‘*Mochlodon*’ (most specimens examined for this taxon pertain to *Zalmoxes*, albeit a few belong to *Rhabdodon* and *Mochlodon* as well). Based on the morphology and the distribution of these joints, it was concluded that the more derived ornithopods (including ‘*Mochlodon*’) utilised a transverse power stroke to chew their food that was accomplished by the mobilisation of the upper jaws (i.e. pleurokinesis; Weishampel 1984). The presence of this kind of cranial kinesis and the associated chewing mechanism was later suggested specifically for *Zalmoxes* as well (Weishampel et al. 2003), although the authors noted a deviation from the general pleurokinetic bauplan characterising the derived ornithopods, one that probably limited the degree of intracranial mobility and might represent an adaptation to process hard food items. Lately, the pleurokinetic skull model has been questioned in some hadrosaurs (Rybczynski et al. 2008; Cuthbertson et al. 2012). As no articulated cranial material, upon which the conditions for pleurokinesis can be demonstrated (Holliday and Witmer 2008), is yet available for *Zalmoxes* or, indeed, for any other rhabdodontid either, the occurrence of such a feeding mechanism cannot be currently confirmed for these basal ornithopods. Thus, the description of more complete and articulated cranial elements would greatly increase our knowledge of potential intracranial kinesis and the functioning of their masticatory apparatus.

Furthermore, large jaw adductor muscle chambers in *Zalmoxes* coupled with robust jaws and a well-developed coronoid process of the lower jaw are indicators of a high bite strength (Weishampel et al. 2003). Taken together with the mesiodistally enlarged teeth of certain rhabdodontids (i.e. *Matheronodon*) and the high-angled wear-surface of the teeth, these features indicate that the masticatory apparatus of at least some rhabdodontids was adapted for powerful slicing action (Godefroit et al. 2017), an interpretation very similar to those of Seeley (1881) and Nopcsa (1902) discussed above. Moreover, it was suggested that the relatively narrow jaw tips (Fig. 5E, F), which, in life, were most likely covered by a keratinous beak, could indicate that *Zalmoxes* was a selective feeder (Weishampel et al. 2003). Godefroit et al. (2017) further argued that the enlarged teeth of *Matheronodon* represent an adaptation for the crushing of tough and woody or fibrous food items. Taking the palaeobotanical data of various rhabdodontid-bearing localities into consideration, Godefroit et al. (2017) hypothesised that rhabdodontids fed primarily on tough plant parts with a high sclerenchyma fibre content, like the palms *Sabalites* and *Pandanites*, both of which are known from the Campanian Grünbach Formation of Austria (Kvaček and Herman 2004), the Maastrichtian of north-eastern

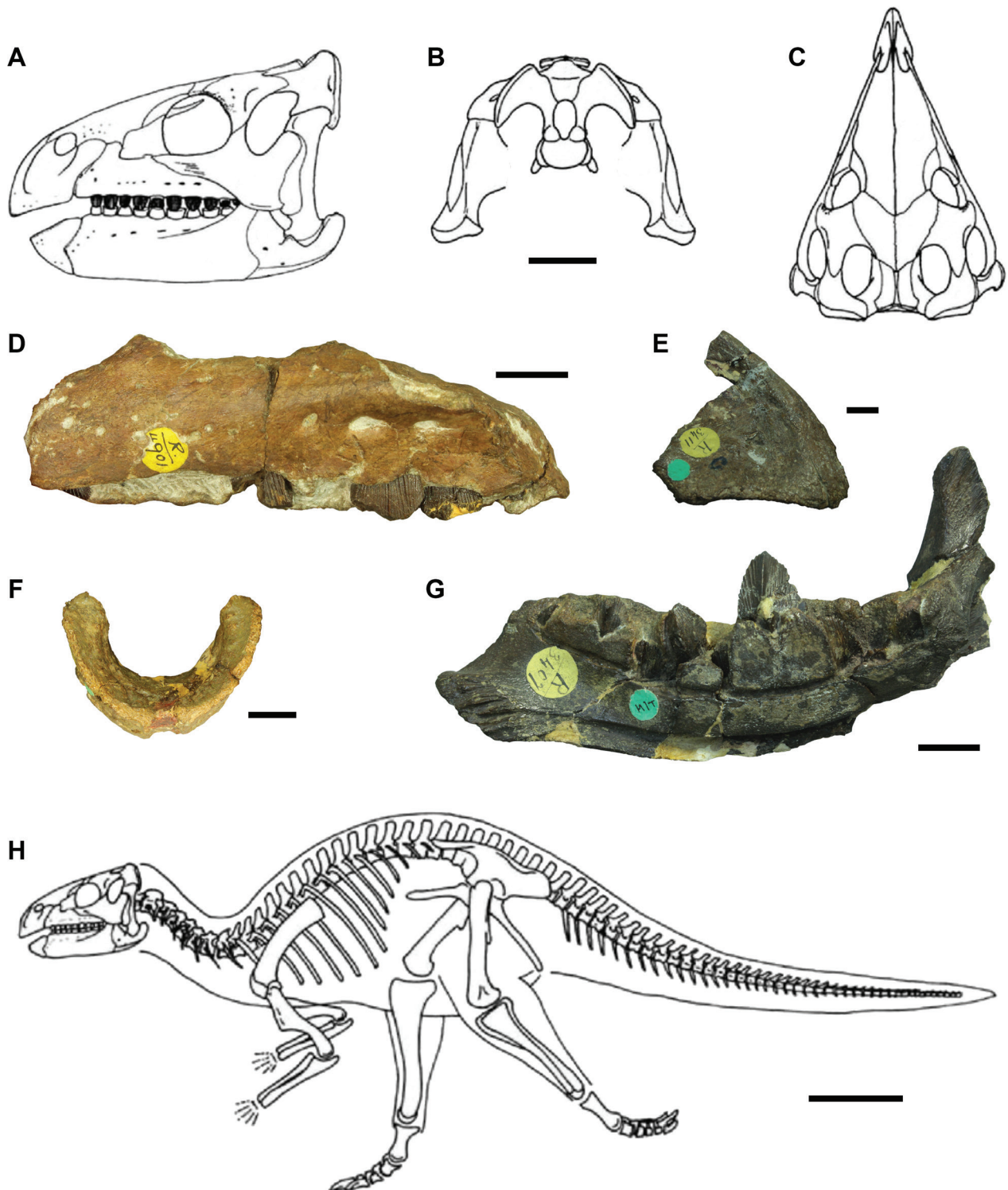


Figure 5. Anatomy of the Rhabdodontidae. A–C. Skull reconstruction of *Z. robustus* in left lateral view (A), posterior view (B), and dorsal view (C). Modified after Weishampel et al. (2003). D. Maxillary of *Z. robustus* (NHMUK R.4901) in medial view. E. Premaxillary of *Z. robustus* (NHMUK R.3411) in right lateral view. F. Prementary of *Z. robustus* (NHMUK R.3410) in dorsal view. G. Right dentary of *Z. robustus* (NHMUK R.3407) in medial view. H. Skeletal reconstruction of *Zalmoxes robustus*. Modified after Weishampel et al. (2003). All specimens figured (i.e. D–G) are historical Nopcsa specimens from his Quarry 1 (for details, see text). Photos (D–G) kindly provided by János Magyar. Scale bars: 5 cm (A–C); 1 cm (D–G); 20 cm (H).

Spain (Marmi et al. 2010, 2014) and the Maastrichtian of Transylvania (Popa et al. 2014).

Apart from cranial anatomy, two independent lines of evidence have also been used to infer the feeding ecology

of rhabdodontids – stable isotope analysis and multiproxy dentition analysis. Stable isotope analysis of rhabdodontid teeth from the Hațeg Basin suggested that these animals mainly ingested C3 plants (Bojar et al. 2010). Remarkably,

the similarity of $\delta^{13}\text{C}$ values between rhabdodontid and hadrosauroid teeth from the same locality of the Hațeg Basin was interpreted by Bojar et al. (2010) to reflect the absence of large-scale habitat partitioning between representatives of the two ornithopod clades. Furthermore, dental microwear analysis has been applied to teeth of *Mochlodon vorosi* from Iharkút (Hungary) revealing straight and parallel micro-striations that likely reflect orthal jaw movement, while the high tooth formation rates in this taxon imply an abrasive diet (Virág and Ósi 2017). The dental microwear pattern of *Mochlodon vorosi* further indicates that this animal was a low-browsing herbivore (browsing height up to 1 m above ground level) that fed on particularly tough vegetation (Ósi et al. 2022). Meanwhile, differences found in microwear pattern between this rhabdodontid and hadrosaurs likely reflect different feeding ecologies (Ósi et al. 2022), an observation that is consistent with (and explains) the large-scale habitat sharing of rhabdodontids and hadrosauroids noted in the Romanian faunas by Bojar et al. (2010). Despite a similar and partially overlapping browsing height in *Mochlodon* and hadrosaurs, the rhabdodontid probably fed on higher-growing plants, which were either tougher or were processed more vigorously (Ósi et al. 2022). Similarly, a different microwear pattern identified in the ankylosaurian *Hungarosaurus* (as compared to *M. vorosi*) demonstrates different feeding strategies and niche partitioning between these two sympatric herbivorous dinosaurs, with *Hungarosaurus* probably feeding on softer plants and/or processing its fodder less intensively (Ósi et al. 2022).

Recently, Augustin et al. (2022) suggested that niche partitioning was probably present between the two sympatric rhabdodontid genera from the Hațeg Basin, *Zalmoxes* and *Transylvanosaurus*. Although they attained a roughly similar body size, *Transylvanosaurus* differs considerably from the sympatric *Zalmoxes* in its cranial morphology having had a much wider and lower skull (Augustin et al. 2022). The markedly different skull proportions, such as a larger attachment site for *m. rectus capitis ventralis* and *m. protractor pterygoideus* in *Transylvanosaurus*, most likely were correlated with different development of the corresponding muscles involved in the feeding process (for details, see Augustin et al. 2022). Ultimately, such differences might reflect distinct feeding adaptations and corresponding niche partitioning between the sympatric rhabdodontids from the Hațeg Basin (Augustin et al. 2022). Generally, the co-occurrence of at least two rhabdodontid species was not uncommon: in the upper Campanian–lower Maastrichtian of north-eastern Spain, *Rhabdodon* sp. occurs alongside *Pareisactus evrostos* (Pereda-Suberbiola and Sanz 1999; Párraga and Prieto-Márquez 2019), while coeval deposits of southern France yielded the two species *Rhabdodon priscus* and *R. septimanicus*, as well as *Matheronodon provincialis* (Buffetaut and Le Loeuff 1991; Chanthasit 2010; Godefroit et al. 2017). Conversely, only one rhabdodontid has, so far, been described from the slightly older European deposits, including *Mochlodon vorosi* from the Santonian of western Hungary, *Mochlodon suessi* from the lower Campanian

of eastern Austria (Seeley 1881; Ósi et al. 2012) and cf. *Rhabdodon priscus* from the lower Campanian of southern France (Buffetaut et al. 1996). Apparently, the co-occurrence of at least two rhabdodontids is characteristic for the later part of their evolutionary history (i.e. Late Campanian–Maastrichtian), whereas single species occurrences are present earlier (i.e. during the Santonian–Early Campanian). The question of whether this pattern is a true evolutionary phenomenon or simply the result of a more extensive fossil record in the later part of the Late Cretaceous cannot be answered conclusively for the time being.

Interestingly, the different sympatric rhabdodontids largely overlapped in body size, as is the case for *Rhabdodon* and *Pareisactus* from northern Spain (Párraga and Prieto-Márquez 2019), *Rhabdodon* and *Matheronodon* from southern France (Chanthasit 2010; Godefroit et al. 2017), as well as *Zalmoxes* and *Transylvanosaurus* from western Romania (Weishampel et al. 2003; Ósi et al. 2012; Augustin et al. 2022). Whether niche partitioning was commonly present between the different sympatric rhabdodontids (as suggested for *Transylvanosaurus* and *Zalmoxes*) is currently unknown, but it is to be expected given their largely overlapping body sizes (and thus feeding heights/ranges). At least for some taxa, the different shapes and proportions of the dentaries (*Rhabdodon priscus* versus *R. septimanicus*), as well as that of the dentition itself (*Rhabdodon* versus *Matheronodon*), definitively suggest some kind of difference in skull shape and proportions and, accordingly, in feeding mechanisms and food preferences and, thus, some degree of niche partitioning. Such niche partitioning may be better understood in the future either based on new and more complete discoveries of these different taxa and/or by using other, complementary approaches. Several methods commonly used to reconstruct certain palaeoecological aspects in fossil vertebrates have yet to be applied rigorously to rhabdodontids. This includes, but is not limited to, stable isotope analysis of their bones and teeth, dental microwear analysis, finite element analysis, biomechanics and myological reconstructions. Some of these, but not others, have already been applied to select taxa; as outlined above, stable isotope analysis has only been used for *Zalmoxes* so far, while dental microwear analysis has only been used for *Mochlodon vorosi*.

In addition to the habitat preferences and feeding ecology of rhabdodontids, several remarks about their posture and locomotion have been made. In their monograph on *Zalmoxes*, Weishampel et al. (2003) noted that it was a medium-sized ornithopod with a comparatively stocky build (Fig. 5H), with several peculiarities of the postcranium suggesting that its locomotion differed from that of other ornithopods and that it had a particularly wide gait when walking and running. Subsequently, Dumbravă et al. (2013) reconstructed the musculature of the *Zalmoxes* hind limb, based mainly on the partial *Z. shqiperorum* skeleton from Nălaț-Vad (see also Godefroit et al. 2009) and other material from this locality, concluding that the rather ventral position of the fourth trochanter on the femur indicates that

Z. shqiperorum was not a particularly fast runner. Although rhabdodontids are mostly envisioned as bipedal animals (for *Zalmoxes*, see Weishampel et al. 1991: fig. 11 and Weishampel et al. 2003: fig. 36; for *Rhabdodon*, see Garcia et al. 1999: fig. 2; for *Mochlodon*, see Ösi et al. 2012: fig. 15), at least *Rhabdodon* was also portrayed as quadrupedal (Pincemaille-Quillevere 2002: fig. 1; Chanthasit 2010: p. 121). This uncertainty concerning the posture and locomotion of rhabdodontids is primarily due to a lack of relatively complete and articulated skeletons (albeit see Vremir et al. 2017). Even the most complete rhabdodontid skeletons described thus far (i.e. MHN AIX PV 199 assigned to *Rhabdodon priscus* and UBB NVZ1 assigned to *Zalmoxes shqiperorum*) lack substantial parts of the postcranium, such as the front limbs (in MHN AIX PV 199) or the majority of the vertebral column (in UBB NVZ1).

Recently, Dieudonné et al. (2023) used several proxies for the posture of ornithopods (based on hind limb morphology) to evaluate the possible posture of rhabdodontomorphs. They concluded that the ‘Vegagete ornithopod’ and *Mochlodon vorosi* switched from quadrupedality to bipedality during ontogeny, whereas *Muttaborrasaurus* and some derived rhabdodontids of the Late Cretaceous (i.e. *Zalmoxes* and *Rhabdodon*) retained a quadrupedal posture until late in ontogeny or even into adulthood. Moreover, based on the histology of long bones, these authors suggested that the rhabdodontomorph ‘Vegagete ornithopod’ grew very rapidly and likely had a high basal metabolic rate (Dieudonné et al. 2023). Conversely, the bone histology of *Zalmoxes* likely indicates relatively slow growth (Benton et al. 2010). Ösi et al. (2012) examined the growth stage of several different rhabdodontids based on histological thin sections of *Mochlodon vorosi*, *M. suessi*, *Zalmoxes robustus*, *Z. shqiperorum* and *Rhabdodon* spp. and concluded that they all had largely similar growth rates, despite their varying adult body sizes with reconstructed (sub-)adult body lengths of 1.4 m in *M. suessi*, 1.8 m in *M. vorosi*, 2.4 m in *Z. robustus*, 2.5 m in *Z. shqiperorum* and 5.9 m in *Rhabdodon* spp. Similarly, Prondvai (2014) found a consistent growth pattern in the three rhabdodontids examined (i.e. *Rhabdodon*, *Zalmoxes*, *Mochlodon*) that is characterised by the early onset of cyclical growth and secondary remodelling, although *Rhabdodon* seems to have undergone a prolonged phase of fast growth compared to *Zalmoxes* and *Mochlodon*. Interestingly, Ösi et al. (2012) were able to show that the ancestral body size of rhabdodontids was likely close to that of *Zalmoxes* by mapping the femoral length on to the results of their phylogenetic analysis. Therefore, *Zalmoxes* likely did not undergo dwarfism, as has been reconstructed for other dinosaurs from the latest Cretaceous Transylvanian Island, such as for the titanosaur *Magyarosaurus* (Stein et al. 2010) and, instead, *Rhabdodon* underwent autapomorphic gigantism, whereas *Mochlodon* might have been characterised by phylogenetic body size reduction (Ösi et al. 2012).

Interestingly, rhabdodontids seem to have died out well before the K/Pg extinction event in Western Europe (i.e. in the early late Maastrichtian), while they survived much

longer (i.e. well into the late Maastrichtian) in Eastern Europe (at the least, in Romania). In the Ibero-Armorican realm, the titanosaur-rhabdodontid-nodosaurid fauna of the Late Campanian–early Maastrichtian was replaced by a hadrosauroid-titanosaur dominated fauna in the later Maastrichtian, with rhabdodontids and nodosaurids apparently going extinct by the early late Maastrichtian, approximately 69 Ma ago (Le Loeuff et al. 1994; Buffetaut et al. 1997; Vila et al. 2016). Several vertebrate groups were affected by this faunal turnover in Ibero-Armorica, the main herbivores of the assemblage first of all; meanwhile and remarkably, such a faunal change did not occur in the Transylvanian realm despite the same clades being also represented there and all major herbivorous taxa appear to have survived for the quasi-entirety of the time span covered by the local fossil record, i.e. from the latest Campanian to late Maastrichtian (Csiki-Sava et al. 2016). Therefore, the Transylvanian landmass seems to be characterised by relatively higher-level faunal stability when compared to the Ibero-Armorican Island (Csiki-Sava et al. 2015, 2016). The reasons leading to the disappearance of rhabdodontids in Western Europe in the early late Maastrichtian are not entirely clear, but it has been hypothesised that palaeogeographic changes might have resulted in the immigration of new taxa on to the Ibero-Armorican landmass (Vila et al. 2016). In particular, the arrival of different clades of hadrosauroids and their subsequent dominance in the Maastrichtian faunas of the Ibero-Armorican Island might have caused the extinction of rhabdodontids, as they potentially occupied similar ecological niches (Vila et al. 2016; but see above). However, it cannot be ruled out that rhabdodontids (and nodosaurids) were already in decline because of another environmental or ecological factor(s) and hadrosauroids simply took advantage of unoccupied niches vacated through the demise of the former taxa (Vila et al. 2016).

One possible environmental factor that might have changed during this time interval, with impact on to the noted faunal replacement, is the nature of the primary producers, i.e. the structure and taxonomic composition of the vegetation supporting the megaherbivores. Although data from related forms in Western Europe are still scarce, tooth structure and tooth wear suggest that *Mochlodon* (and, by extension, possibly all rhabdodontids) and *Hungarosaurus* (and, by extension, possibly all struthiosaurine nodosaurids) show a tooth wear characterised by high number of pits, more typical of browsers (Ösi et al. 2022). The extremely wide teeth of *Matheronodon* were also adapted to cut tougher plant parts (Godefroit et al. 2017). In contrast, microwear patterns of hadrosauroid teeth are known to be scratch-dominated (Fiorillo 2011; Mallon and Anderson 2014; A. Ösi pers. obs.), which may indicate a fundamentally grazer-type lifestyle (Williams et al. 2009). What is clear concerning the faunal turnover in the western European fauna is that herbivorous groups with pit-dominated microwear patterns (rhabdodontids and nodosaurids) are followed by hadrosauroids with a scratch-dominated microwear pattern. This may indicate

a change in the available plant food, for example, the development of more open areas and the spread of a ‘grassland’-type ground vegetation. In contrast, the eastern part of the Archipelago may not have undergone such a dramatic change in flora, allowing rhabdodontids and nodosaurids to persist until the end of the Cretaceous. All this is only a hypothesis until at least more details of the floral record and evolution supports it. Regardless of the exact cause(s) of their demise in Western Europe, rhabdodontids survived until shortly before the K/Pg extinction event in Transylvania and were amongst the last non-avian dinosaurs still present before the end of the Cretaceous.

Acknowledgements

This contribution originated from, and took shape during, the PhD research activity of FJA, who would like to thank his two supervisors Hervé Bocherens and Andreas T. Matzke (both University of Tübingen) for their support and insightful discussions. AÖ was supported by the NKFIH OTKA K 131597 project. We would also like to thank János Magyar (Eötvös Loránd University, Budapest) and Eric Buffetaut (Paris Sciences et Lettres Research University) for providing several photos of rhabdodontid specimens. Finally, we are very grateful to the editor Florian Witzmann for his support during the publication process as well as to the two reviewers Daniel Madzia and Penélope Cruzado-Caballero for their comments and suggestions that significantly improved the quality of the manuscript.

References

- Abel O (1919) Die Stämme der Wirbeltiere. Vereinigung wissenschaftlicher Verleger Walter de Gruyter & Co., Berlin und Leipzig. <https://doi.org/10.5962/bhl.title.2114>
- Allain R, Suberbiola XP (2003) Dinosaurs of France. *Comptes Rendus Palevol* 2: 27–44. [https://doi.org/10.1016/S1631-0683\(03\)00002-2](https://doi.org/10.1016/S1631-0683(03)00002-2)
- Andrzejewski KA, Winkler DA, Jacobs LL (2019) A new basal ornithopod (Dinosauria: Ornithischia) from the Early Cretaceous of Texas. *PLoS ONE* 14: e0207935. <https://doi.org/10.1371/journal.pone.0207935>
- Augustin FJ, Bastiaans D, Dumbravă MD, Csiki-Sava Z (2022) A new ornithopod dinosaur, *Transylvanosaurus platycephalus* gen. et sp. nov. (Dinosauria: Ornithischia), from the Upper Cretaceous of the Hațeg Basin, Romania. *Journal of Vertebrate Paleontology* 42: e2133610. <https://doi.org/10.1080/02724634.2022.2133610>
- Augustin FJ, Csiki-Sava Z, Matzke AT, Botfalvai G, Rabi M (2021) A new latest Cretaceous pleurodiran turtle (Testudinata: *Dortokidae*) from the Hațeg Basin (Romania) documents end-Cretaceous faunal provinciality and selective survival during the K-Pg extinction. *Journal of Systematic Palaeontology* 19: 1059–1081. <https://doi.org/10.1080/14772019.2021.2009583>
- Augustin FJ, Dumbravă MD, Bastiaans D, Csiki-Sava Z (2023) Reappraisal of the braincase anatomy of the ornithopod dinosaurs *Telmatosaurus* and *Zalmoxes* from the Upper Cretaceous of the Hațeg Basin (Romania) and the taxonomic reassessment of some previously referred specimens. *PalZ* 97: 129–145. <https://doi.org/10.1007/s12542-022-00621-x>
- Barta DE, Norell MA (2021) The osteology of *Haya griva* (Dinosauria: Ornithischia) from the Late Cretaceous of Mongolia. *Bulletin of the American Museum of Natural History* 445: 1–111. <https://doi.org/10.1206/0003-0090.445.1.1>
- Bartholomai A, Molnar RE (1981) *Muttaborrasaurus*, a new iguanodontid (Ornithischia: Ornithopoda) dinosaur from the Lower Cretaceous of Queensland. *Memoirs of the Queensland Museum* 20: 319–349.
- Bell PR, Brougham T, Herne MC, Frauenfelder T, Smith ET (2019) *Fostoria dhimbangunmal*, gen. et sp. nov., a new iguanodontian (Dinosauria, Ornithopoda) from the mid-Cretaceous of Lightning Ridge, New South Wales, Australia. *Journal of Vertebrate Paleontology* 39: e1564757. <https://doi.org/10.1080/02724634.2019.1564757>
- Bell PR, Herne MC, Brougham T, Smith ET (2018) Ornithopod diversity in the Griman Creek Formation (Cenomanian), New South Wales, Australia. *PeerJ* 6: e6008. <https://doi.org/10.7717/peerj.6008>
- Benton MJ, Csiki Z, Grigorescu D, et al (2010) Dinosaurs and the island rule: the dwarfed dinosaurs from Hațeg Island. *Palaeogeography, Palaeoclimatology, Palaeoecology* 293: 438–454. <https://doi.org/10.1016/j.palaeo.2010.01.026>
- Blanco A (2021) Importance of the postcranial skeleton in eusuchian phylogeny: reassessing the systematics of allodaposuchid crocodylians. *PLoS ONE* 16: e0251900. <https://doi.org/10.1371/journal.pone.0251900>
- Blanco A, Brochu CA (2017) Intra- and interspecific variability in allodaposuchid crocodylomorphs and the status of western European taxa. *Historical Biology* 29: 495–508. <https://doi.org/10.1080/08912963.2016.1201081>
- Bojar A-V, Csiki Z, Grigorescu D (2010) Stable isotope distribution in Maastrichtian vertebrates and paleosols from the Hațeg Basin, South Carpathians. *Palaeogeography, Palaeoclimatology, Palaeoecology* 293: 329–342. <https://doi.org/10.1016/j.palaeo.2009.08.027>
- Botfalvai G, Csiki-Sava Z, Grigorescu D, Vasile Ș (2017) Taphonomical and palaeoecological investigation of the Late Cretaceous (Maastrichtian) Tuștea vertebrate assemblage (Romania; Hațeg Basin) - insights into a unique dinosaur nesting locality. *Palaeogeography, Palaeoclimatology, Palaeoecology* 468: 228–262. <https://doi.org/10.1016/j.palaeo.2016.12.003>
- Boyd CA (2015) The systematic relationships and biogeographic history of ornithischian dinosaurs. *PeerJ* 3: e1523. <https://doi.org/10.7717/peerj.1523>
- Brinkmann W (1986) *Rhabdodon* Matheron, 1869 (Reptilia, Ornithischia): proposed conservation by suppression of *Rhabdodon* Fleishmann, 1831 (Reptilia, Serpentes). *Bulletin of Zoological Nomenclature* 43: 269–272. <https://doi.org/10.5962/bhl.part.447>
- Brinkmann W (1988) Zur Fundgeschichte und Systematik der Ornithopoden (Ornithischia, Reptilia) aus der Ober-Kreide von Europa. *Documenta Naturae* 45: 1–157.
- Brusatte SL, Dumbravă M, Vremir M, Csiki-Sava Z, Totoianu R, Norell MA (2017) A catalog of *Zalmoxes* (Dinosauria: Ornithopoda) specimens from the Upper Cretaceous Nălaț-Vad locality, Hațeg Basin, Romania. *American Museum Novitates* 3884: 1–36. <https://doi.org/10.1206/3884.1>
- Brusatte SL, Vremir M, Watanabe A, Csiki-Sava Z (2013) An infant ornithopod dinosaur tibia from the Late Cretaceous of Sebes, Romania. *Terra Sebus, Acta Musei Sabesiensis* 5: 627–644.

- Buffetaut E, Costa G, Le Loeuff J, Michel M, Jean-Claude R, Xavier V, Haiyan T (1996) An Early Campanian vertebrate fauna from the Villeveyrac Basin (Hérault, Southern France). *Neues Jahrbuch für Geologie und Paläontologie - Monatshefte* 1(1996): 1–16. <https://doi.org/10.1127/njgpm/1996/1996/1>
- Buffetaut E, Le Loeuff J (1991) Une nouvelle espèce de *Rhabdodon* (Dinosauria, Ornithischia) du Crétacé supérieur de l'Hérault (Sud de la France). *Comptes Rendus de l'Académie des Sciences, Sér 2, Mécanique, physique, chimie, sciences de l'univers, sciences de la terre* 312: 943–948.
- Buffetaut E, Le Loeuff J, Cavin L, Duffaud S, Gheerbrant E, Laurent Y, Martin M, Rage J-C, Tong H, Vasse D (1997) Late Cretaceous non-marine vertebrates from southern France: A review of recent finds. *Geobios* 30: 101–108. [https://doi.org/10.1016/S0016-6995\(97\)80015-0](https://doi.org/10.1016/S0016-6995(97)80015-0)
- Bunzel E (1871) Die Reptilfauna der Gosau-Formation in der Neuen Welt bei Wiener-Neustadt. *Abhandlungen der Kaiserlich Königlichen Geologischen Reichsanstalt* 5: 1–18.
- Butler RJ, Upchurch P, Norman DB (2008) The phylogeny of the ornithischian dinosaurs. *Journal of Systematic Palaeontology* 6: 1–40. <https://doi.org/10.1017/S1477201907002271>
- Chanthasit P (2010) The ornithopod dinosaur *Rhabdodon* from the Late Cretaceous of France: anatomy, systematics and paleobiology. Université Claude Bernard.
- Codrea V, Vremir M, Jipa C, Godefroit P, Csiki Z, Smith T, Fărcaș C (2010) More than just Nopcsa's Transylvanian dinosaurs: A look outside the Hațeg Basin. *Palaeogeography, Palaeoclimatology, Palaeoecology* 293: 391–405. <https://doi.org/10.1016/j.palaeo.2009.10.027>
- Codrea VA, Godefroit P (2008) New Late Cretaceous dinosaur findings from northwestern Transylvania (Romania). *Comptes Rendus Palevol* 7: 289–295. <https://doi.org/10.1016/j.crpv.2008.03.008>
- Codrea VA, Vremir M, Jipa C, et al. (2012) First discovery of Maastrichtian (latest Cretaceous) terrestrial vertebrates in Rusca Montană Basin (Romania). In: Godefroit P (Ed.) *Bernissart Dinosaurs and Early Cretaceous Terrestrial Ecosystems*. Indiana University Press, Bloomington, 570–581.
- Cooper MR (1985) A revision of the ornithischian dinosaur *Kangnasaurus coetzeei* Haughton, with a classification of the Ornithischia. *Annals of the South African Museum* 95: 281.
- Csiki Z, Grigorescu D, Codrea VA, Therrien F (2010) Taphonomic modes in the Maastrichtian continental deposits of the Hațeg Basin, Romania – palaeoecological and palaeobiological inferences. *Palaeogeography, Palaeoclimatology, Palaeoecology* 293: 375–390. <https://doi.org/10.1016/j.palaeo.2009.10.013>
- Csiki-Sava Z, Buffetaut E, Ősi A, Pereda-Suberbiola X, Brusatte SL (2015) Island life in the Cretaceous – faunal composition, biogeography, evolution, and extinction of land-living vertebrates on the Late Cretaceous European archipelago. *ZooKeys* 469: 1–161. <https://doi.org/10.3897/zookeys.469.8439>
- Csiki-Sava Z, Vremir M, Vasile Ș, Brusatte SL, Dyke G, Naish D, Norell MA, Totoianu R (2016) The east side story – the Transylvanian latest Cretaceous continental vertebrate record and its implications for understanding Cretaceous–Paleogene boundary events. *Cretaceous Research* 57: 662–698. <https://doi.org/10.1016/j.cretres.2015.09.003>
- Cuthbertson RS, Tirabasso A, Rybczynski N, Holmes RB (2012) Kinetic limitations of intracranial joints in *Brachylophosaurus canadensis* and *Edmontosaurus regalis* (Dinosauria: Hadrosauridae), and their implications for the chewing mechanics of hadrosaurids. *The Anatomical Record* 295: 968–979. <https://doi.org/10.1002/ar.22458>
- Dieudonné PE, Baldor FT-F, Huerta-Hurtado P (2020) Unrelated ornithopods with similar tooth morphology in the vicinity of Salas de los Infantes (Burgos Province, Spain): an intriguing case-study. *Journal of Iberian Geology* 46: 403–417. <https://doi.org/10.1007/s41513-020-00140-1>
- Dieudonné P-E, Cruzado-Caballero P, Godefroit P, Tortosa T (2021) A new phylogeny of cerapodan dinosaurs. *Historical Biology* 33: 2335–2355. <https://doi.org/10.1080/08912963.2020.1793979>
- Dieudonné P-É, Fernández-Baldor FT, Stein K (2023) Histogenesis and growth dynamics of the tiny Vegagete rhabdodontomorph hindlimb (Ornithischia, Ornithopoda): Paleoeological and evolutionary implications. *Cretaceous Research* 141: 105342. <https://doi.org/10.1016/j.cretres.2022.105342>
- Dieudonné P-E, Tortosa T, Torcida Fernández-Baldor FT, Canudo JJ, Díaz-Martínez I (2016) An unexpected early rhabdodontid from Europe (Lower Cretaceous of Salas de los Infantes, Burgos Province, Spain) and a re-examination of basal iguanodontian relationships. *PLoS ONE* 11: e0156251. <https://doi.org/10.1371/journal.pone.0156251>
- Dumbravă M, Codrea VA, Solomon A, Razvan A (2013) Hind leg myology of the Maastrichtian (latest Cretaceous) euornithischian dinosaur *Zalmoxes shquiperorum* from the Hațeg Basin, Romania: preliminary data. *Oltenia Studii și comunicări Științele Naturii* 29: 7–18.
- Fiorillo AR (2011) Microwear patterns on the teeth of northern high latitude hadrosaurs with comments on microwear patterns in hadrosaurs as a function of latitude and seasonal ecological constraints. *Palaeontologia Electronica* 14: 1–17.
- Fleischmann FL (1831) *Dalmatiae Nova Serpantum Genera*. Heyder, Erlangen.
- García G, Pincemaille M, Vianey-Liaud M, Marandat B, Lorenz E, Cheylan G, Cappetta H, Michaux J, Sudre J (1999) Découverte du premier squelette presque complet de *Rhabdodon priscus* (Dinosauria, Ornithopoda) du Maastrichtien inférieur de Provence. *Comptes Rendus de l'Académie des Sciences - Series IIA - Earth and Planetary Science* 328: 415–421. [https://doi.org/10.1016/S1251-8050\(99\)80108-6](https://doi.org/10.1016/S1251-8050(99)80108-6)
- Gheerbrant E, Teodori D (2021) An enigmatic specialized new eutherian mammal from the Late Cretaceous of Western Europe (Northern Pyrenees). *Comptes Rendus Palevol* 20: 207–223. <https://doi.org/10.5852/cr-palevol2021v20a13>
- Godefroit P, Codrea V, Weishampel DB (2009) Osteology of *Zalmoxes shquiperorum* (Dinosauria, Ornithopoda), based on new specimens from the Upper Cretaceous of Nălaț-Vad (Romania). *Geodiversitas* 31: 525–553. <https://doi.org/10.5252/g2009n3a3>
- Godefroit P, García G, Gomez B, Stein K, Cincotta A, Lefèvre U, Valentin X (2017) Extreme tooth enlargement in a new Late Cretaceous rhabdodontid dinosaur from Southern France. *Scientific Reports* 7: 13098. <https://doi.org/10.1038/s41598-017-13160-2>
- Grigorescu D (2010) The Latest Cretaceous fauna with dinosaurs and mammals from the Hațeg Basin – a historical overview. *Palaeogeography, Palaeoclimatology, Palaeoecology* 293: 271–282. <https://doi.org/10.1016/j.palaeo.2010.01.030>
- Grigorescu D (1983) A stratigraphic, taphonomic and paleoecologic approach to a “forgotten land”: the dinosaur-bearing deposits from the Hațeg Basin (Transylvania-Romania). *Acta Palaeontologica Polonica* 28: 103–121.
- Herne MC, Nair JP, Evans AR, Tait AM (2019) New small-bodied ornithopods (Dinosauria, Neornithischia) from the Early Cretaceous Wonthaggi Formation (Strzelecki Group) of the Australian-Antarctic rift system, with revision of *Qantassaurus intrepidus* Rich and

- Vickers-Rich, 1999. *Journal of Paleontology* 93: 543–584. <https://doi.org/10.1017/jpa.2018.95>
- Holliday CM, Witmer LM (2008) Cranial kinesis in dinosaurs: intracranial joints, protractor muscles, and their significance for cranial evolution and function in diapsids. *Journal of Vertebrate Paleontology* 28: 1073–1088. <https://doi.org/10.1671/0272-4634-28.4.1073>
- Huene F von (1956) *Paläontologie und Phylogenie der niederen Tetrapoden*. Gustav Fischer Verlag, Jena.
- International Commission on Zoological Nomenclature (1988) Opinion 1483. *Rhabdodon* Matheron, 1869 (Reptilia, Ornithischia): conserved. *Bulletin of Zoological Nomenclature* 45: 85–86.
- Jianu C-M (1994) A right dentary of *Rhabdodon priscus* Matheron 1869 (Reptilia: Ornithischia) from the Maastrichtian of the Hateg Basin (Romania). *Sargetia* 16: 29–35.
- Kvaček J, Herman AB (2004) Monocotyledons from the Early Campanian (Cretaceous) of Grünbach, Lower Austria. *Review of Palaeobotany and Palynology* 128: 323–353. [https://doi.org/10.1016/S0034-6667\(03\)00154-4](https://doi.org/10.1016/S0034-6667(03)00154-4)
- Lapparent AF de (1947) Les dinosauriens du Crétacé supérieur du Midi de la France. *Mémoires de la Société géologique de France* 26: 1–54.
- Le Loeuff J, Buffetaut E, Martin M (1994) The last stages of dinosaur faunal history in Europe: a succession of Maastrichtian dinosaur assemblages from the Corbières (southern France). *Geological Magazine* 131: 625–630. <https://doi.org/10.1017/S0016756800012413>
- Madzia D, Boyd CA, Mazuch M (2018) A basal ornithomimid dinosaur from the Cenomanian of the Czech Republic. *Journal of Systematic Palaeontology* 16: 967–979. <https://doi.org/10.1080/14772019.2017.1371258>
- Madzia D, Jagt JWM, Mulder EWA (2020) Osteology, phylogenetic affinities and taxonomic status of the enigmatic late Maastrichtian ornithomimid taxon *Orthomerus dolloi* (Dinosauria, Ornithischia). *Cretaceous Research* 108: 104334. <https://doi.org/10.1016/j.cretres.2019.104334>
- Madzia D, Arbour VM, Boyd CA, Farke AA, Cruzado-Caballero P, Evans DC (2021) The phylogenetic nomenclature of ornithischian dinosaurs. *PeerJ* 9: e12362. <https://doi.org/10.7717/peerj.12362>
- Mallon JC, Anderson JS (2014) The functional and palaeoecological implications of tooth morphology and wear for the megaherbivorous dinosaurs from the Dinosaur Park Formation (upper Campanian) of Alberta, Canada. *PLoS ONE* 9: e98605. <https://doi.org/10.1371/journal.pone.0098605>
- Marmi J, Gomez B, Martín-Closas C, Villalba-Breva S, Daviero-Gomez V (2014) Diversified fossil plant assemblages from the Maastrichtian in Isona (southeastern Pyrenees). *Review of Palaeobotany and Palynology* 206: 45–59. <https://doi.org/10.1016/j.revpalbo.2014.03.003>
- Marmi J, Gomez B, Martín-Closas C, Villalba-Breva S (2010) A reconstruction of the fossil palm *Sabalites longirhachis* (Unger) J. Kvaček et Herman from the Maastrichtian of Pyrenees. *Review of Palaeobotany and Palynology* 163: 73–83. <https://doi.org/10.1016/j.revpalbo.2010.10.007>
- Maryanska T, Osmólska H (1985) On ornithischian phylogeny. *Acta Palaeontologica Polonica* 30: 137–150.
- Matheron P (1869) Notice sur les reptiles fossiles des dépôts fluviolacustres crétacés du bassin à lignite de Fuveau. *Mémoires de l'Académie impériale des Sciences, Belles-Lettres et Arts de Marseille*, 1–39.
- Matheron P (1846) Sur les terrains traversés par le souterrain de la Nerthe, près Marseille. *Bulletin de la Société géologique de France* 4: 261–269.
- Matheron P (1892) Sur les animaux vertébrés dans les couches d'eau douce crétacées du midi de la France. *Compte Rendu de la Association Française pour l'Avancement des Sciences* 20: 382–383.
- McDonald AT (2012) Phylogeny of basal iguanodonts (Dinosauria: Ornithischia): An update. *PLoS ONE* 7: e36745. <https://doi.org/10.1371/journal.pone.0036745>
- McDonald AT, Kirkland JJ, DeBlieux DD, Madsen SK, Cavin J, Milner AR, Panzarin L (2010) New Basal Iguanodonts from the Cedar Mountain Formation of Utah and the Evolution of Thumb-Spiked Dinosaurs. *PLoS ONE* 5: e14075. <https://doi.org/10.1371/journal.pone.0014075>
- Milner AR, Norman DB (1984) The biogeography of advanced ornithomimid dinosaurs (Archosauria: Ornithischia)—a cladistic-vicariance model. In: Reif W-E, Westphal F (Eds) *Third Symposium on Mesozoic Terrestrial Ecosystems, Short Papers*. Attempto Verlag, Tübingen, 145–150.
- Müller AH (1968) *Lehrbuch der Paläozoologie*. Band III Vertebraten: Teil 2: Reptilien und Vögel. Gustav Fischer Verlag, Jena.
- Narváez I, Brochu CA, Escaso F, Pérez-García A, Ortega F (2016) New Spanish Late Cretaceous eusuchian reveals the synchronic and sympatric presence of two allodaposuchids. *Cretaceous Research* 65: 112–125. <https://doi.org/10.1016/j.cretres.2016.04.018>
- Nopcsa F (1897) Vorläufiger Bericht über das Auftreten von oberer Kreide im Hátszeg Thale in Siebenbürgen. *Verhandlungen der kaiserlich-königlichen Akademie der Wissenschaften* 14: 273–274.
- Nopcsa F (1899a) Jegyzetek Hátszeg vidékének geológiájához. *Földtani Közlöny* 29: 332–335.
- Nopcsa F (1899b) Bemerkungen zur Geologie der Gegend von Hátszeg. *Földtani Közlöny* 29: 360–362.
- Nopcsa F (1900) Dinosaurierreste aus Siebenbürgen I: Schädel von *Limnosaurus transylvanicus* nov. gen et sp. *Denkschriften der königlichen Akademie der Wissenschaften Mathematisch-Naturwissenschaftliche Classe* 68: 555–591.
- Nopcsa F (1901) Synopsis und Abstammung der Dinosaurier. *Földtani Közlöny* 31: 247–279.
- Nopcsa F (1902) Dinosaurierreste aus Siebenbürgen II. Schädelreste von *Mochlodon*. Mit einem Anhang: zur Phylogenie der Ornithomimiden. *Denkschriften der königlichen Akademie der Wissenschaften Mathematisch-Naturwissenschaftliche Klasse* 72: 149–175.
- Nopcsa F (1903) Sitzung der mathematisch-naturwissenschaftlichen Klasse vom 4. Juni 1903. Sonderabdruck aus dem akademischen Anzeiger 14.
- Nopcsa F (1904) Dinosaurierreste aus Siebenbürgen III. Weitere Schädelreste von *Mochlodon*. *Denkschriften der königlichen Akademie der Wissenschaften Mathematisch-Naturwissenschaftliche Klasse*, Wien 74: 229–263.
- Nopcsa F (1905) Zur Geologie der Gegend zwischen Gyulafehervár, Déva, Ruzskabanya und der Rumänischen Landesgrenze. *Mitteilungen aus dem Jahrbuche der königlich ungarischen geologischen Reichsanstalt, Budapest* 14: 93–279.
- Nopcsa F (1914) Die Lebensbedingungen der obercretacischen Dinosaurier Siebenbürgens. *Centralblatt für Mineralogie, Geologie und Paläontologie*, 564–574.
- Nopcsa F (1915) Die Dinosaurier der siebenbürgischen Landesteile Ungarns. *Mitteilungen aus dem Jahrbuche der königlich ungarischen geologischen Reichsanstalt, Budapest* 23: 3–24.
- Nopcsa F (1923) On the geological importance of the primitive reptilian fauna in the uppermost Cretaceous of Hungary; with a description of a new tortoise (*Kallokibotio*). *Quarterly Journal of*

- the Geological Society 79: 100–116. <https://doi.org/10.1144/GSL.JGS.1923.079.01-04.08>
- Normcsa F (1925) Dinosaurierreste aus Siebenbürgen IV. Die Wirbelsäule von Rhabdodon und Orthomerus. *Palaeontologica Hungarica* 1: 273–304.
- Normcsa F (1929) Sexual differences in ornithopodous dinosaurs. *Palaeobiologica* 2: 188–201.
- Normcsa F (1934) The Influence of Geological and Climatological Factors on the Distribution of Non-Marine Fossil Reptiles and Stegocephalia. *Quarterly Journal of the Geological Society* 90: 76–140. <https://doi.org/10.1144/GSL.JGS.1934.090.01-04.05>
- Norman DB (1984) A systematic reappraisal of the reptile order Ornithischia. In: Reif W-E, Westphal F (Eds) *Third Symposium on Mesozoic Terrestrial Ecosystems, Short Papers*. Attempto Verlag, Tübingen, 157–162.
- Norman DB (1985) On the cranial morphology and evolution of ornithopod dinosaurs. In: Hearn JP, Hodges JK, Zoological Society of London (Eds) *Advances in animal conservation: the proceedings of a symposium held at the Zoological Society of London on 31st May and 1st June 1984*. Clarendon Press, Oxford University Press, Oxford [Oxfordshire]: New York, 521–547.
- Norman DB (1990) A review of *Vectisaurus*, with comments on the family Iguanodontidae. In: Carpenter K, Currie PJ (Eds) *Dinosaur systematics: approaches and perspectives*. Cambridge University Press, Cambridge, 147–161. <https://doi.org/10.1017/CBO9780511608377.014>
- Norman DB, Weishampel DB (1990) Iguanodontidae and related ornithopods. In: Weishampel DB, Dodson P, Osmólska H (Eds) *The Dinosauria*. University of California Press, Berkeley, 510–533.
- Norman DB (2004) Basal Iguanodontia. In: Weishampel DB, Dodson P, Osmólska H (Eds) *The Dinosauria*, 2nd ed. University of California Press, Berkeley, 413–437. <https://doi.org/10.1525/california/9780520242098.003.0022>
- Ortega F, Bardet N, Barroso-Barcenilla F, Callapez PM, Cambra-Moo O, Daviero-Gómez V, Díez Díaz V, Domingo L, Elvira A, Escaso F, García-Oliva M, Gómez B, Houssaye A, Knoll F, Marcos-Fernández F, Martín M, Mocho P, Narváez I, Pérez-García A, Peyrot D, Segura M, Serrano H, Torices A, Vidal D, Sanz JL (2015) The biota of the Upper Cretaceous site of Lo Hueco (Cuenca, Spain). *Journal of Iberian Geology* 41: 83–99. https://doi.org/10.5209/rev_JIGE.2015.v41.n1.48657
- Ortega F, Escaso F, Gasulla JM, Dantas P, Sanz JL (2006) Dinosaurios de la Península Ibérica. *Estudios Geológicos* 62: 219–240. <https://doi.org/10.3989/egol.0662122>
- Ősi A (2004) The first dinosaur remains from the Upper Cretaceous of Hungary (Csehbánya Formation, Bakony Mts). *Geobios* 37: 749–753. <https://doi.org/10.1016/j.geobios.2003.06.005>
- Ősi A, Barrett PM, Evans AR, Nagy AL, Szenti I, Kukovecz Á, Magyar J, Segesdi M, Gere K, Jón V (2022) Multi-proxy dentition analyses reveal niche partitioning between sympatric herbivorous dinosaurs. *Scientific Reports* 12: 20813. <https://doi.org/10.1038/s41598-022-24816-z>
- Ősi A, Prondvai E, Butler RJ, Weishampel DB (2012) Phylogeny, histology and inferred body size evolution in a new rhabdodontid dinosaur from the Late Cretaceous of Hungary. *PLoS One* 7: e44318. <https://doi.org/10.1371/journal.pone.0044318>
- Párraga J, Prieto-Márquez A (2019) *Pareisactus evrostos*, a new basal iguanodontian (Dinosauria: Ornithopoda) from the Upper Cretaceous of southwestern Europe. *Zootaxa* 4555: 247–258. <https://doi.org/10.11646/zootaxa.4555.2.5>
- Pereda-Suberbiola X, Corral JC, Astibia H, Badiola A, Bardet N, Berreteaga A, Buffetaut E, Buscalioni A, Cappetta H, Cavin L, Díez Díaz V, Gheerbrant E, Murelaga X, Ortega F, Pérez-García A, Poyato-Ariza F, Rage J-C, Sanz J, Torices A (2015) Late cretaceous continental and marine vertebrate assemblages from the Laño quarry (Basque-Cantabrian Region, Iberian Peninsula): an update. *Journal of Iberian Geology* 41: 101–124. https://doi.org/10.5209/rev_JIGE.2015.v41.n1.48658
- Pereda-Suberbiola X, Sanz JL (1999) The ornithopod dinosaur *Rhabdodon* from the upper Cretaceous of Laño (Iberian Peninsula). *Estudios del Museo de Ciencias Naturales de Alava* 14: 257–272.
- Pincemaille-Quillevere M (2002) Description d'un squelette partiel de *Rhabdodon priscus* (Euornithopoda) du Crétacé supérieur de Vitrolles (Bouches du Rhône, France). *Oryctos* 4: 39–70.
- Pincemaille-Quillevere M, Buffetaut E, Quillevere F (2006) Osteological description of the braincase of *Rhabdodon* (Dinosauria, Euornithopoda) and phylogenetic implications. *Bulletin de la Société Géologique de France* 177: 97–104. <https://doi.org/10.2113/gssgfbull.177.2.97>
- Poole K (2022) Phylogeny of iguanodontian dinosaurs and the evolution of quadrupedality. *Palaeontol Electron* 25: 1–65. <https://doi.org/10.26879/702>
- Popa ME, Kvaček J, Vasile Ş, Csiki-Sava Z (2014) Maastrichtian monocotyledons of the Rusca Montană and Hațeg basins, South Carpathians, Romania. *Review of Palaeobotany and Palynology* 210: 89–101. <https://doi.org/10.1016/j.revpalbo.2014.08.004>
- Prondvai E (2014) Comparative bone histology of rhabdodontid dinosaurs. *Palaeovertebrata* 38: e1. <https://doi.org/10.18563/pv.38.2.e1>
- Rabi M, Vremir M, Tong H (2013) Preliminary overview of Late Cretaceous turtle diversity in eastern central Europe (Austria, Hungary, and Romania). In: Brinkman D, Holroyd P, Gardner J (Eds) *Morphology and Evolution of Turtles. Vertebrate Paleobiology and Paleoanthropology*. Springer, Dordrecht, 307–336. https://doi.org/10.1007/978-94-007-4309-0_19
- Romer AS (1933) *Vertebrate paleontology*. University of Chicago Press, Chicago. <https://doi.org/10.2307/1437149>
- Romer AS (1956) *Osteology of the reptiles*. University of Chicago Press, Chicago.
- Romer AS (1945) *Vertebrate paleontology*. 2nd Edn. University of Chicago Press, Chicago.
- Rybczynski N, Błoskie A, Tirabasso A, Błoskie P, Cuthbertson R, Holliday CM (2008) A three-dimensional animation model of *Edmontosaurus* (Hadrosauridae) for testing chewing hypotheses. *Palaeontologia Electronica* 11: 1–14.
- Sachs S, Hornung JJ (2006) Juvenile ornithopod (Dinosauria: Rhabdodontidae) remains from the Upper Cretaceous (Lower Campanian, Gosau Group) of Muthmannsdorf (Lower Austria). *Geobios* 39: 415–425. <https://doi.org/10.1016/j.geobios.2005.01.003>
- Seeley HG (1881) The reptile fauna of the Gosau Formation preserved in the Geological Museum of the University of Vienna: with a note on the geological horizon of the fossils at Neue Welt, west of Wiener Neustadt, by Edw. Suess, Ph.D., F.M.G.S., &c., Professor of Geology in the University of Vienna, &c. *Quarterly Journal of the Geological Society* 37: 620–706. <https://doi.org/10.1144/GSL.JGS.1881.037.01-04.49>
- Sereno PC (1986) Phylogeny of the bird-hipped dinosaurs. *National Geographic Research* 2: 234–256.
- Sereno PC (1984) The phylogeny of the Ornithischia: a reappraisal. In: Reif W-E, Westphal F (Eds) *Third Symposium on Mesozoic Terrestrial Ecosystems, Short Papers*. Attempto Verlag, Tübingen, 219–226.

- Sereno PC (2005) Stem Archosauria—TaxonSearch. <http://taxonsearch.uchicago.edu/> [Accessed 7 August 2023]
- Steel R (1969) Handbuch der Paläoherpetologie - Encyclopedia of Paleoherpertology. Part 15: Ornithischia. Gustav Fischer Verlag, Stuttgart.
- Stein K, Csiki Z, Rogers KC, Weishampel DB, Redelstorff R, Carballido JL, Sander PM (2010) Small body size and extreme cortical bone remodeling indicate phyletic dwarfism in *Magyarosaurus dacus* (Sauropoda: Titanosauria). PNAS 107: 9258–9263. <https://doi.org/10.1073/pnas.1000781107>
- Summesberger H, Machalski M, Wagneich M (2007) First record of the late Campanian heteromorph ammonite *Nostoceras hyatti* from the Alpine Cretaceous (Grünbach, Gosau Group, Lower Austria). Acta Geologica Polonica 57: 443–451.
- Taquet P (2001) Philippe Matheron et Paul Gervais: deux pionniers de la découverte et de l'étude des os et des œufs de dinosaures de Provence (France). Geodiversitas 23: 611–623.
- Therrien F (2006) Depositional environments and fluvial system changes in the dinosaur-bearing Sânpetru Formation (Late Cretaceous, Romania): post-orogenic sedimentation in an active extensional basin. Sedimentary Geology 192: 183–205. <https://doi.org/10.1016/j.sedgeo.2006.04.002>
- Therrien F, Zelenitsky DK, Weishampel DB (2009) Palaeoenvironmental reconstruction of the Late Cretaceous Sânpetru Formation (Hațeg Basin, Romania) using paleosols and implications for the “disappearance” of dinosaurs. Palaeogeography, Palaeoclimatology, Palaeoecology 272: 37–52. <https://doi.org/10.1016/j.palaeo.2008.10.023>
- Valentin X, Godefroit P, Tabuce R, Vianey-Liaud M, Wu W, Garcia G (2012) First Late Maastrichtian (Latest Cretaceous) Vertebrate Assemblages from Provence (Vitrolles-la-Plaine, Southern France). In: Godefroit P (Ed.) Bernissart dinosaurs and early Cretaceous terrestrial ecosystems. Indiana University Press, Bloomington, 583–597.
- Verdú FJ, Royo-Torres R, Cobos A, Alcalá L (2020) Systematics and paleobiology of a new articulated axial specimen referred to *Iguanodon cf. galvensis* (Ornithopoda, Iguanodontoida). Journal of Vertebrate Paleontology 40: e1878202. <https://doi.org/10.1080/02724634.2021.1878202>
- Verdú FJ, Royo-Torres R, Cobos A, Alcalá L (2018) New systematic and phylogenetic data about the early Barremian *Iguanodon galvensis* (Ornithopoda: Iguanodontoida) from Spain. Historical Biology 30: 437–474. <https://doi.org/10.1080/08912963.2017.1287179>
- Vila B, Sellés AG, Brusatte SL (2016) Diversity and faunal changes in the latest Cretaceous dinosaur communities of southwestern Europe. Cretaceous Research 57: 552–564. <https://doi.org/10.1016/j.cretres.2015.07.003>
- Virág A, Ősi A (2017) Morphometry, Microstructure, and Wear Pattern of Neornithischian Dinosaur Teeth From the Upper Cretaceous Iharkút Locality (Hungary). The Anatomical Record 300: 1439–1463. <https://doi.org/10.1002/ar.23592>
- Vremir M (2010) New faunal elements from the Late Cretaceous (Maastrichtian) continental deposits of Sebeș area (Transylvania). Acta Musei Sabesiensis 2: 635–684.
- Vremir M, Bălc R, Csiki-Sava Z, Brusatte SL, Dyke G, Naish D, Norell MA (2014) Petrești-Arini – An important but ephemeral Upper Cretaceous continental vertebrate site in the southwestern Transylvanian Basin, Romania. Cretaceous Research 49: 13–38. <https://doi.org/10.1016/j.cretres.2014.02.002>
- Vremir M, Csiki-Sava Z, Brusatte SL, Totoianu R, Norell M (2017) A rhabdodontid dinosaur skeleton from the uppermost Campanian/lowermost Maastrichtian of Sebes (Transylvanian Basin). In: 15th Annual Meeting of the European Association of Vertebrate Palaeontologists Munich, Germany, 1st to 3rd August 2017, Information and Abstracts. Zitteliana 91: 94–95.
- Vremir M, Dyke GJ, Totoianu R (2015) Repertoire of the Late Cretaceous vertebrate localities from Sebeș area, Alba County (Romania). Terra Sebus, Acta Musei Sabesiensis 7: 695–724.
- Weishampel DB (1984) Evolution of jaw mechanisms in ornithopod dinosaurs. Advances in Anatomy Embryology and Cell Biology 87: 1–109. https://doi.org/10.1007/978-3-642-69533-9_1
- Weishampel DB, Barrett PM, Coria RA, Le Loeuff J, Xing X, Xijin Z, Sahni A, Gomani EMP, Noto CR (2004) Dinosaur distribution. In: Weishampel DB, Dodson P, Osmólska H (Eds) The Dinosauria, 2nd ed. University of California Press, Berkeley, 517–606. <https://doi.org/10.1525/california/9780520242098.003.0027>
- Weishampel DB, Grigorescu D, Norman DB (1991) The dinosaurs of Transylvania. National Geographic Research & Exploration 7: 196–215.
- Weishampel DB, Jianu C, Csiki Z, Norman DB (2003) Osteology and phylogeny of *Zalmoxes* (n. g.), an unusual euornithopod dinosaur from the latest Cretaceous of Romania. Journal of Systematic Palaeontology 1: 65–123. <https://doi.org/10.1017/S1477201903001032>
- Weishampel DB, Jianu C-M, Csiki Z, Norman DB (1998) *Rhabdodon*, an unusual euornithopod dinosaur from the Late Cretaceous of western Romania. Journal of Vertebrate Paleontology 18: 85A.
- Weishampel DB, Reif W-E (1984) The Work of Franz Baron Nopcsa (1877–1933): Dinosaurs, Evolution and Theoretical Tectonics. Jahrbuch der Geologisches Bundesanstalt 127: 187–203.
- Weishampel DB, Weishampel JB (1983) Annotated localities of ornithopod dinosaurs: implications to Mesozoic paleobiogeography. The Mosasaur 1: 43–87. https://doi.org/10.1007/978-3-642-69533-9_11
- Williams VS, Barrett PM, Purnell MA (2009) Quantitative analysis of dental microwear in hadrosaurid dinosaurs, and the implications for hypotheses of jaw mechanics and feeding. PNAS 106: 11194–11199. <https://doi.org/10.1073/pnas.0812631106>
- Yang Y, Wu W, Dieudonné P-E, Godefroit P (2020) A new basal ornithopod dinosaur from the Lower Cretaceous of China. PeerJ 8: e9832. <https://doi.org/10.7717/peerj.9832>
- Zanno LE, Gates TA, Avrahami HM, Tucker RT, Makovicky PJ (2023) An early-diverging iguanodontian (Dinosauria: Rhabdodontomorpha) from the Late Cretaceous of North America. PLoS ONE 18: e0286042. <https://doi.org/10.1371/journal.pone.0286042>

Possible fungus-eating cucujiformian beetle larvae with setiferous processes from Cretaceous and Miocene ambers

Ana Zippel¹, Carolin Haug^{1,2}, Zeynep Elverdi³, Patrick Müller⁴, Joachim T. Haug^{1,2}

1 Ludwig-Maximilians-Universität München (LMU Munich), Biocenter, Großhaderner Str. 2, 82152 Planegg-Martinsried, Munich, Germany

2 GeoBio-Center at LMU, Richard-Wagner-Str. 10, 80333 München, Germany

3 Istanbul Technical University (İTÜ), Faculty of Science and Letters, Ayazağa Campus, 34469 Maslak-Istanbul, Turkey

4 Kreuzbergstr. 90, 66482 Zweibrücken, Germany

<https://zoobank.org/CA1BA8BF-F123-40F1-B97E-5C86B3B42327>

Corresponding author: Ana Zippel (ana.zippel@palaeo-evo-devo.info)

Academic editor: Florian Witzmann ♦ Received 4 April 2023 ♦ Accepted 6 August 2023 ♦ Published 28 August 2023

Abstract

Beetle larvae represent important components of the modern-day fauna. This should have been the case in the past as well. Yet, fossil beetle larvae are rare, or at least are rare in the literature, as identifying a beetle larva to a narrower taxonomic group is very challenging. This is even more complicated if prominent features have evolved convergently in several lineages. Yet, even in such cases, an ecological interpretation of the fossils is possible if the convergent character is coupled to a specific life habit. For example, different, not closely related, beetle larvae that possess setiferous processes. We here report on three beetle larvae, one from Miocene Mexican and two from Cretaceous Kachin amber, Myanmar. These larvae possess setiferous processes, most similar to the processes of modern representatives of Cucujiformia, especially of the groups Endomychidae, Erotylidae, Cerylonidae and Coccinelidae. Considering the shape of the entire habitus, we see the most similarities between the new larvae and the modern larvae of Endomychidae. However, the new larvae and the larvae of modern representatives differ in certain aspects, most prominently in the body size. The fossils are smaller than their extant counterparts with setiferous processes. Hence the fossils could represent larvae of Endomychidae, but the case remains unclear. Despite this uncertainty, we suggest a lifestyle of the fossil larvae as fungus-eaters on rotting wood. This lifestyle is not only known from extant larvae of Endomychidae, but also from other larvae with similar processes.

Key Words

Endomychidae, fossils, fungus-eating, Myanmar amber, palaeoecology

Introduction

Beetle larvae are very important components of the modern fauna. This importance is caused by the fact that the group of beetles, Coleoptera, is extremely species-rich with only slightly fewer than 400,000 formally described species, and also by the various ecological roles fulfilled by beetle larvae. Given their importance in the modern fauna, it is astonishing that fossil beetle larvae, which could inform us about the evolutionary history of these important faunal components, are relatively underrepresented in the literature.

This under-representation seems to be coupled to the fact that many fossil beetle larvae can prove quite difficult

to be interpreted in a phylogenetic or taxonomic frame (Klausnitzer 1978). This has led to controversies over the identification of fossil larvae (e.g. Grimaldi et al. 2005 vs. Beutel et al. 2016; Zippel et al. 2022a vs. Batelka and Engel 2022). Nevertheless, controversies over the phylogenetic interpretation of fossils are also common in adults (Cai et al. 2017 vs. Li et al. 2022a; Clarke et al. 2019). Even more problematic in this respect is that some fossil larvae differ in certain aspects from all known modern forms. In some cases, this may mean that the fossils possess an unusual combination of characters (“chimeras”; Haug et al. 2019a) not found in modern forms, but the individual characters are well-known in different modern larvae

(e.g. Zippel et al. 2023). In other cases, the fossil larvae may retain plesiomorphies (see discussions in Haug et al. 2021a and Zippel et al. 2022a; see Batelka and Engel 2022 and Rasnitsyn and Müller 2023 for an alternative view).

Yet, some beetle larvae have rather prominent features that allow the recognition of a fossil as a representative of a specific group with quite some certainty. The aquatic larvae of whirligig beetles (Gyrinidae) are very conspicuous due to their body shape in combination with the lateral processes projecting from their trunk and hence can easily be identified also as fossils (Zhao et al. 2019; Gustafson et al. 2020). Also larvae of water penny beetles (Psephenidae), likewise aquatic, with their often flat and round appearance can be easily identified (Wedmann et al. 2011; Hayashi et al. 2020). Many larvae of false flower beetles (Scraptiidae) have an enlarged trunk end, which provides also a good identifier in the case of fossils (Larsson 1978; Haug and Haug 2019; Zippel et al. 2022b). Larvae of Texas beetles (Brachypsectridae) have quite peculiar processes on their trunk segments and well-specialised head and mouthpart shapes, which have also been identified in fossils preserved in amber from different ages including the Cretaceous (Zhao et al. 2020; Haug et al. 2021b), Eocene (Scheven 2004; Klausnitzer 2009; Haug et al. 2021b) and Miocene (Poinar 1992; Wu 1996; Poinar and Poinar 1999; Woodruff 2002; Scheven 2004; Klausnitzer 2009).

There are other groups of beetles that have larvae with prominent processes on the trunk (Haug et al. 2021b fig. 15 p. 177). Within the group Cucujiformia, larvae of several lineages have setiferous lateral protrusions, apparently as a result of independent convergent evolution. We here report new fossil beetle larvae preserved in about 100-million-year-old Kachin amber, Myanmar and about 25-million-year-old Mexican amber. They also possess lateral protrusions resembling those of different cucujiformian larvae, but also differing from these in certain aspects. We discuss the implications of these new fossils concerning the evolution of larval characters in beetles and the importance of reporting fossil larvae.

Material and methods

Material

At the centre of this study are three new fossil specimens: SNHMB.G 8195, SNHMB.G 8196, and PED 1955. Two specimens (SNHMB.G 8195, with an old depository number MEX 011, and SNHMB.G 8196, with an old depository number BUB 1259) came from one of the authors (PM) and are now deposited in the Staatliches Naturhistorisches Museum Braunschweig, Germany. One specimen (PED 1955) is deposited in the Palaeo-Evo-Devo Research Group Collection of Arthropods at the Ludwig-Maximilians-Universität München, Germany. All three specimens were legally purchased.

Specimen SNHMB.G 8195 originates from approximately 25-million-year-old Miocene Mexican amber.

Specimens SNHMB.G 8196 and PED 1955 originate from about 100-million-year-old Kachin amber, Myanmar. SNHMB.G 8196 was acquired by one of the authors (PM) in the year 2016. Specimen PED 1955 was acquired from the trading platform ebay.com from the trader burmite-miner.

Three specimens of extant fungus-eating larvae of Endomychidae from the Coleoptera Collection of the Natural History Museum of Denmark, Copenhagen (NHMD) are included for comparison. The specimens were preserved in glass jars and vials filled with ethanol without a depository number, organised alphabetically by the group and the land of origin. The specimen of *Endomychus biguttatus* was collected by Riley, C. J. in Tennessee on 17.02.1890. The specimen of *Endomychus coccineus* was collected under the bark of beech in Bonn, Germany on 1.6.1925. The specimen of *Eumorphus quadriguttatus* was collected in Sarawak in Borneo. Unfortunately, the labels within the vials were not well-readable and therefore we cannot provide more information on the extant specimens.

Documentation methods

All three of the fossil specimens were documented on a Keyence VHX-6000 digital microscope in front of white and black backgrounds. The specimens were documented with different illumination settings: cross-polarised co-axial and low-angle ring light (Haug et al. 2013a, 2018). All images were recorded as composite images (see Haug et al. 2008, 2011; Kerp and Bomfleur 2011) with the built-in HDR function (cf. Haug et al. 2013b). All of the images were further processed with Adobe Photoshop CS2. Drawings of specimens from the literature were drawn with the free software Inkscape.

The extant specimens were photographed in the Coleoptera Collection at the National History Museum of Denmark (NHMD) in Copenhagen with macro-photography equipment. Each specimen was stored with multiple other specimens in 70% ethanol. For photographing purposes, each specimen of interest was placed in a separate Petri dish with 70% ethanol and covered with a coverslip. A Canon Rebel T3i digital camera equipped with a Canon MP-E 65 mm macro lens was used. A Yonguno YN24EX E-TTL twin flash provided illumination. Polarisers were placed on the lens and flashes (perpendicular to each other in order to produce cross-polarised light). Stacks were further processed with Combine ZP (Haug et al. 2008, 2011).

Morphological terminology

The usual ‘entomological’ terminology within the text is amended with more descriptive morphological terminology within the first description of a specimen. This is done in order to enhance the comprehensibility for non-experts. The descriptive terms apply to all of the specimens but are not repeated to facilitate easier reading of the text.

Results

Description of fossil specimen SNHMB.G 8195

Small larva. Total body length ~1.86 mm. Body oval in dorsal view, flattened dorso-ventrally, parallel-sided (Fig. 1A–C), differentiated into anterior head and posterior trunk. Head partially torn, partially inaccessible, possibly partly retracted under tergite of anterior part of trunk. No stemmata discernible. Labrum (derivative of ocular segment) partly discernible (Fig. 1E) with at

least three strong setae on anterior rim (Fig. 1E arrow). Antennae (appendages of post-ocular segment 1) not accessible. Intercalary segment (post-ocular segment 2) without externally recognizable structures. Mandibles (appendages of post-ocular segment 3) not accessible. Maxillae (appendages of post-ocular segment 4) with maxillary palp, partially discernible (Fig. 1E). Labium (appendages of post-ocular segment 5) not accessible.

Trunk further differentiated into anterior thorax and posterior abdomen. Thorax with three segments (pro-, meso- and metathorax). Prothorax sub-rectangular in

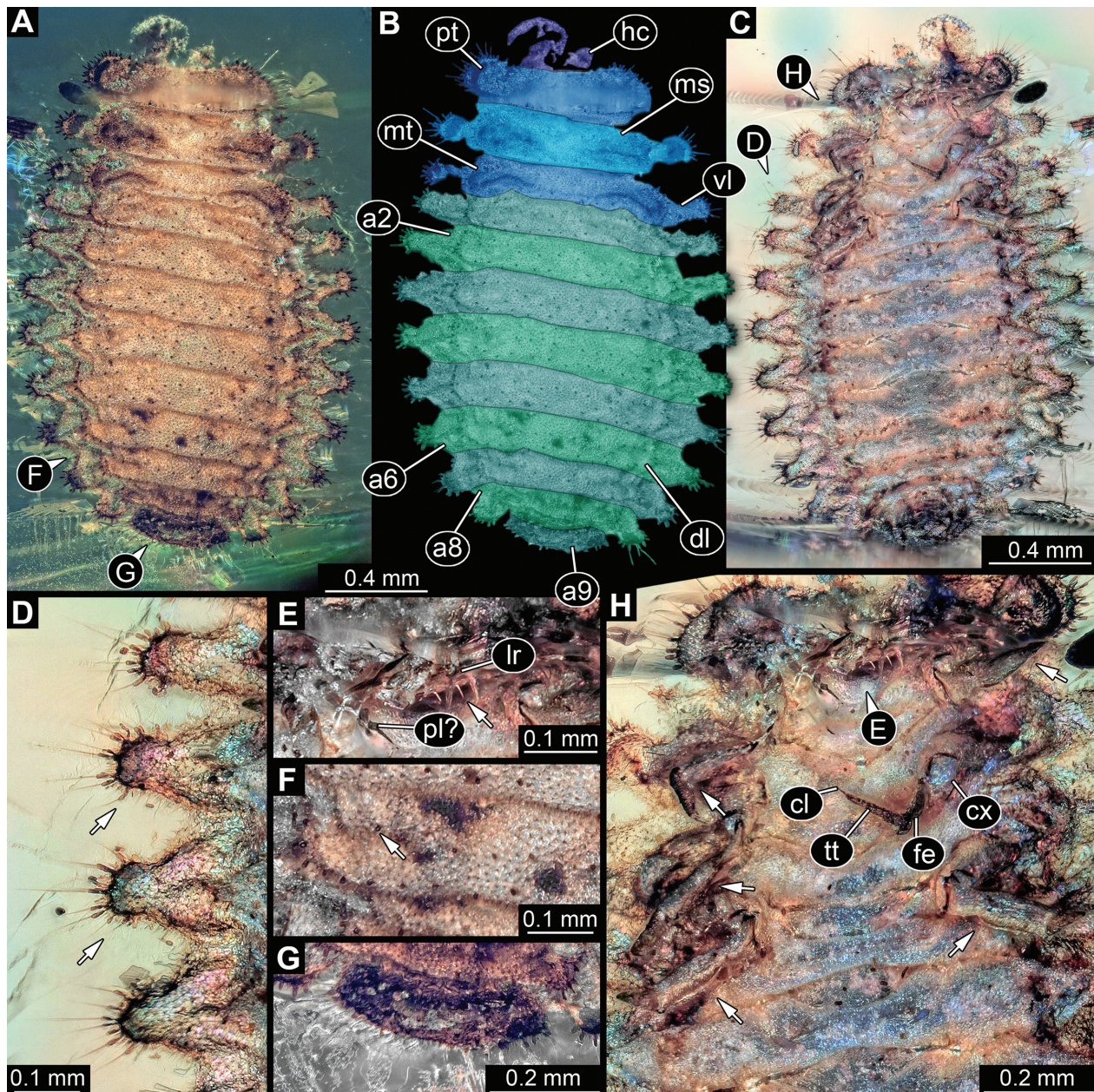


Figure 1. Fossil specimen SNHMB.G 8195, larva of Cucujiformia: **A.** Habitus in dorsal view; **B.** Colour-marked version of **A.**; **C.** Habitus in ventral view; **D.** Close-up of lateral processes with specialized hairs (arrows) in ventral view; **E.** Close-up of probable head region in ventral view, arrow marks the strong hairs of possible labrum; **F.** Close-up of body surface in dorsal view, arrow marks the darker coloured wart; **G.** Close-up of abdomen segment 9 in dorsal view; **H.** Close-up of anterior part of the body in ventral view, arrows mark legs. **Abbreviations:** a2–9 = abdomen segments 2–9; cl = claw; cx = coxa; dl = dorso-lateral process; fe = femur; hc = head capsule; lr = labrum; ms = mesothorax; mt = metathorax; pl? = possible palp; pt = prothorax; tt = tibio-tarsus; vl = ventro-lateral process.

dorsal view, wider than long, $4.2\times$ (~ 0.17 mm long) with convex lateral edges. Meso- and metathorax sub-similar in shape, sub-rectangular in dorsal view, with convex lateral edges drawn out into lateral processes, one per lateral edge. Mesothorax wider than long, $5.2\times$ (~ 0.19 mm long; width including lateral processes). Metathorax wider than long, $8.2\times$ (~ 1.11 mm long; width including lateral processes; Fig. 1A–C). Legs discernible, with five elements (Fig. 1H arrows): coxa (~ 0.14 mm long), trochanter (~ 0.08 mm long), femur (~ 0.16 mm long), tibio-tarsus (~ 0.14 mm long) and a claw (~ 0.02 mm long).

Abdomen segments 1–8 sub-similar, sub-rectangular in dorsal view, with convex lateral edges drawn out into lateral processes, one per lateral edge (Fig. 1D). Abdomen segments 1–8 wider than long (between 0.13–0.19 mm long and between 0.67–1.32 mm wide, including lateral processes). Abdomen segment 9 sub-trapezoid in dorsal view, wider than long, $3.4\times$ (~ 0.12 mm long) (Fig. 1G). Trunk end (with possible pygopod) not discernible.

Dorsal surface of body bears very short irregularities of integument (asperities), not possible to interpret whether they are short setae or small spines, and small dark-coloured warts (Fig. 1F arrow). Lateral processes of trunk segments bear laterally relatively long tubercles (appear like enlarged warts) with longer simple setae distally (0.11–0.13 mm long). Abdomen segment 9 bears similar tubercles with longer simple setae posteriorly (Fig. 1G).

Description of fossil specimen SNHMB.G 8196

Small larva. Total body length ~ 2.47 mm. Body oval in dorsal view, flattened dorso-ventrally, parallel-sided (Fig. 2A–C), differentiated into anterior head and posterior trunk. Head semi-circular in dorsal view, partially covered in Verlumung (ventral view). No stemmata discernible. Labrum partly discernible with at least four shorter setae on anterior rim (Fig. 2E). Antennae discernible, elongated in dorsal view (~ 0.13 mm long), with at least three antennomers (elements of an antenna). Most distal element bears at least four strong setae distally (Fig. 2E). Intercalary segment without externally recognizable structures. Mandibles, maxillae and labium not accessible.

Trunk further differentiated into anterior thorax and posterior abdomen. Thorax with three segments (pro-, meso- and metathorax; Fig. 2B). Prothorax semi-ovaloid in dorsal view, wider than long, $4.1\times$ (~ 0.2 mm long) with convex lateral edges drawn out into lateral processes, one per lateral edge. Meso- and metathorax sub-similar in shape, sub-rectangular in dorsal view, with convex lateral edges drawn out into lateral processes, one per lateral edge. Mesothorax wider than long, $4.4\times$ (~ 0.22 mm long; width including lateral processes). Metathorax wider than long, $5.2\times$ (~ 0.2 mm long; width including lateral processes) (Fig. 2A–C). Legs partially discernible, partially covered in Verlumung, with presumed five elements (Fig. 2D arrows): coxa, trochanter (not accessible), femur (partially accessible), tibio-tarsus and a claw.

Abdomen segments 1–7 sub-similar, sub-rectangular in dorsal view, with convex lateral edges drawn out into lateral processes, one per lateral edge (Fig. 2A–C). Abdomen segment 8 sub-similar, but with lateral edges and lateral processes orientated posteriorly. Abdomen segments 1–8 wider than long (between 0.13–0.18 mm long and between 0.54–1.04 mm wide, including lateral processes). Abdomen segment 9 sub-trapezoid, wider than long, $1.7\times$ (~ 0.19 mm long), with anterior rim medially convex and posterior rim medially concave in dorsal view (Fig. 2F). Trunk end not accessible, covered by Verlumung (Fig. 2A).

Dorsal surface of body bears short irregularities of integument (asperities) and small dark-coloured warts (Fig. 2C). Anterior and lateral rims of head capsule bear multiple setae. Lateral processes of trunk segments bear laterally tubercles (appear like enlarged warts) with longer fringed setae (setae with distal tip forked in multiple smaller branches), distally (0.05–0.25 mm long) (Fig. 2F). Abdomen segment 9 bears similar tubercles with longer simple setae posteriorly, but also shorter ones which are broader distally and possibly fringed (Fig. 2F).

Description of fossil specimen PED 1955

Small larva. Total body length ~ 2.41 mm. Body oval, slightly elongated in dorsal view, flattened dorso-ventrally, parallel-sided (Fig. 3A–C), differentiated into anterior head and posterior trunk. Head sub-trapezoid in ventral view, wider than long, $2.4\times$ (~ 0.13 mm long); partially covered by other inclusions (dorsal view) (Fig. 3C), partially covered by Verlumung (ventral view) (Fig. 3A), possibly partly retracted under anterior part of trunk. No stemmata discernible. Labrum not clearly discernible (Fig. 3A). Antennae only partially accessible, only one antenna partially discernible (Fig. 3A arrow). Intercalary segment without externally recognizable structures. Mandibles not clearly accessible. Maxillae not clearly accessible. Labium not clearly accessible.

Trunk further differentiated into anterior thorax and posterior abdomen (Fig. 3B). Thorax with three segments (pro-, meso- and metathorax). Prothorax sub-rectangular in dorsal view, wider than long, $3.4\times$ (~ 0.18 mm long) with convex lateral edges. Meso- and metathorax sub-similar in shape, sub-rectangular in dorsal view, with convex lateral edges drawn out into lateral processes, one per lateral edge. Mesothorax wider than long, $4.2\times$ (~ 0.17 mm long; width including lateral processes). Metathorax wider than long, $4.8\times$ (~ 0.17 mm long; width including lateral processes) (Fig. 3A–C). Legs discernible, with five elements (Figs 3A, D): coxa, trochanter, femur, tibio-tarsus and a claw (Fig. 3D arrow).

Abdomen segments 1–8 sub-similar, sub-rectangular in dorsal view, with convex lateral edges drawn out into lateral processes, one per lateral edge. Abdomen segments 1–8 wider than long (between 0.15–0.23 mm long and between 0.67–0.84 mm wide, including lateral

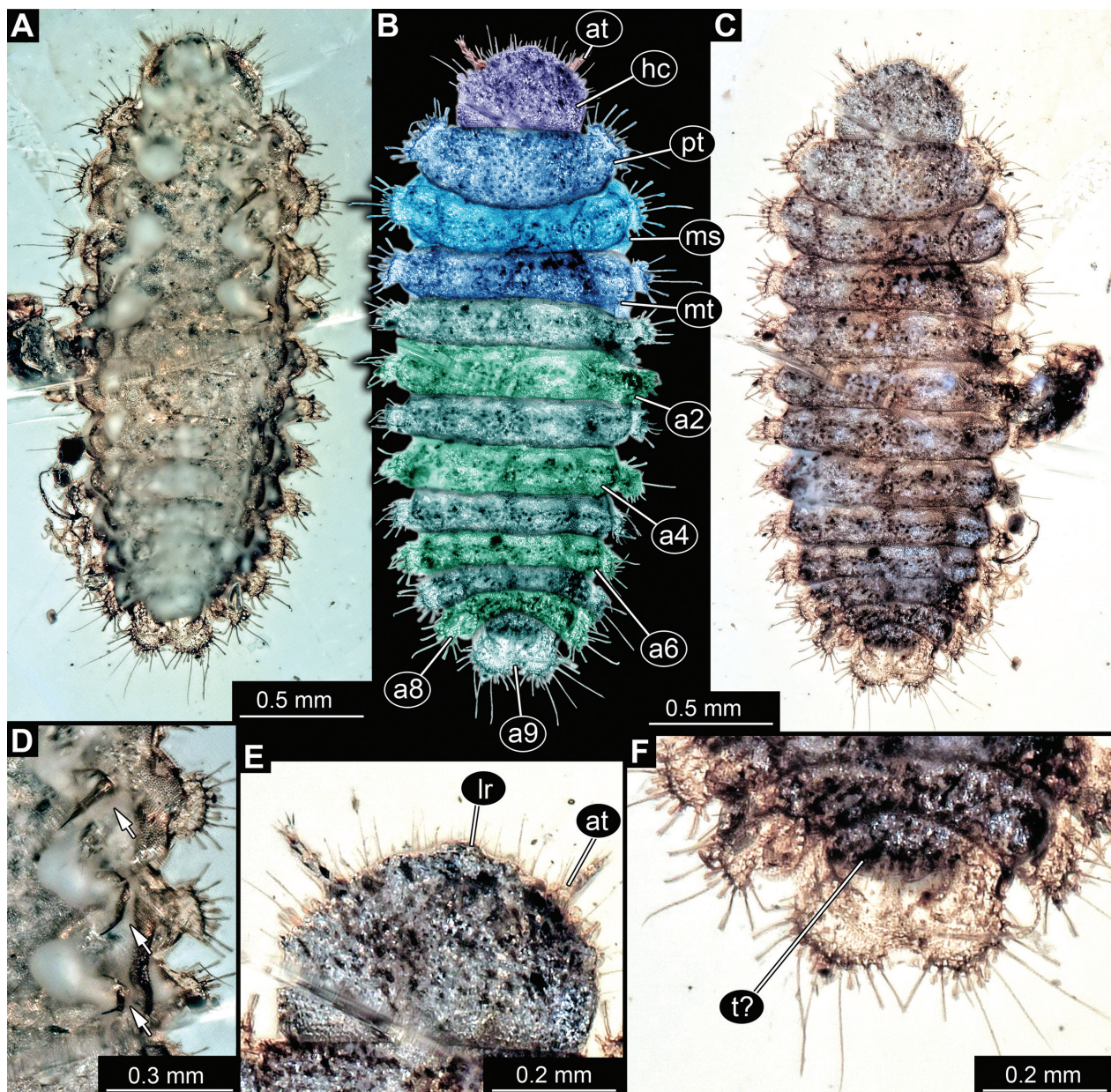


Figure 2. Fossil specimen SNHMB.G 8196, larva of Cucujiformia: **A.** Habitus in ventral view; **B.** Colour-marked version of **C**; **C.** Habitus in dorsal view; **D.** Close-up of legs and lateral processes with hairs in ventral view, arrows mark the legs; **E.** Close-up of head in ventral view; **F.** Close-up of posterior part of abdomen. **Abbreviations:** a2–9 – abdomen segments 2–9; at – antenna; hc – head capsule; lr – labrum; ms – mesothorax; mt – metathorax; pt – prothorax; t? – possible trunk end.

processes). Abdomen segment 9 sub-trapezoid, wider than long, 2.5× (~0.14 mm long), with posterior rim medially concave in ventral view and posteriorly with two processes (possible urogomphi; ~0.09 mm long), cone-shaped (with distal tips posteriorly orientated; Fig. 3E). Trunk end (with possible pygopod) partly discernible in ventral view (Fig. 3E: t?), surrounded by abdomen segment 9, closer to anterior rim of abdomen segment 9 than to its posterior rim.

Dorsal surface of body with paired darker patches per all three thorax and abdomen tergites 1–8. Within patches small dark-coloured warts discernible (Fig. 3C). Similar patches on lateral processes discernible. Lateral processes of trunk segments bear laterally setae which are broader

distally and possibly fringed (maximally 0.18 mm long) (Fig. 3F). Abdomen segment 9 bears similar fringed setae along lateral and posterior edge, but also single simple longer setae near posterior processes (Fig. 3A, E).

Description of extant specimen of *Endomychus biguttatus*

Small larva. Total body length ~4.89 mm. Body oval in dorsal view, flattened dorso-ventrally (Fig. 4A, E), differentiated into anterior head and posterior trunk. Head hypognathous (mouth parts facing downwards), ovaloid in ventral view, completely hidden by first sclerite of

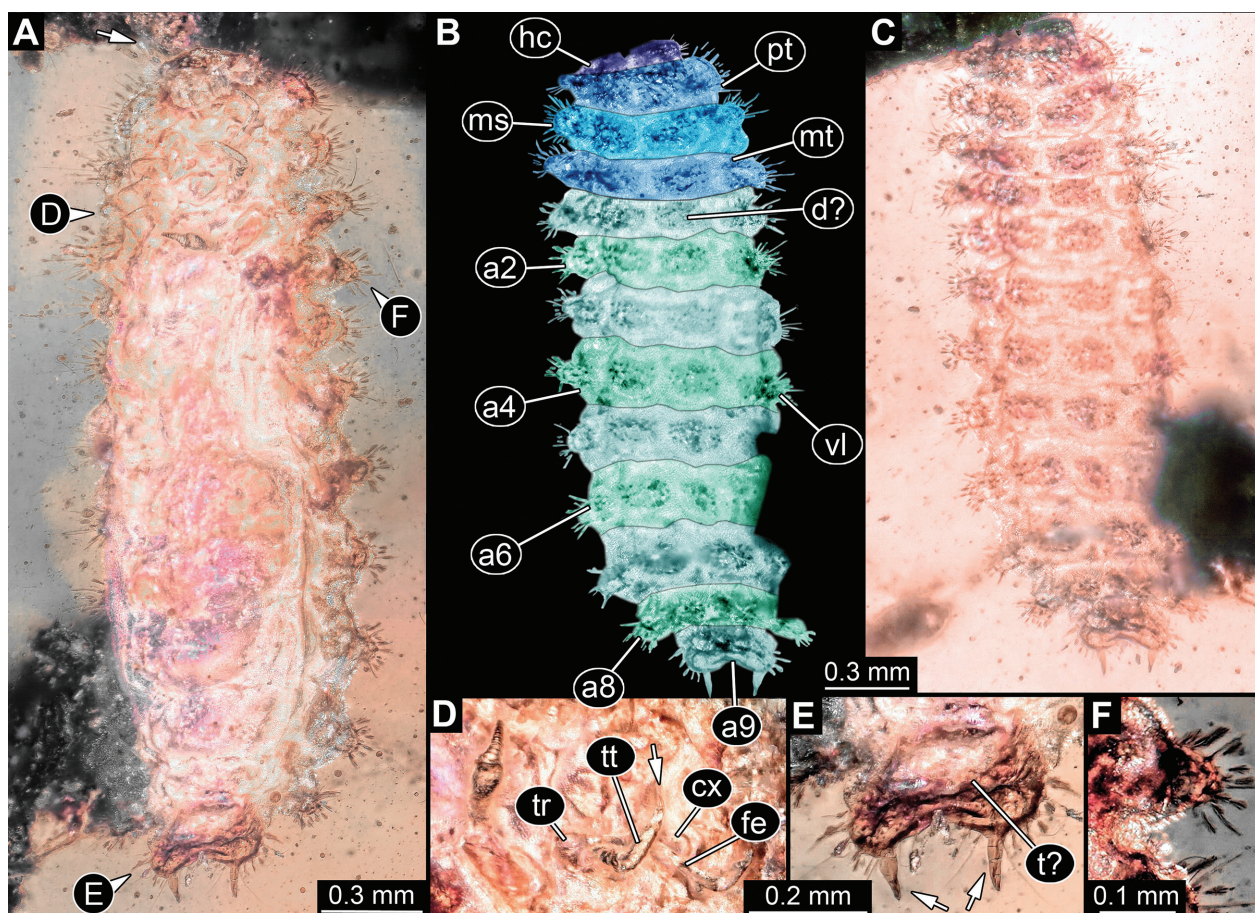


Figure 3. Fossil specimen PED 1955, larva of Cucujiformia: **A.** Habitus in ventral view, arrow marks the possible antenna; **B.** Colour-marked version of **C**; **C.** Habitus in dorsal view; **D.** Close-up of legs in ventral view, arrow marks the claw (image was turned 90 degrees to the right); **E.** Close-up of abdomen segment 9 in ventral view, arrows mark the posterior processes; **F.** Close-up of ventro-lateral processes with specialized hairs. **Abbreviations:** a2–9 – abdomen segments 2–9; cx – coxa; d? – possible dorso-lateral process; fe – femur; hc – head capsule; ms – mesothorax; mt – metathorax; pt – prothorax; t? – possible trunk end; tr – trochanter; tt – tibio-tarsus; vl – ventro-lateral process.

anterior part of trunk in dorsal view, wider than long, $1.8\times$ (~ 0.51 mm long). No stemmata discernible in ventral view, four stemmata on each side presumed. Labrum discernible, wider than long, with anterior rim medially slightly concave in ventral view (Fig. 4D). Antennae discernible, one partially covered by other body parts, elongated, longer than wide (~ 0.51 mm long), with three antennomeres (elements of an antenna). Intercalary segment without externally recognizable structures (Fig. 4B). Mandibles not discernible in ventral view. Maxillae discernible, each with cardo proximo-laterally, sub-triangular in ventral view; with stipes in middle, elongate in ventral view; with single endite medially, longer than wide, with multiple short setae; and maxillary palp distally (Fig. 4D). Palp, longer than wide (~ 0.18 mm long), with three palpomeres (elements of a palp), on membranous area. Labium sub-trapezoid in ventral view, with a pair of palps. Each palp longer than wide (~ 0.07 mm long), with two palpomeres (elements of a palp) on membranous area (Fig. 4D).

Trunk further differentiated into anterior thorax and posterior abdomen. Thorax with three segments (pro-,

meso- and metathorax). Prothorax semi-circular in dorsal view, with convex posterior edge, wider than long, $2\times$ at maximum width (~ 1.06 mm long). Lateral edges of prothorax postero-laterally drawn out; medially longitudinal line discernible (Fig. 4A). Meso- and metathorax sub-similar in shape, sub-trapezoid in dorsal view, with convex lateral edges; medially with distinct longitudinal line. Edges of tergite drawn out posteriorly into dorso-lateral processes, one per lateral edge. Mesothorax wider than long, $4.2\times$ (~ 0.59 mm long; width including lateral processes). Metathorax wider than long, $3.9\times$ (~ 0.64 mm long; width including lateral processes; Fig. 4). Legs discernible, with five elements (Fig. 4F): coxa (~ 0.62 mm long), trochanter (~ 0.22 mm long), femur (~ 0.47 mm long), tibio-tarsus (~ 0.55 mm long) and a claw (~ 0.15 mm long).

Abdomen segments 1–8 sub-similar, sub-rectangular in dorsal view, with convex lateral edges drawn out into lateral processes, a dorso-lateral and a ventro-lateral one per edge (Fig. 4G). Abdomen segments 1–8 wider than long (between 0.26 – 0.39 mm long and between 1.11 – 2.64 mm wide, including lateral processes). Abdomen

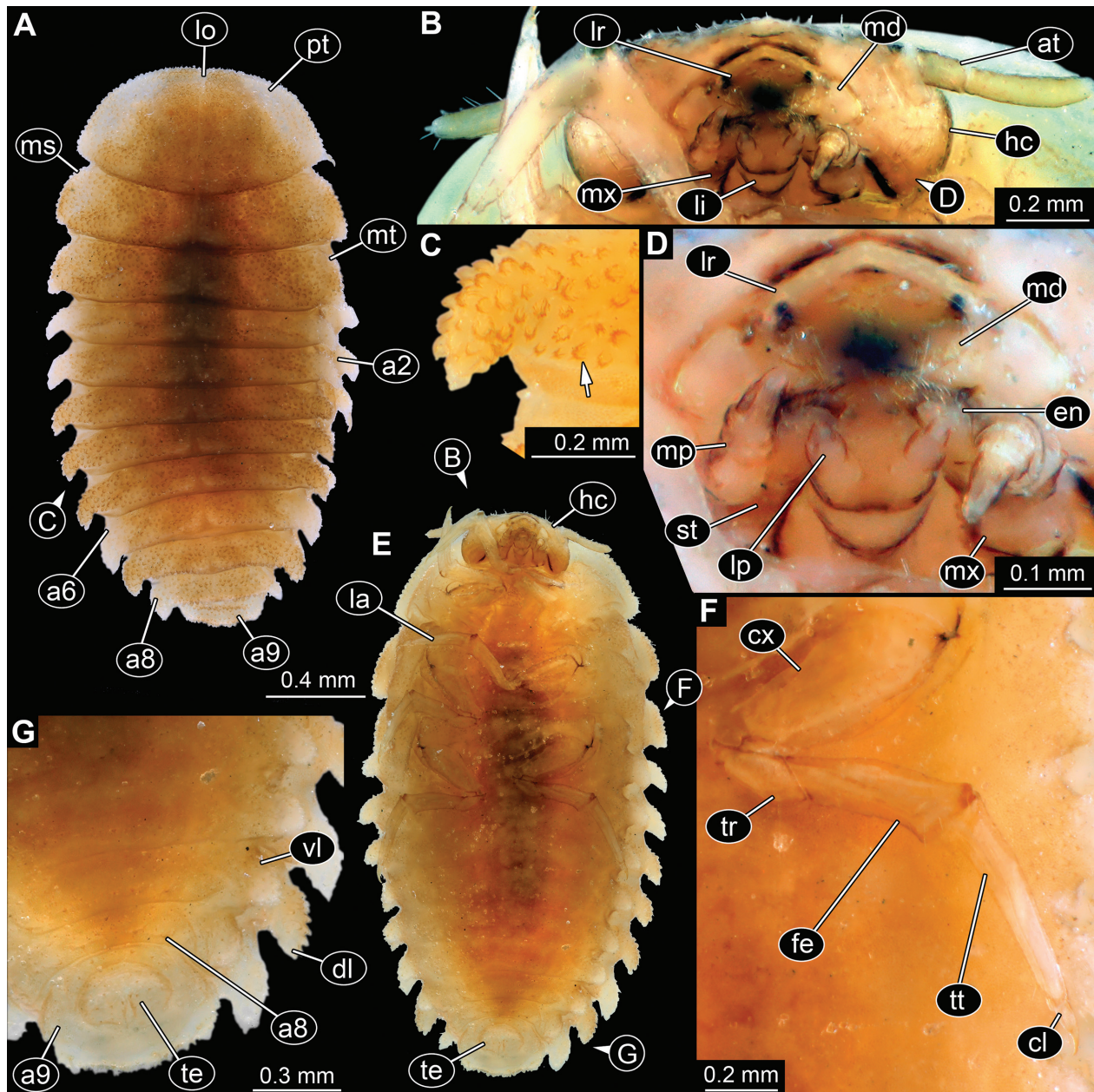


Figure 4. Extant specimen of larva of *Endomychus biguttatus*, Endomychidae: **A.** Habitus in dorsal view; **B.** Close-up of head in ventral view; **C.** Close-up of dorso-lateral process in dorsal view, arrow marks a wart; **D.** Close-up of mouth parts in ventral view; **E.** Habitus in ventral view; **F.** Close-up of a leg in ventral view; **G.** Close-up of posterior part of abdomen in ventral view. **Abbreviations:** a2–9 – abdomen segments 2–9; at – antenna; cl – claw; cx – coxa; dl – dorso-lateral process; en – endite; fe – femur; hc – head capsule; la – locomotory appendages (legs); li – labium; lo – longitudinal line; lp – labial palp; lr – labrum; md – mandible; mp – maxillary palp; ms – mesothorax; mt – metathorax; mx – maxilla; pt – prothorax; st – stipes; te – trunk end; tr – trochanter; tt – tibio-tarsus; vl – ventro-lateral process.

segment 9 sub-trapezoid in dorsal view, wider than long, $4.3\times$ (~0.16 mm long) (Fig. 4A). Trunk end (with possible pygopod) only accessible in ventral view, ovaloid, with indentation medio-posteriorly, dorsally not visible as concealed by abdomen segment 9, closer to anterior rim of abdomen segment 9 than to its posterior rim (Fig. 4G).

Dorsal surface of body, including the processes, bears small darker-coloured warts (Fig. 4C arrow). Abdomen segment 9 bears similar tubercles also posteriorly (Fig. 4).

Description of extant specimen of *Endomychus coccineus*

Small larva. Total body length ~6.44 mm. Body oval in dorsal view, flattened dorso-ventrally (Fig. 5A, D), differentiated into anterior head and posterior trunk. Head hypognathous (mouth parts facing downwards), semi-circular in dorsal view, wider than long, $1.2\times$ (~0.81 mm long), with two lighter lines discernible (arms of moulting suture) (Fig. 5C arrows). Single stemma

discernible, but additional three per side presumed (Fig. 5G). Labrum discernible, wider than long (~0.27 mm wide) (Fig. 5C). Antennae discernible, elongated, longer than wide (~0.55 mm long), with three antennomeres (elements of an antenna) (Fig. 5C). Intercalary segment without externally recognizable structures. Mandibles partially discernible, mostly concealed by other mouth parts (Fig. 5G). Maxillae discernible, each with cardo proximo-laterally, sub-triangular in ventral view; with stipes in middle, elongate in ventral view; with single

endite medially, longer than wide, with multiple short setae; and maxillary palp distally (Fig. 5G). Palp longer than wide (~0.21 mm long), with three palpomeres (elements of a palp), at proximal part membranous area discernible. Labium sub-trapezoid in ventral view, with a pair of palps. Each palp longer than wide (~0.08 mm long), with two palpomeres (elements of a palp), on proximal part membranous area discernible (Fig. 5G).

Trunk further differentiated into anterior thorax and posterior abdomen. Thorax with three segments (pro-

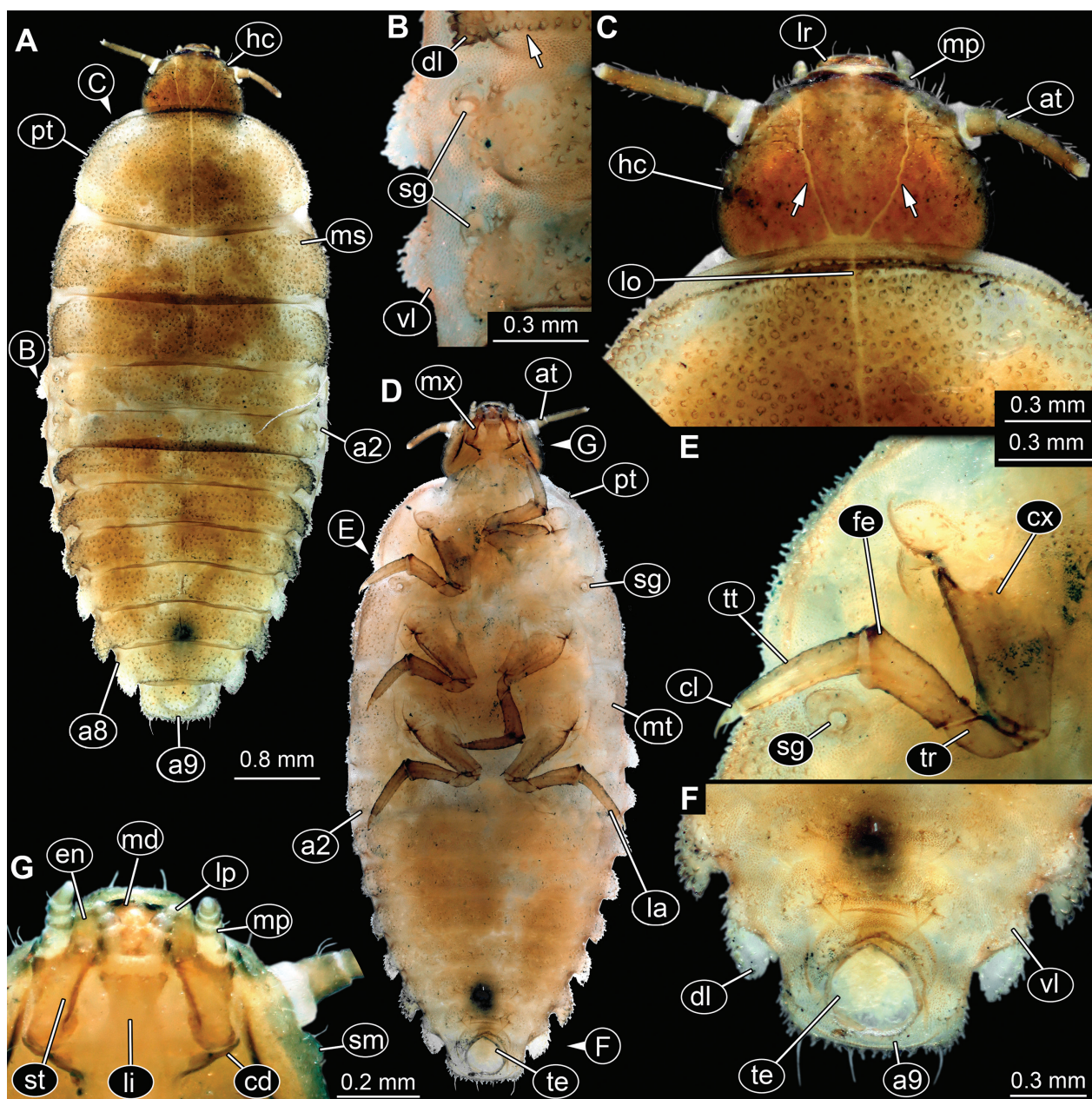


Figure 5. Extant specimen of larva of *Endomychus coccineus*, Endomychidae: **A.** Habitus in dorsal view; **B.** Close-up of lateral processes and stigmata in dorsal view, arrow marks a wart; **C.** Close-up of head in dorsal view, arrows mark the arms of epicranial suture; **D.** Habitus in ventral view; **E.** Close-up of a leg in ventral view; **F.** Close-up of posterior part of abdomen in ventral view; **G.** Close-up of head in ventral view. **Abbreviations:** a2–9 – abdomen segments 2–9; at – antenna; cd – cardo; cl – claw; cx – coxa; dl – dorso-lateral process; en – endite; fe – femur; hc – head capsule; la – locomotory appendages (legs); li – labium; lo – longitudinal line; lp – labial palp; lr – labrum; md – mandible; mp – maxillary palp; ms – mesothorax; mt – metathorax; mx – maxilla; pt – prothorax; sg – stigma; sm – stemma; st – stipes; te = trunk end; tr – trochanter; tt – tibio-tarsus; vl – ventro-lateral process.

meso- and metathorax). Prothorax semi-circular in dorsal view, with posterior edge convex, wider than long, $1.7\times$ at maximum width (~ 1.22 mm long). Lateral edges of prothorax postero-laterally drawn out; medially with prominent longitudinal line (Fig. 5A). Meso- and metathorax sub-similar in shape, sub-rectangular in dorsal view, with convex lateral edges; medially with prominent longitudinal line. Edges drawn out posteriorly into short dorso-lateral processes, one per lateral edge (Fig. 5A). Mesothorax wider than long, $3.3\times$ (~ 0.77 mm long; width including lateral processes). Metathorax wider than long, $3.1\times$ (~ 0.84 mm long; width including lateral processes) (Fig. 5A). Legs discernible, with five elements (Fig. 5E): coxa (~ 0.69 mm long), trochanter (~ 0.27 mm long), femur (~ 0.45 mm long), tibio-tarsus (~ 0.57 mm long) and a claw (~ 0.12 mm long).

Abdomen segments 1–8 sub-similar, sub-rectangular in dorsal view, with convex lateral edges drawn out into lateral processes, a dorso-lateral and a ventro-lateral one per edge (Fig. 5A, B, F). Abdomen segments 1–8 wider than long (between 0.19–0.41 mm long and between 1.17–2.74 mm wide, including lateral processes). Abdomen segment 9 sub-rectangular in dorsal view, wider than long, $1.3\times$ (~ 0.55 mm long) (Fig. 5A). Trunk end (with possible pygopod) only accessible in ventral view, sub-circular in shape, dorsally not visible as concealed by abdomen segment 9, closer to anterior rim of abdomen segment 9 than to its posterior rim (Fig. 5F).

Dorsal surface of body, including the processes, bears small darker-coloured warts (Fig. 5A, C). Abdomen segment 9 bears similar tubercles also posteriorly and some longer simple setae.

Description of extant specimen of *Eumorphus quadriguttatus*

Larva. Total body length ~ 11.57 mm. Body oval in dorsal view, flattened dorso-ventrally (Fig. 6A), differentiated into anterior head and posterior trunk. Head hypognathous (mouth parts facing downwards), sub-pentagonal in ventral view, partially hidden by first sclerite of anterior part of trunk in dorsal view, wider than long, $2.4\times$ (~ 1.03 mm long), with two lighter lines discernible (arms of epicranial suture), anterior rim with short setae. Multiple stemmata discernible (Fig. 6B arrows), exact number not obvious. Labrum discernible, wider than long, $2.3\times$ (~ 0.22 mm wide), sub-pentagonal in ventral view, with anterior rim medially slightly concave and multiple setae antero-laterally (Fig. 6C). Antennae discernible, elongated, longer than wide (~ 0.8 mm long), with three antennomeres (elements of an antenna), at proximal part membranous area discernible. Intercalary segment without externally recognizable structures. Mandibles partially discernible, mostly hidden by other mouth parts (Fig. 6C). Maxillae partially discernible, with cardo inaccessible; with partially discernible stipes in the middle; with single endite medially, with multiple short setae; and maxillary palp distally (Fig. 6C). Palp longer than

wide (~ 0.38 mm long), with three palpomeres (elements of a palp), at proximal part membranous area discernible. Labium (appendages of post-ocular segment 5) partially discernible, with a pair of palps. Each palp longer than wide (~ 0.11 mm long), with two palpomeres (elements of a palp), at proximal part membranous area discernible.

Trunk further differentiated into anterior thorax and posterior abdomen. Thorax with three segments (pro-, meso- and metathorax). Prothorax semi-circular in dorsal view, wider than long, $2.3\times$ at maximum width (~ 1.7 mm long). Tergite of prothorax bears antero-laterally cone-shaped processes with multiple setae, one per side; medially longitudinal line discernible. Antero-lateral processes ~ 1.2 mm long. Meso- and metathorax subsimilar in shape, sub-rectangular in dorsal view, with convex lateral edges; medially longitudinal line discernible. Lateral edges of tergites convex, bear antero-laterally cone-shaped processes with multiple setae, one per side. Mesothorax wider than long, $3.6\times$ (~ 1.35 mm long; width without lateral processes). Metathorax wider than long, $5\times$ (~ 1.1 mm long; width without lateral processes; Fig. 6A). Antero-lateral processes between 1.64–1.66 mm long. Legs discernible, with five elements (Fig. 6D): coxa (~ 1.06 mm long), trochanter (~ 0.53 mm long), femur (~ 0.89 mm long), tibio-tarsus (~ 1.49 mm long) and a claw (~ 0.16 mm long).

Abdomen segments 1–8 sub-similar, sub-rectangular in dorsal view. Lateral edges of tergites convex, bear laterally cone-shaped processes with multiple setae, a dorso-lateral and a ventro-lateral one per edge (Fig. 6A), ventral processes shorter than dorsal ones. Abdomen segments 1–8 wider than long (between 0.74–0.98 mm long and between 3.32–6.44 mm wide, without lateral processes). Abdomen segment 9 only partially accessible in dorsal view, sub-hexagonal in ventral view, wider than long, $1.7\times$ (~ 0.98 mm long) (Fig. 6E). Postero-lateral edges of abdomen segment 9 posteriorly drawn out into processes (~ 0.41 mm long) with multiple setae. Trunk end (with possible pygopod) only accessible in ventral view, sub-circular, dorsally not visible while concealed by abdomen segment 9, wider than long, $2.2\times$ (~ 0.43 mm long), closer to anterior rim of abdomen segment 9 than to its posterior rim (Fig. 6E).

Discussion

Identity of the new fossils: beetle larvae of Cucujiformia

All three new fossils have a segmented body arranged into a head and a trunk, which is further differentiated into a thorax with three leg-bearing segments (and no wings) and an abdomen with legless segments (Figs 1–3). Also, no genitalia or compound eyes are accessible. This character combination indicates that the new fossils are immature stages of the group Holometabola (Lawrence 1991a). In addition, abdomen leg derivatives, such as sometimes seen in Lepidoptera and Hymenoptera, and antennae with

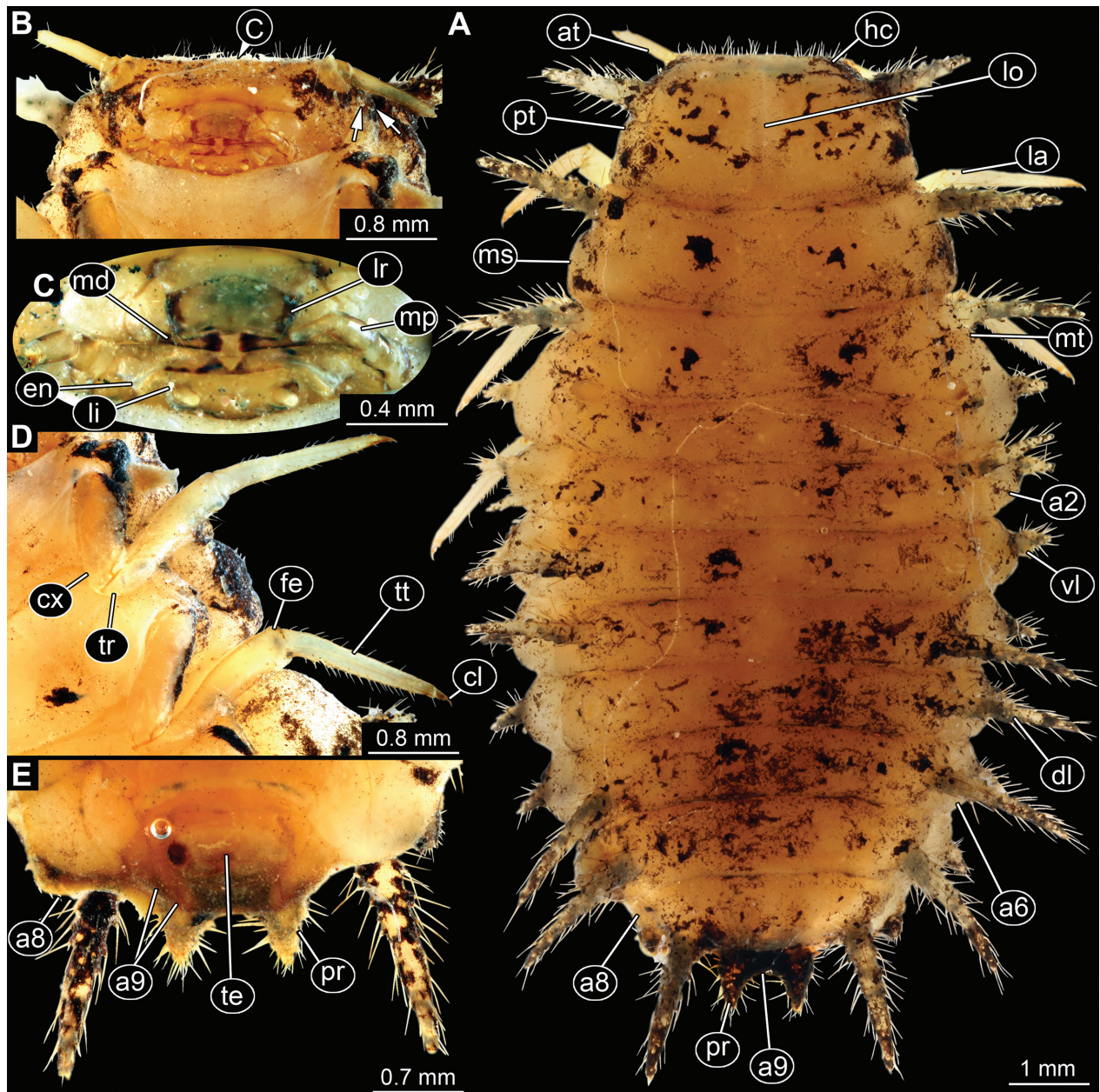


Figure 6. Extant specimen of larva of *Eumorphus quadriguttatus*, Endomychidae: **A.** Habitus in dorsal view; **B.** Close-up of head in ventral view, arrows mark stemmata; **C.** Close-up of mouth parts in ventral view; **D.** Close-up of legs in ventral view; **E.** Close-up of posterior part of abdomen in ventral view. **Abbreviations:** a2–9 – abdomen segments 2–9; at – antenna; cl – claw; cx – coxa; dl – dorso-lateral process; en – endite; fe – femur; hc – head capsule; la – locomotory appendages (legs); li – labium; lo – longitudinal line; lr – labrum; md – mandible; mp – maxillary palp; ms – mesothorax; mt – metathorax; pr – process; pt – prothorax; te – trunk end; tr – trochanter; tt – tibio-tarsus; vl – ventro-lateral process.

more than four elements, such as seen in early lineages of Hymenoptera (Lawrence 1991a), are also not discernible.

The lack of certain characteristics and a strongly sclerotized head capsule (Peterson 1957; Beutel and Lawrence 2005) imply that the new fossils are immature stages of beetles (Coleoptera). More precisely, the legs with five elements imply that these are the immatures of either Myxophaga or Polyphaga. However, the larvae of Myxophaga have spiracle gills on most of the abdomen segments (Beutel 2005), which are not discernible on any of the new fossils. The dorso-ventrally flattened

habitus with multiple trunk processes of the new fossil larvae resembles the habitus of some larvae of the group Cucujiformia. More precisely, larvae with such processes are known in Erotylidae (pleasing fungus beetles; Fig. 7E, H; Lawrence 1991b; Ruta et al. 2011; Zaitsev et al. 2016), Cerylonidae (minute bark beetles; Lawrence 1991c), Coccinellidae (ladybird beetles; Kapur 1950; LeSage 1991), or Endomychidae (handsome fungus beetles; Figs 4–6, 7A–D, F, G, I–L; Leschen and Carlton 1988; Lawrence 1991d; Burakowski 1997; McHugh and Pakaluk 1997; Zaitsev 2022a, 2022b) and other ingroups.

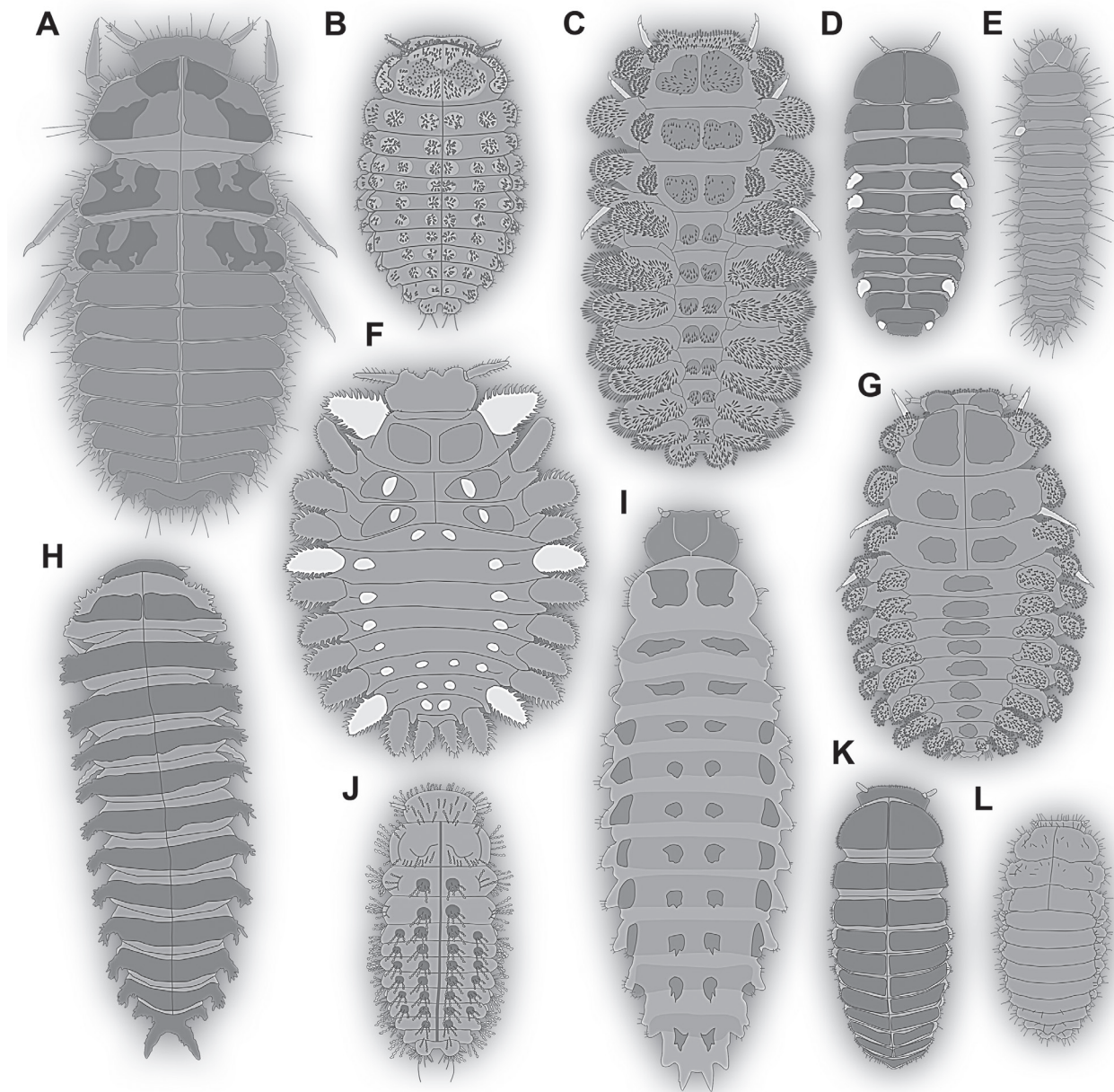


Figure 7. Examples of extant larvae of Endomychidae (A–D, F, G, I–L) and Erotylidae (E, H) with processes, modified after literature: **A.** *Stenotarsus commodus* from McHugh and Pakaluk (1997 fig. 42 p. 74); **B.** *Mycetina cruciata* from Burakowski (1997 fig. 1 p. 210); **C.** *Andrytus* from McHugh and Pakaluk (1997 fig. 1 p. 60); **D.** *Endomychus coccineus* from Tomaszewska and Zaitsev (2012 fig. 29b p. 89); **E.** *Cryptophilus integer* from Ruta et al. (2011 fig. 2 p. 4); **F.** *Amphisternus corallifer* from Yoshitomi and Sogoh (2018 fig. 1 p. 225); **G.** *Epipocus* from McHugh and Pakaluk (1997 fig. 18 p. 66); **H.** *Episcapha morawitzi* from Zaitsev et al. (2016 fig. 23 p. 372); **I.** *Lycoperdina dux* from Tomaszewska and Zaitsev (2012 fig. 29a p. 89); **J.** First stage larva of *Mycetina cruciata* from Burakowski (1997 fig. 20 p. 212); **K.** Last stage larva of *Ectomychus basalis* from Tomaszewska and Zaitsev (2012 fig. 2 p. 83); **L.** *Mycetina marginalis* from Tomaszewska and Zaitsev (2012 fig. 28c p. 86).

After McKenna et al. (2015) Erotylidae is an ingroup of Cucujoidea; Cerylonidae, Coccinellidae and Endomychidae are all ingroups of Coccinelloidea. Since in both groups, Cucujoidea and Coccinelloidea, processes are present rather often, it could be argued that this overall habitus is ancestral for either both groups or even their shared stem-species (\approx ancestor) and has been lost in all other ingroups of Cucujoidea and Coccinelloidea. Nevertheless, it is also possible, if not even more likely, that the ingroups

with processes developed them several times independently through convergent evolution.

Convergence is a quite common phenomenon among beetles in general and also beetle larvae (see also Haug et al. 2023b). Coleoptera as a whole and also many ingroups of it are extremely species-rich. This extreme species richness indicates that many lineages underwent rather rapid speciation events. This should have led to many different species with rather similar overall morphology. When

several of these species were exposed to similar selective pressures, it should not be surprising that several of these evolved similar morphological traits.

Differences among the extant larvae of Endomychidae and the new fossils

The new fossil larvae resemble in some characters the larvae of extant representatives of Endomychidae (cf. Figs 1–3 and Figs 4–6). Similarities to the modern larvae include the dorso-ventrally flattened body, the antennae morphology in SNHMB.G 8196, the lateral processes and their position on the body, and the specialised setae of the processes (Figs 1–3, 7). Additionally, the shapes of abdomen segment 9 of SNHMB.G 8196 and SNHMB.G 8195 in dorsal view are similar to the shapes of abdomen segment 9 of certain modern larvae.

However, there are multiple differences between the new fossils and the extant larvae of Endomychidae. The new fossil larvae are relatively small in body size compared to the extant larval representatives with lateral processes (Burakowski 1997; McHugh and Pakaluk 1997; Tomaszewska and Zaitsev 2012; Yoshitomi and Sogoh 2018; also to the new extant specimens described here in Figs 4–6). It is possible that not all here described larvae are of the same life stage. Nevertheless, the difference in size between the extant and fossil larvae is obvious. A comparable effect of differences in size over time was already described from larvae of other insect groups (Zippel et al. 2022b), but also adults in Myanmar amber (e.g., Wichard 2021). Hence the fossil larvae could be later-stage larvae of overall small-sized animals.

In addition to the difference in body shape among the new fossils, they also differ in the morphology of the tergite of the abdomen segment 9. Each of the fossils has a different shape of this tergite in dorsal view. The fossil specimen SNHMB.G 8195 has a fan-shaped tergite that has no medial indentation of the posterior rim. A rather similar morphology is present in extant larvae of *Endomychus* (Figs 4, 5 and Leschen and Carlton 1988). The fossil specimen SNHMB.G 8196 has the posterior rim of the tergite medially indented and laterally convex. The tergite seems almost bilobed. A similar morphology is known in extant larvae of *Mycetina* (Tomaszewska and Zaitsev 2012; Zaitsev 2022a). However, the shape of the head capsule of the new fossil and the extant larvae differs greatly (cf. Fig. 2 and Tomaszewska and Zaitsev 2012: fig. 28.c; Zaitsev 2022a: figs 3, 29, 58). Indeed, the specimen SNHMB.G 8196 resembles in some characters the larva of *Sticholotis ruficeps* (Coccinellidae). On one hand, the modern larva has similar lateral processes and head shape to the fossil. On the other hand, the tergite of the abdomen segment 9 of the modern larva differs from the tergite seen in the new fossil (Escalona and Ślipiński 2010, fig. 37). The tergite of abdomen segment 9 is narrow and medially convex but not indented. Among the three new fossils, only the

specimen SNHMB.G 8195 has a tergite without the medial indentation. However, the tergite of the larva of *Sticholotis ruficeps* is much narrower than the tergite of the specimen SNHMB.G 8195.

The fossil larva PED 1955 is the most slender one of the new fossils. Its tergite of abdomen segment 9 has a similar shape to that of SNHMB.G 8196, but it has additional posterior processes, which possibly represent urogomphi; see Fig. 3). Urogomphi are rare in extant larvae of Endomychidae (Tomaszewska 2005). A combination of a medially indented posterior rim of abdomen tergite 9 and possible urogomphi (as seen in specimen PED 1955) seems unknown in extant larvae of Endomychidae. The distal parts of the possible urogomphi resemble more those of the larvae of *Omosita nearctica* (Nitidulidae; Williams et al. 2021 their fig. 3) than the known posterior processes of larvae of Endomychidae (for comparison check the larva of *Eumorphus quadriguttatus* in Fig. 6).

Overall, the differences could mean that the fossils are not representatives of the group Endomychidae, they may not even be closely related to the group. As pointed out, there are several groups with larvae carrying lateral processes comparable to those of the fossils (Endomychidae and Erotylidae; Fig. 7; Genung et al. 1980; Carlton et al. 2000; Skelley 2009; Ruta et al. 2011; Zaitsev et al. 2016, Coccinellidae; Ślipiński and Tomaszewska 2005, fig. 10.33.7.B, Escalona and Ślipiński 2010, fig. 37). The new fossils may be more closely related to either of these groups or represent one (or even more) additional lineage(s) that is (are) now extinct, which evolved larvae with such processes. Yet, it is also possible that the morphology of the fossils, with their combinations of characters, is no longer present among the extant larvae of Endomychidae, but that they represent early offshoots of the group. Examples of today's extinct morphologies have been recognised for some groups of Holometabola (Badano et al. 2018, 2021; Haug et al. 2019a, 2019b, 2021c, 2022a; Zippel et al. 2021, 2023). Despite the uncertainty of interpretation and limited access to crucial characters, it seems likely that the new fossils are larvae of the group Cucujiformia, with some implications that the fossil SNHMB.G 8195 is a representative of Endomychidae. However, the relationship of the other two fossils, SNHMB.G 8196 and PED 1955, to the ingroups of Cucujiformia remain uncertain.

Adult representatives of Endomychidae are known in Kachin amber (Tomaszewska et al. 2018, 2022; Li et al. 2022b). Interestingly, even though the evolutionary history of Coccinellidae was traced back to the Cretaceous (McKenna et al. 2019), not a single fossil of Coccinellidae is known from that period. The oldest fossil reported is of an adult from the Eocene French Oise amber (Kirejtshuk and Nel 2012). Additional fossils have been also reported from Eocene Baltic amber (Szawaryn and Szwedo 2018; Szawaryn 2019; Szawaryn and Tomaszewska 2020). Hence, a possible relationship of the specimens to the representatives of Coccinellidae must be interpreted carefully.

Ecology of the new fossils

Many of the extant larvae of Cucujiformia spend most of their immature life in decaying wood infested with fungi. Some of the examples are larvae with setiferous processes of the groups Erotylidae, Cerylonidae and Endomychidae (Leschen and Carlton 1988; Lawrence 1991b, 1991c, 1991d; Burakowski 1997; McHugh and Pakaluk 1997; Leschen et al. 2005; Ruta et al. 2011; Zaitsev et al. 2016; Zaitsev 2022a, 2022b). Few representatives have a dorso-ventrally flattened body that allows them to live within small crevices, often directly underneath the bark (Leschen et al. 2005; Ślipiński and Lawrence 2005; Tomaszewska 2005). Some are even obligatory fungus-feeders and are specialized in a single species of fungi (Tomaszewska 2005). The processes with specialized setae are probably helping in defence or hunting, which would explain why so many larval representatives of Coccinellidae also still have a similar morphology (Ślipiński and Tomaszewska 2005). The processes might also be helpful in feeding upon the fungi-infested wood. If we presume that these larvae are not predaceous (as larvae of Brachypsectridae; Haug et al. 2021b or most of the larvae of Coccinellidae; Ślipiński and Tomaszewska 2005), the processes will unlikely be used for any hunting strategy. Therefore, it is much more likely that the processes have a role in defence mechanisms such as camouflaging. Cloaking as a defence mechanism is one of the behaviours already known from some larvae of Endomychidae (Tomaszewska 2005) and can be seen in other holometabolans as well (Wang et al. 2016; Machado et al. 2019; Haug et al. 2022b, 2022c, 2022d). The processes of the new larvae may help in cloaking themselves with hyphae or spores of the fungi as well. Such camouflage is probably additionally useful to stay unnoticed by a predator (Tomaszewska 2005) and have easier access to food. Similar strategies of decorating with hyphae are also seen in the brood care of some adults of Endomychidae. The female representatives of *Endomychus biguttatus* wrap hyphae around the individual eggs to physically protect them (Leschen 1994).

In some species the first-stage larvae do not have strongly pronounced processes, for example, the first instar of *Endomychus biguttatus* (Fig. 1; Leschen and Carlton 1988, their fig. 3). It has only slightly posteriorly drawn out lateral edges of trunk segments. However, the later stages, which are also much larger in size, have much more pronounced processes. This can naturally be due to the growth of the animal. Alternatively, it is possible that having the processes is of advantage only for the older (often also relatively larger) stages. Smaller larvae might rather have an “escape strategy” than a “camouflage one”. If we consider their often small size, the “escape strategy” might be the less costly one since they can easily fit in small crevices in the bark or wood.

Despite the overall uncertainty of the interpretation of the new larvae, it seems likely that they had a similar lifestyle to extant larvae with similar setiferous processes.

Therefore it seems most likely that they were wood-associated. In the case of the specimen SNHMB.G 8195, which has many characters similar to the modern larvae of Endomychidae, a similar lifestyle of feeding upon fungi can be presumed as well. However, in the cases of the specimens PED 1955 and SNHMB.G 8196, we cannot surely imply such a lifestyle because some modern representatives of Cucujiformia lead different lifestyles. For example, the modern larvae of Coccinellidae can be mycophagous, phytophagous, or predaceous, but Leschen (2000) and Ślipiński and Tomaszewska (2005) implied that the predaceous lifestyle is likely a derived one. Therefore, even if one of the new fossil specimens would be an early representative of Coccinellidae, a fungus-feeding lifestyle of the fossil representatives would still be possible.

Diversity of ecological roles

Wood-associated lifestyles of specimens preserved in amber are not surprising. In Kachin amber (Cretaceous, Myanmar) many different wood-associated ecological roles have been recognised (Peris 2020; Peris and Rust 2020), including hard-wood borers (Peris 2020; Haug et al. 2021a), soft-wood borers (Zippel et al. 2022b, in press a), submerged wood borers (Zippel et al. in press b), predators of wood-eating larvae (Haug et al. 2021b; Peris et al. 2022), but also larvae that possibly feed on fungi-infested rotting wood (Tomaszewska et al. 2018; Zippel et al. 2023; Haug et al. 2023b). The new fossils add to the latter category but possess a rather different overall appearance than the already known forms.

In younger ambers in the Eocene also numerous wood-associated larvae of different types are known (Larsson 1978; Klausnitzer 2003; Gröhn 2015; Haug et al. 2021b, 2023a; Zippel et al. 2022c). In Miocene amber many of these wood-associated larvae have so far not been reported, besides the “wood predators” (Haug et al. 2021b). Recognising one of the new larvae (specimen SNHMB.G 8195) as a possible wood-associated fungus feeder is, therefore, an important amendment to the Miocene amber fauna.

Conclusion

The three new larvae are an important addition to the amber fauna of the Cretaceous and Miocene. All new fossils are likely larvae of the group Cucujiformia, with characteristic setiferous processes and some other characters shared with modern larvae of Endomychidae. The characteristic setiferous processes are present in many larvae of Cucujiformia, not only in Endomychidae. It seems likely that setiferous processes in the larvae of different ingroups of Cucujiformia evolved as a response to similar selective pressures and are the result of convergent evolution. The processes in the new fossils might have had a function in hunting, but also in defence and camouflaging. They likely helped while, at least some of, the new larvae were feeding on fungi.

Acknowledgements

We thank Artem Zaitsev, Moscow, and an anonymous reviewer for their helpful input and suggestions about the manuscript. This study benefited from the help of various people and institutions; we thank them for their support. Lars Vilhelmsen, Alexey Solodovnikov, and Martin V. Sørensen, all Copenhagen, are thanked for providing access to specimens at NHMD and for their help and support. J. Matthias Starck, Munich, is thanked for his long-time support. We thank Mike Reich, Braunschweig, for his help curating the two new fossil specimens. JTH is kindly supported by the Volkswagen Foundation with a Lichtenberg Professorship and by the German Research Foundation (DFG Ha-6300/6-1). This study also benefited from SYNTHESYS+ grant (DK-TAF-TA4-007) that supported AZ for her three-weeks-stay in Copenhagen, Denmark. We are grateful to all people providing free software used in this project. This is LEON publication #56.

References

- Badano D, Engel MS, Basso A, Wang B, Ceretti P (2018) Diverse Cretaceous larvae reveal the evolutionary and behavioural history of antlions and lacewings. *Nature Communications* 9(1): 3257. <https://doi.org/10.1038/s41467-018-05484-y>
- Badano D, Fratini M, Magueri L, Palermo F, Pieroni N, Cedola A, Haug JT, Weiterschan T, Velten J, Mei M, di Giulio A, Ceretti P (2021) X-ray microtomography and phylogenomics provide insights into the morphology and evolution of an enigmatic Mesozoic insect larva. *Systematic Entomology* 46(3): 672–684. <https://doi.org/10.1111/syen.12482>
- Batelka J, Engel MS (2022) The first fossil tumbling flower beetle larva is a symphytan (Hymenoptera). *Acta Entomologica Musei Nationalis Pragae* 62: 57–59. <https://doi.org/10.37520/aemnp.2022.005>
- Beutel RG (2005) *Myxophaga* Crowson, 1955. In: Kristensen NP, Beutel RG (Eds) *Handbook of zoology, vol. IV Arthropoda: Insecta*. In: Leschen RAB, Beutel RG Lawrence JF (volume Eds) Part 38. Coleoptera, vol. 1: morphology and systematics (Archostemata, Adephaga, Myxophaga, Polyphaga (partim)). 1st ed. Walter De Gruyter, Berlin (NY), 43–44. <https://doi.org/10.1515/9783110904550.43>
- Beutel RG, Lawrence JF (2005) 4. Coleoptera, Morphology. In: Kristensen NP, Beutel RG (Eds) *Handbook of zoology, vol. IV Arthropoda: Insecta*. In: Leschen RAB, Beutel RG Lawrence JF (volume Eds) Part 38. Coleoptera, vol. 1: morphology and systematics (Archostemata, Adephaga, Myxophaga, Polyphaga (partim)). 1st ed. Walter De Gruyter, Berlin (NY), 23–27. <https://doi.org/10.1515/9783110904550>
- Beutel RG, Zhang WW, Pohl H, Wappler T, Bai M (2016) A miniaturized beetle larva in Cretaceous Burmese amber: Reinterpretation of a fossil “strepsipteran triungulin”. *Insect Systematics & Evolution* 47(1): 83–91. <https://doi.org/10.1163/1876312X-46052134>
- Burakowski B (1997) Descriptions of larva and pupa of *Mycetina cruciata* (Schaller)(Coleoptera, Endomychidae). *Annales Zoologici* 47(1–2): 209–214.
- Cai CY, Háva J, Huang DY (2017) The earliest *Attagenus* species (Coleoptera: Dermestidae: Attageninae) from Upper Cretaceous Burmese amber. *Cretaceous Research* 72: 95–99. <https://doi.org/10.1016/j.cretres.2016.12.018>
- Carlton CE, Townsend VR, Van Zandt PA, Mopper S (2000) Description of the larva of *Loberus impressus* (Coleoptera: Languriidae: Xenoscelinae) with notes on its natural history. *Annals of the Entomological Society of America* 93(3): 356–361. [https://doi.org/10.1603/0013-8746\(2000\)093\[0356:DOTLOL\]2.0.CO;2](https://doi.org/10.1603/0013-8746(2000)093[0356:DOTLOL]2.0.CO;2)
- Clarke DJ, Limaye A, McKenna DD, Oberprieler RG (2019) The weevil fauna preserved in Burmese amber—snapshot of a unique, extinct lineage (Coleoptera: Curculionidae). *Diversity (Basel)* 11(1): 1. <https://doi.org/10.3390/d11010001>
- Escalona HE, Ślipiński A (2010) *Sticholotis ruficeps* Weise: new synonymies and description of its mature larva (Coleoptera: Coccinellidae: Sticholotidini). *Annales Zoologici* 60(3): 309–318. <https://doi.org/10.3161/000345410X535307>
- Genung WG, Woodruff RE, Grissell EE (1980) *Languria erythrocephalus*: Host plants, immature stages, parasites, and habits (Coleoptera: Languriidae). *The Florida Entomologist* 63(2): 206–210. <https://doi.org/10.2307/3494441>
- Grimaldi D, Kathirithamby J, Schawaroch V (2005) Strepsiptera and triungula in Cretaceous amber. *Insect Systematics & Evolution* 36(1): 1–20. <https://doi.org/10.1163/187631205788912787>
- Gröhn C (2015) *Einschlüsse im baltischen Bernstein*. Verlag Wachholtz, Kiel, 424 pp.
- Gustafson GT, Michat MC, Balke M (2020) Burmese amber reveals a new stem lineage of whirligig beetle (Coleoptera: Gyridae) based on the larval stage. *Zoological Journal of the Linnean Society* 189(4): 1232–1248. <https://doi.org/10.1093/zoolinnean/zlz161>
- Haug JT, Haug C (2019) Beetle larvae with unusually large terminal ends and a fossil that beats them all (Scraptiidae, Coleoptera). *PeerJ* 7: e7871. <https://doi.org/10.7717/peerj.7871>
- Haug JT, Haug C, Ehrlich M (2008) First fossil stomatopod larva (Arthropoda: Crustacea) and a new way of documenting Solnhofen fossils (Upper Jurassic, Southern Germany). *Palaeodiversity* 1: 103–109.
- Haug JT, Haug C, Kutschera V, Mayer G, Maas A, Liebau S, Castellani C, Wolfram U, Clarkson ENK, Waloszek D (2011) Autofluorescence imaging, an excellent tool for comparative morphology. *Journal of Microscopy* 244(3): 259–272. <https://doi.org/10.1111/j.1365-2818.2011.03534.x>
- Haug JT, Müller CHG, Sombke A (2013a) A centipede nymph in Baltic amber and a new approach to document amber fossils. *Organisms, Diversity & Evolution* 13(3): 425–432. <https://doi.org/10.1007/s13127-013-0129-3>
- Haug C, Shannon KR, Nyborg T, Vega FJ (2013b) Isolated mantis shrimp dactyli from the Pliocene of North Carolina and their bearing on the history of Stomatopoda. *Boletín de la Sociedad Geológica Mexicana* 65(2): 273–284. <https://doi.org/10.18268/BSGM2013v65n2a9>
- Haug JT, Müller P, Haug C (2018) The ride of the parasite: A 100-million-year old mantis lacewing larva captured while mounting its spider host. *Zoological Letters* 4(1): 31. <https://doi.org/10.1186/s40851-018-0116-9>
- Haug C, Herrera-Flórez AF, Müller P, Haug JT (2019a) Cretaceous chimeras—an unusual 100-million-year old neuropteran larva from the “experimental phase” of insect evolution. *Palaeodiversity* 12(1): 1–11. <https://doi.org/10.18476/pale.v12.a1>
- Haug JT, Müller P, Haug C (2019b) A 100-million-year old predator: A fossil neuropteran larva with unusually elongated mouthparts. *Zoological Letters* 5(1): 1–14. <https://doi.org/10.1186/s40851-019-0144-0>
- Haug C, Haug GT, Zippel A, van der Wal S, Haug JT (2021a) The earliest record of fossil solid-wood-borer larvae—Immature beetles in

- 99 million-year-old Myanmar amber. *Palaeoentomology* 4(4): 390–404. <https://doi.org/10.11646/palaeoentomology.4.4.14>
- Haug JT, Zippel A, Haug GT, Hoffeins C, Hoffeins H-W, Hammel JU, Baranov V, Haug C (2021b) Texas beetle larvae (Brachypsectridae) – the last 100 million years reviewed. *Palaeodiversity* 14(1): 161–183. <https://doi.org/10.18476/pale.v14.a8>
- Haug GT, Baranov V, Wizen G, Pazinato PG, Mueller P, Haug C, Haug JT (2021c) The morphological diversity of long-necked lacewing larvae (Neuroptera: Myrmeleontiformia). *Bulletin of Geosciences* 96(4): 1–27. <https://doi.org/10.3140/bull.geosci.1807>
- Haug C, Zippel A, Hassenbach C, Haug GT, Haug JT (2022a) A split-footed lacewing larva from about 100-million-year-old amber indicates a now extinct hunting strategy for neuropterans. *Bulletin of Geosciences* 97: 453–464. <https://doi.org/10.3140/bull.geosci.1861>
- Haug C, Posada Zuluaga V, Zippel A, Braig F, Müller P, Gröhn C, Weiterschan T, Wunderlich J, Haug GT, Haug JT (2022b) The morphological diversity of antlion larvae and their closest relatives over 100 million years. *Insects* 13(7): 587. <https://doi.org/10.3390/insects13070587>
- Haug GT, Haug C, van der Wal S, Müller P, Haug JT (2022c) Split-footed lacewings declined over time: Indications from the morphological diversity of their antlion-like larvae. *PalZ* 96(1): 29–50. <https://doi.org/10.1007/s12542-021-00550-1>
- Haug JT, Linhart S, Haug GT, Gröhn C, Hoffeins C, Hoffeins H-W, Müller P, Weiterschan T, Wunderlich J, Haug C (2022d) The diversity of aphidlion-like larvae over the last 130 million years. *Insects* 13(4): 336. <https://doi.org/10.3390/insects13040336>
- Haug C, Baranov VA, Hörnig MK, Gauweiler J, Hammel JU, Perkovsky EE, Haug JT (2023a) 35 million-year-old solid-wood-borer beetle larvae support the idea of stressed Eocene amber forests. *Palaeobiodiversity and Palaeoenvironments* 103(3): 521–530. <https://doi.org/10.1007/s12549-022-00552-0>
- Haug C, Zippel A, Müller P, Haug JT (2023b) Unusual larviform beetles in 100-million-year-old Kachin amber resemble immatures of trilobite beetles and fireflies. *PalZ* 2023: 1–12. <https://doi.org/10.1007/s12542-023-00648-8>
- Hayashi M, Aiba H, Nakano E, Takahashi Y, Sato T (2020) Fossilized water pennies (Coleoptera: Psephenidae) in the Middle Pleistocene lake deposits in Shiobara site, Tochigi Prefecture, Japan. *Japanese Journal of Systematic Entomology* 26: 84–86.
- Kapur AP (1950) The biology and external morphology of the larvae of Epilachninae (Coleoptera, Coccinellidae). *Bulletin of Entomological Research* 41(1): 161–208. <https://doi.org/10.1017/S0007485300027565>
- Kerp H, Bomfleur B (2011) Photography of plant fossils— New techniques, old tricks. *Review of Palaeobotany and Palynology* 166(3–4): 117–151. <https://doi.org/10.1016/j.revpalbo.2011.05.001>
- Kirejtshuk AG, Nel A (2012) The oldest representatives of the family Coccinellidae (Coleoptera: Polyphaga) from the lowermost Eocene Oise amber (France). *Zoosystematica Rossica* 21(1): 131–144. <https://doi.org/10.31610/zsr/2012.21.1.131>
- Klausnitzer B (1978) Ordnung Coleoptera (Larven). Bestimmungsbücher zur Boden-Fauna Europas, vol 10. Akademie Verlag, Berlin, 378 pp. https://doi.org/10.1007/978-94-009-9975-6_2
- Klausnitzer B (2003) Käferlarven (Insecta: Coleoptera) in Baltischem Bernstein-Möglichkeiten und Grenzen der Bestimmung. *Entomologische Abhandlungen* 61: 103–108.
- Klausnitzer B (2009) Bemerkungen zu rezenten und fossilen Larven (Bernstein) der Gattung *Brachypsectra* LeConte (Coleoptera, Brachypsectridae). *Contributions to Natural History* 12: 721–742.
- Larsson SG (1978) Baltic Amber: A Palaeobiological Study. *Entomograph I. Scandinavian Scientific Press, Klampenborg*, 192 pp.
- Lawrence JF (1991a) Order Coleoptera. Beetles. Diagnosis. In: Stehr FD (Ed.) *Immature Insects*, Vol. 2. Kendall/Hunt Publishing Co., Dubuque, Iowa, 144–146.
- Lawrence JF (1991b) Order Coleoptera. Beetles. Erotylidae (Cucujoidea)(including Dacnidae). Pleasing fungus beetles. In: Stehr FD (Ed.) *Immature Insects*, Vol. 2. Kendall/Hunt Publishing Co., Dubuque, Iowa, 473–475.
- Lawrence JF (1991c) Order Coleoptera. Beetles. Cerylonidae (Cucujoidea)(= Cerylidae; including Aculagnathidae, Anommatidae, Dolosidae, Euxestidae, Murmidiidae). In: Stehr FD (Ed.) *Immature Insects*, Vol. 2. Kendall/Hunt Publishing Co., Dubuque, Iowa, 480–481.
- Lawrence JF (1991d) Order Coleoptera. Beetles. Endomychidae (Cucujoidea)(including Merophysidae, Mycetacidae). In: Stehr FD (Ed.) *Immature Insects*, Vol. 2. Kendall/Hunt Publishing Co., Dubuque, Iowa, 482–485.
- LeSage L (1991) Order Coleoptera. Beetles. Coccinellidae (Cucujoidea). The lady beetles, lady birds. In: Stehr FD (Ed.) *Immature Insects*, Vol. 2. Kendall/Hunt Publishing Co., Dubuque, Iowa, 485–494.
- Leschen RAB (1994) Ecological and behavioral correlates among mycophagous Coleoptera. *Folia Entomologica Mexicana* 92: 9–19.
- Leschen RAB (2000) Beetles feeding on bugs (Coleoptera, Hemiptera): Repeated shifts from mycophagous ancestors. *Invertebrate Systematics* 14(6): 917–929. <https://doi.org/10.1071/IT00025>
- Leschen RAB, Carlton CE (1988) Immature stages of *Endomychus biguttatus* Say (Coleoptera: Endomychidae) with observations on the alimentary canal. *Journal of the Kansas Entomological Society* 61(3): 321–327. <https://www.jstor.org/stable/25085008>
- Leschen RAB, Skelley AB, McHugh JV (2005) 10.7. Erotylidae Leach, 1815. In: Kristensen NP, Beutel RG (Eds) *Handbook of zoology*, vol. IV Arthropoda: Insecta. In: Leschen RAB, Beutel RG Lawrence JF (volume Eds) Part 38. Coleoptera, vol. 2: morphology and systematics (Elateroidea, Bostrichiformia, Cucujiformia Partim). 1st ed. Walter De Gruyter, Berlin (NY), 311–319. <https://doi.org/10.1515/9783110911213.311>
- Li Y-D, Huang D-Y, Cai C-Y (2022a) “*Attagenus*” *burmiticus* from mid-Cretaceous amber reinterpreted as a member of Orphilinae (Coleoptera: Dermestidae). *Palaeoentomology* 5(4): 390–394. <https://doi.org/10.11646/palaeoentomology.5.4.12>
- Li Y-D, Tomaszewska W, Huang DY, Cai CY (2022b) *Rhomeocalpsua torosa* gen. et sp. nov., a unique lineage of Endomychidae from mid-Cretaceous Burmese amber (Coleoptera: Coccinelloidea). *Palaeoentomology* 5(2): 146–154. <https://doi.org/10.11646/palaeoentomology.5.2.7>
- Machado RJ, Gillung JP, Winterton SL, Garzón-Orduña IJ, Lemmon AR, Lemmon EM, Oswald JD (2019) Owlflies are derived antlions: Anchored phylogenomics supports a new phylogeny and classification of Myrmeleontidae (Neuroptera). *Systematic Entomology* 44(2): 418–450. <https://doi.org/10.1111/syen.12334>
- McHugh JV, Pakaluk J (1997) Review of the larval stages of Epipocinae. *Annales Zoologici* 47(1–2): 59–77. [Insecta: Coleoptera: Endomychidae]
- McKenna DD, Wild AL, Kanda K, Bellamy CL, Beutel RG, Caterino MS, Farnum CW, Hawks DC, Ivie MA, Jameson ML, Leschen RAB, Marvldi AE, McHugh JV, Newton AF, Robertson JA, Thayer MK, Whiting MF, Lawrence JF, Ślipiński A, Maddison DR, Farrell BD (2015) The beetle tree of life reveals that Coleoptera survived

- end-Permian mass extinction to diversify during the Cretaceous terrestrial revolution. *Systematic Entomology* 40(4): 835–880. <https://doi.org/10.1111/syen.12132>
- McKenna DD, Shin S, Ahrens D, Balke M, Beza-Beza C, Clarke DJ, Donath A, Escalona HE, Friedrich F, Letsch H, Liu S, Maddison D, Mayer C, Misof B, Murin PJ, Niehuis O, Peters RS, Podsiadlowski L, Pohl H, Scully ED, Yan EV, Zhou X, Ślipiński A, Beutel RG (2019) The evolution and genomic basis of beetle diversity. *Proceedings of the National Academy of Sciences of the United States of America* 116(49): 24729–24737. <https://doi.org/10.1073/pnas.1909655116>
- Peris D (2020) Coleoptera in amber from Cretaceous resiniferous forests. *Cretaceous Research* 113: 104484. <https://doi.org/10.1016/j.cretres.2020.104484>
- Peris D, Rust J (2020) Cretaceous beetles (Insecta: Coleoptera) in amber: the palaeoecology of this most diverse group of insects. *Zoological Journal of the Linnean Society* 189(4): 1085–1104. <https://doi.org/10.1093/zoolinnean/zlz118>
- Peris D, Mähler B, Kolibáč J (2022) Review of the Family Thaneroceridae (Coleoptera: Cleroidea) and the Description of *Thanerosus* gen. nov. from Cretaceous Amber Using Micro-CT Scanning. *Insects* 13(5): 438. <https://doi.org/10.3390/insects13050438>
- Peterson A (1957) Larvae of insects. An Introduction to Nearctic Species. Part II. Coleoptera, Diptera, Neuroptera, Siphonaptera, Mecoptera, Trichoptera (Vol. 2). 3rd ed. Ohio State University, Columbus, Ohio, 416 pp.
- Poinar GO (1992) Life in Amber. Stanford University Press, Stanford, California, [viii +] 118 pp. <https://doi.org/10.1515/9781503623545>
- Poinar GO, Poinar R (1999) The amber forest: a reconstruction of a vanished world. Princeton, Princeton University Press, Princeton, New Jersey, [xiii +] 229 pp.
- Rasnitsyn AP, Müller P (2023) Identity of the larva described by Zippel et al. (2022) in the mid-Cretaceous Burmese (Kachin) amber (Hymenoptera, Tenthredinoidea, Blasticotomidae = Xyelotomidae syn. Nov.). *Palaeoentomology* 6(1): 13–16. <https://doi.org/10.11646/palaeoentomology.6.1.4>
- Ruta R, Jałoszyński P, Sienkiewicz P, Konwerski S (2011) Erotylidae (Insecta, Coleoptera) of Poland—problematic taxa, updated keys and new records. *ZooKeys* 134: 1–13. <https://doi.org/10.3897/zookeys.134.1673>
- Scheven J (2004) Bernstein-Einschlüsse: Eine untergegangene Welt bezeugt die Schöpfung. Erinnerungen an die Welt vor der Sintflut. Kuratorium Lebendige Vorwelt, Hofheim a. T., 160 pp.
- Skelly PE (2009) Pleasing fungus beetles of the West Indies (Coleoptera: Erotylidae: Erotylinae). *Insecta Mundi* 82: 1–94.
- Ślipiński A, Lawrence J (2005) 10.29. Cerylonidae Billberg, 1820. In: Kristensen NP, Beutel RG (Eds) Handbook of zoology, vol. IV Arthropoda: Insecta. In: Leschen RAB, Beutel RG Lawrence JF (volume Eds) Part 38. Coleoptera, vol. 2: morphology and systematics (Elateroidea, Bostrichiformia, Cucujiformia partim). 1st ed. Walter De Gruyter, Berlin (NY), 422–432. <https://doi.org/10.1515/9783110911213.422>
- Ślipiński A, Tomaszewska W (2005) 10.33. Coccinellidae Latreille, 1802. In: Kristensen NP, Beutel RG (Eds) Handbook of zoology, vol. IV Arthropoda: Insecta. In: Leschen RAB, Beutel RG Lawrence JF (volume Eds) Part 38. Coleoptera, vol. 2: morphology and systematics (Elateroidea, Bostrichiformia, Cucujiformia partim). 1st ed. Walter De Gruyter, Berlin (NY), 454–472. <https://doi.org/10.1515/9783110911213.454>
- Szawaryn K (2019) Unexpected diversity of whitefly predators in Eocene Baltic amber – new fossil *Serangium* species (Coleoptera: Coccinellidae). *Zootaxa* 4571(2): 270–276. <https://doi.org/10.11646/zootaxa.4571.2.7>
- Szawaryn K, Szewo J (2018) Have ladybird beetles and whiteflies co-existed for at least 40 Mya? *Palaontologische Zeitschrift* 92(4): 593–603. <https://doi.org/10.1007/s12542-018-0409-5>
- Szawaryn K, Tomaszewska W (2020) The first fossil Sticholotidini ladybird beetle (Coleoptera: Coccinellidae) reveals a transition zone through northern Europe during the Eocene. *Papers in Palaeontology* 6(4): 651–659. <https://doi.org/10.1002/spp2.1321>
- Tomaszewska W (2005) 10.32. Endomychidae Leach, 1815. In: Kristensen NP, Beutel RG (Eds) Handbook of zoology, vol. IV Arthropoda: Insecta. In: Leschen RAB, Beutel RG Lawrence JF (volume Eds) Part 38. Coleoptera, vol. 2: morphology and systematics (Elateroidea, Bostrichiformia, Cucujiformia partim). 1st ed. Walter De Gruyter, Berlin (NY), 442–454. <https://doi.org/10.1515/9783110911213.442>
- Tomaszewska W, Zaitsev AA (2012) Larva of *Ectomychus basalis* Gorham (Coleoptera, Endomychidae, Stenotarsinae) and its phylogenetic implication. *Deutsche Entomologische Zeitschrift* 59: 81–90.
- Tomaszewska W, Ślipiński A, Bai M, Zhang W, Ren D (2018) The oldest representatives of Endomychidae (Coleoptera: Coccinelloidea) from the Upper Cretaceous Burmese amber. *Cretaceous Research* 91: 287–298. <https://doi.org/10.1016/j.cretres.2018.07.001>
- Tomaszewska W, Szawaryn K, Arriaga-Varela E (2022) First member of ‘higher Endomychidae’ (Coleoptera: Coccinelloidea) from the Mid-Cretaceous amber of Myanmar and new insights into the time of origin of the handsome fungus beetles. *Insects* 13(8): 690. <https://doi.org/10.3390/insects13080690>
- Wang B, Xia F, Engel MS, Perrichot V, Shi G, Zhang H, Chen J, Jarzembowski EA, Wappler T, Rust J (2016) Debris-carrying camouflage among diverse lineages of Cretaceous insects. *Science Advances* 2(6): e1501918. <https://doi.org/10.1126/sciadv.1501918>
- Wedmann S, Hörnschemeyer T, Schmied H (2011) Fossil water-penny beetles (Coleoptera: Psephenidae: Eubrianacinae) from the Eocene of Europe, with remarks on their phylogenetic position and biogeography. *Palaeontology* 54(5): 965–980. <https://doi.org/10.1111/j.1475-4983.2011.01088.x>
- Wichard W (2021) Overview of the caddisflies (Insecta, Trichoptera) in mid-Cretaceous Burmese amber. *Cretaceous Research* 119: 104707. <https://doi.org/10.1016/j.cretres.2020.104707>
- Williams KA, Clitheroe C-L, Villet MH, Midgley JM (2021) The first record of *Omosita nearctica* Kirejtshuk (Coleoptera, Nitidulidae) in South Africa, with the first description of its mature larva. *African Invertebrates* 62(1): 257–271. <https://doi.org/10.3897/afrinvertebr.62.58842>
- Woodruff RE (2002) A new species of the beetle genus *Brachypsectra* from the Dominican Republic, with fossil connections (Coleoptera: Brachypsectridae). *Insecta Mundi* 549: 161–170. <https://digitalcommons.unl.edu/insectamundi>
- Wu RJC (1996) Secrets of a Lost World: Dominican Amber and its Inclusions. Self-published by the author, Santo Domingo, 222 pp.
- Yoshitomi H, Sogoh K (2018) Description of the larva of *Amphisternus corallifer* Gerstaecker (Coleoptera: Endomychidae), with specimens list of the genus *Amphisternus* preserved in EUMJ. *Japanese Journal of Systematic Entomology* 24(2): 225–229.
- Zaitsev AA (2022a) Larval description of two species of *Mycetina* Mulsant, 1846 (Coleoptera: Endomychidae: Lycoperdininae) from

- Russian Far East. Russian Entomological Journal 31(4): 392–406. <https://doi.org/10.15298/rusentj.31.4.09>
- Zaitsev AA (2022b) Larval description of *Lycoperdina smirnoviorum* Gusakov, 2017 (Coleoptera: Endomychidae: Lycoperdininae). Evraziatskii Entomologicheskii Zhurnal 31(2): 144–153. <https://doi.org/10.15298/rusentj.31.2.09>
- Zaitsev AA, Kompantsev AV, Zaitsev AI (2016) A review of larval Enecaustini (Coleoptera: Erotylidae) from Russia. Russian Entomological Journal 25(4): 367–386. <https://doi.org/10.15298/rusentj.25.4.05>
- Zhao X, Zhao X, Jarzembowski E, Wang B (2019) The first whirligig beetle larva from mid-Cretaceous Burmese amber (Coleoptera: Adepaga: Gyrididae). Cretaceous Research 99: 41–45. <https://doi.org/10.1016/j.cretres.2019.02.015>
- Zhao X, Zhao X, Jarzembowski E, Tian Y, Chen L (2020) The first record of brachypsectrid larva from mid-Cretaceous Burmese amber (Coleoptera: Polyphaga). Cretaceous Research 113: 104493. <https://doi.org/10.1016/j.cretres.2020.104493>
- Zippel A, Kiesmüller C, Haug GT, Müller P, Weiterschan T, Haug C, Hörnig MK, Haug JT (2021) Long-headed predators in Cretaceous amber—Fossil findings of an unusual type of lacewing larva. Palaeoentomology 4(5): 475–498. <https://doi.org/10.11646/palaeoentomology.4.5.14>
- Zippel A, Haug C, Müller P, Haug JT (2022a) First fossil tumbling flower beetle-type larva from 99 million-year-old amber. Palaontologische Zeitschrift 96(2): 219–229. <https://doi.org/10.1007/s12542-022-00608-8>
- Zippel A, Haug C, Hoffeins C, Hoffeins H-W, Haug JT (2022b) Expanding the record of larvae of false flower beetles with prominent terminal ends. Rivista Italiana di Paleontologia e Stratigrafia 128(1): 81–104. <https://doi.org/10.54103/2039-4942/17084>
- Zippel A, Baranov VA, Hammel JU, Hörnig MK, Haug C, Haug JT (2022c) The first fossil immature of Elmidae: An unusual riffle beetle larva preserved in Baltic amber. PeerJ 10: e13025. <https://doi.org/10.7717/peerj.13025>
- Zippel A, Haug C, Müller P, Haug JT (2023) The first fossil false click beetle larva preserved in amber. PalZ 97: 209–215. <https://doi.org/10.1007/s12542-022-00638-2>
- Zippel A, Haug C, Yanez Iturbe-Ormaeche B, Haug JT (in press a) Diversity of archostematan beetle larvae through time with new possible fossils. Palaeodiversity.
- Zippel A, Haug C, Müller P, Haug JT (in press b) Elateriform beetle larvae preserved in about 100-million-year-old Kachin amber. PalZ.

